# LUND UNIVERSITY

**Monitoring Wastewater Treatment Systems**

Rosén, Christian

1998

[Link to publication](#)

*Total number of authors:*
1

# Monitoring Wastewater Treatment Systems

Christian Rosén

Lund 1998

ii

# Abstract

This work considers various techniques to extract information from the vast amount of data collected at a modern wastewater treatment plant. If the information extracted is to be considered reliable is highly dependent on the data screening. Data screening includes validation and quality improvement of data. Adequate methods for validation, noise reduction and other forms of quality improvements of wastewater treatment data are discussed. In order to detect deviations and disturbances, the measurement variables can be investigated individually or many variables simultaneously. Single variable detection involves investigation of the basic signal characteristics such as amplitude, mean and spread. Usable methods are discussed and examples are given. In order to detect synergetic effects, techniques capable of investigating several variables simultaneously, are needed. Multivariate statistics based methods, such as principal component analysis (PCA), principal component regression (PCR) and projection to latent structures (PLS), are considered and their applicability discussed. Some possibilities to adapt the methods to the dynamic situation in a wastewater treatment plant are also outlined.

# Acknowledgements

First of all, I would like to thank Dr Ulf Jeppsson at the Dept of Industrial Electrical Engineering and Automation (IEA), who has served as my informal supervisor throughout the study presented in this thesis. Without all the hours of discussion with him, my work would have been substantially more difficult. His ability to find traps and gaps in my reasoning has saved me a lot of time. I would also like to express my gratitude to my supervisor Professor Gustaf Olsson, for the inexhaustible enthusiasm he has shown for my work. He has a tremendous capability to put things into a broader context and to discern the important elements of the research. With a creative and friendly atmosphere everything becomes much easier. This is certainly the case at IEA and I would, therefore, like to thank everyone at IEA for their support.

I would also like to thank the staff at the Ronneby wastewater treatment plant. Without their cooperation providing me with real measurement data, this work would not have been possible. I would also like to thank them for important comments on presentation and visualisation of analysis results.

There are other people who have shown great interest in my work, and I would especially like to thank my father, Dr Björn Rosén for all the discussions we have had over the years and for reading the manuscript and returning valuable feedback. Dr Bengt Carlsson, Uppsala University has also provided valuable contribution by reading my manuscript and providing me with important comments.

This work was financially supported by the Swedish Water and Wastewater Association (VAV), as a part of the VA-forsk research program.

*Lund, November 27, 1998*
*Christian Rosén*

# Contents

# Chapter 1

# Introduction

Over the last centuries the human effects on the hydrologic cycle have increased. In order to establish convenient environments for living as well as agricultural and industrial production, artificial recycles have been created. In addition to the necessity to life, water is used for numerous purposes, for example irrigation, transport of material and energy as well as cleaning. Whatever the purpose is, processing and use normally results in pollution of water. The first ideas of recovery of water quality were based on physical means, such as dilution and sedimentation. However, this became precarious as cities became larger and the importance of hygienic issues increased. Chemical precipitation was introduced to increase the settleability of the waste. Biological treatment of wastewater dates back to the late 19th century (Orhon and Artan 1994). It started with the trickling filter or biological bed, which was developed in the early 20th century (Hammer 1986). Another breakthrough in biological treatment of sewage was the discovery that supplemental aeration of wastewater resulted in purification. In the beginning of the 20th century, experiments were carried out on what was to be called the *activated sludge* process. During the last few decades, wastewater treatment has become an industry of high complexity. Higher demands on efficiency in terms of effluent water quality and economics are important reasons. More knowledge on the physical, chemical and biological processes involved has been obtained, which has resulted in more advanced and efficient configurations. The ability to measure, analyse and control certain substance concentrations, flow rates and other entities has influenced the design and operation of treatment plants considerably.

# 1.1   Motivation

In most process industries, monitoring of the process and the process output is performed to achieve conformity with quality, safety and economic requirements imposed on the production. The level of monitoring differs from various fields and pioneering efforts can be found in, for instance, the petrochemical and pharmaceutical industries. Wastewater treatment industries cannot be considered to be among the most diligent and systematic users of monitoring. Up to today, monitoring in wastewater treatment has mostly focused on a few key effluent entities upon which regulations are enforced by governments or other authorities. However, as more entities are regulated and the regulations become more rigid, the demands on the operation of the processes increase. Minimising the use of resources, for instance, energy, chemicals and man power, and decreasing the amount of sludge products produced, have also become important issues in order to adapt the wastewater treatment processes to the ideas of sustainability. The development towards resource efficient and sustainable systems has led to an increased need of process knowledge. To obtain more knowledge, new and upgraded wastewater treatment plants are equipped with measurement systems for collecting data from a large amount of entities. The measurements are used for monitoring the process and the quality of the process output. Measurements are also used for control directly in control loops or indirectly as a basis for manual control actions. In large wastewater treatment plants the data collecting system may include hundreds or even thousands of measured entities.

An increased amount of data calls for techniques to handle large data sets on-line. The methods for monitoring used today are normally based on time series charts, where the operator can view the different variables as historical trends. It is hard to keep track of more than a few variables and when the number of monitored variables increases, it is difficult to draw any conclusions. To be able to monitor the process behaviour effectively, an extraction of important information must be performed from the large number of measured variables, and this information must then be presented in an understandable and interpretable way.

## 1.2 Objectives and Contributions of the Thesis

The main objective of this thesis is to investigate the first element in the information extraction concept of *detection, diagnosis and consequence analysis* ($D^2C$) of disturbances, faults and deviating events, in on-line measurements from wastewater treatment processes. An investigation of possible methods for detection implies that monitoring methods used in other theoretical and practical areas are investigated and adapted to suit the demands of wastewater treatment process monitoring. Important features of the processes that have to be considered are, for instance, data quality, process dynamics and comprehensibility for operators. The objectives of this thesis are given below.

- Provide techniques on how measurement data can be validated and how the quality of data can be improved. This is important to obtain reliable analysis results. The improvement of the data quality should only marginally influence the process information content of the data.

- Enlighten and demonstrate methods to extract information from single variables and to show the applicability of the methods for detection of disturbances. Single variable analysis involves investigation of amplitude, spread and short as well as long-term variability. It also involves examination of the frequency characteristics of measurement variables.

- Investigate the applicability of and adapt multivariate statistics to the needs of wastewater treatment monitoring. The methods should be able detect deviations and isolate the variables responsible for the deviations. The investigated methods should also provide techniques for easy interpretation.

- As a subordinate objective, the topics discussed above should be presented in a way that makes them understandable for people with different backgrounds. Thus, the thesis should include basic explanations for most of the methods described, but also provide

an adequate bibliography if more information on different methods and techniques is required by the reader.

The objective that people with different backgrounds should be able to read and appreciate the thesis, implies that some readers will consider some parts of the thesis as obvious and perhaps naive. However, since the thesis is written with process engineers as much as the research community in mind, the extra effort to fully explain the basis of methods and techniques presented is worthwhile. The main contributions of this thesis are listed below.

- Methods to improve measurement data quality by digital filtering adapted to the needs of wastewater treatment data analysis, are presented

- Some aspects of single variable analysis of wastewater treatment data are presented. Investigation of both time and frequency domain characteristics of a measurement signal is discussed together with what information that can be obtained when performing such analyses.

- The applicability of multivariate statistics on wastewater treatment data is shown, by examples on simulated and real process data. Techniques for displaying information in a comprehensible way are presented.

## 1.3   Outline of the Thesis

In Chapter 2 some basic concepts in automation and control of wastewater treatment plants are discussed. Information extraction from on-line measurements are discussed on a general level in Chapter 3. Chapter 4 provides methods and techniques for data screening, that is the validation and reconstruction of erroneous data. Filtering, outlier detection and handling of missing values are topics discussed in this chapter. Investigation of individual measurement signals is discussed in Chapter 5. Here, signal features such as amplitude, spread, variability and frequency are used to detect deviations in signals. Chapter 6 is devoted to the theory of multivariate statistics (MVS) and how

MVS can be used for multivariate monitoring of processes. Some practical aspects on building multivariate monitoring models are discussed together with what information can be achieved. The concept of operational modes and how such modes can be used for detection and control, is also discussed. In Chapter 7 multivariate monitoring results on simulated data are presented and in Chapter 8 results from monitoring real wastewater treatment plant data are presented. Conclusions and a summary of results are presented in Chapter 9, which also contain a discussion on implementation aspects and new topics of research in the direction of this thesis.

## 1.4  Publications

The author of this thesis has earlier presented a few reports and articles, which are all in line with the study presented here. Rosén and Olsson (1997a) treats the transformation from data to information and discusses some practical aspects of data collection and information extraction. Rosén and Olsson (1997b) is a report on analysis of on-line data from Pt Loma wastewater treatment plant in San Diego, USA. The incentive of the Pt Loma study was optimisation and increased knowledge of the chemical precipitation at the plant in order to meet more stringent requirements from the government of California. Some early results of detection and isolation of disturbances in wastewater treatment systems are available in Rosén and Olsson (1998). Time delay related issues and fault propagation in multilevel flow models (graph-based diagnosis) are discussed in Rosén (1998).

# Chapter 2

# Basic Concepts

In this chapter some basic concepts are presented. Some important definitions are presented in order to avoid misconceptions caused by different backgrounds of the readers. The principles of wastewater treatment are discussed briefly for the sake of uninitiated reader. The chapter is concluded by a discussion on the differences between static and dynamic process descriptions.

## 2.1   Useful Definitions

In order to allow the reader to become acquainted with the terminology used in this thesis, some basic definitions are presented.

### On-line and Off-line Analysis

In a real monitoring situation, the measurement variables are known up to the present value. No information on the future is available. The analyses carried out can only be based on historic and present values. In this thesis such an analysis is referred to as *on-line* analysis or *causal* analysis. However, it is sometimes valuable to investigate historic time periods of variable measurements in order to obtain information on the process. In such cases, the analysis must not be causal, since the future is known. Analysis of historic time periods is referred to as *off-line* analysis and may be either causal or *non-causal*.

## Measurement Sampling

Measurements are collected in series. A single measurement value is denoted as a *sample*. The distance in time between every sample is the *sampling time*. If several single data series are investigated simultaneously, that is *multivariate* data analysis, a sample refers to all measurements at a specific point in time. Thus, a multivariate sample consists of a single measurement from every variable considered. In this thesis, no distinction is made between a sample and a multivariate sample. Consequently, the term sample is also used in multivariate analysis, even though the correct term would be multivariate sample. In matrix form, a sample corresponds to one row of the data matrix.

## Notation of Measurements

In this thesis, most of the variables of the processes discussed are normally described in vector and matrix format. In order to easily separate scalars, vectors and matrices the following commonly used standard of notation is used. Scalars are written in italic lower case, e.g. $x$. Vectors are written in bold lower case, e.g. $\mathbf{x}$, and matrices are written in bold capitals, e.g. $\mathbf{X}$. Input data to a model or filter are normally denoted by $x$, $\mathbf{x}$ or $\mathbf{X}$, while model or filter output are denoted by $y$, $\mathbf{y}$ or $\mathbf{Y}$. $x(k)$ or $y(k)$ refers to the input or output variable value at time $k$. This can also be written in subscript, *i.e.* $x_i$ or $y_i$. However, some deviations occur due to different tradition in various fields.

## Estimation Terms

There is some confusion due to different conventions in the use of the terms *smoothing, filtering* and *prediction*. The terms seem to be used differently depending on people's backgrounds. In this report the terms have been used in the same way as by Åström and Wittenmark (1997). Assume that an estimate $\hat{y}(k + m)$ is to be constructed from $X_k$, where $X_k$ is a time series of $k$ measurements such that $X_k = \{x(i)|i \leq k\}$. Then it is called
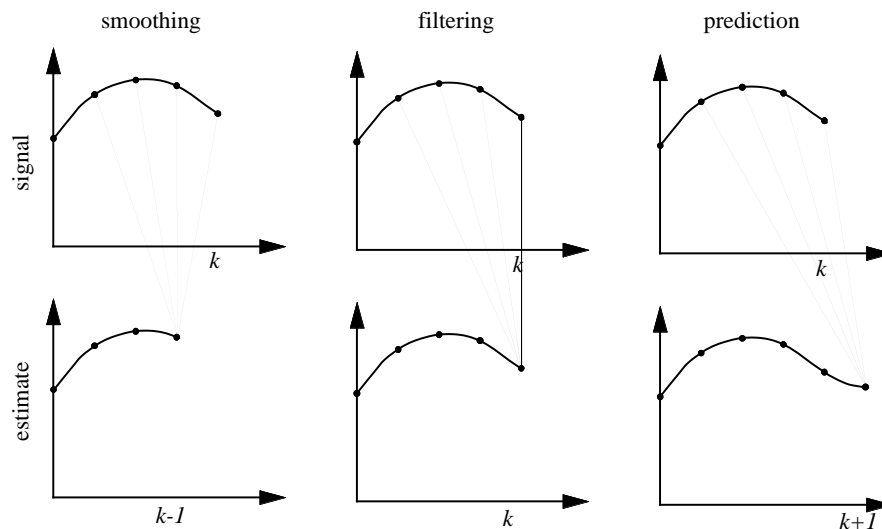
**Figure 2.1** Smoothing, filtering and prediction (Åström and Wittenmark 1997).

- smoothing if $m < 0$,

- filtering if $m = 0$ and

- prediction if $m > 0$.

The distinction between smoothing, filtering and prediction is illustrated in Figure 2.1. This implies that if the term estimation is used nothing is said about the causality of the estimate.

## 2.2 Wastewater Treatment Systems

For readers not familiar with wastewater treatment systems a short description is given. Some basic ideas behind modern wastewater treatment are discussed. For further reading on wastewater treatment in general Henze *et al.* (1995a) is a good reference. For control and automation in wastewater treatment the reader is referred to Olsson and Newell (1998), Van Impe *et al.* (1998) or Andrews (1992).

### Wastewater Treatment Processes

Wastewater treatment processes aim at removal of pollutants in the wastewater by transformation and separation processes. This can be
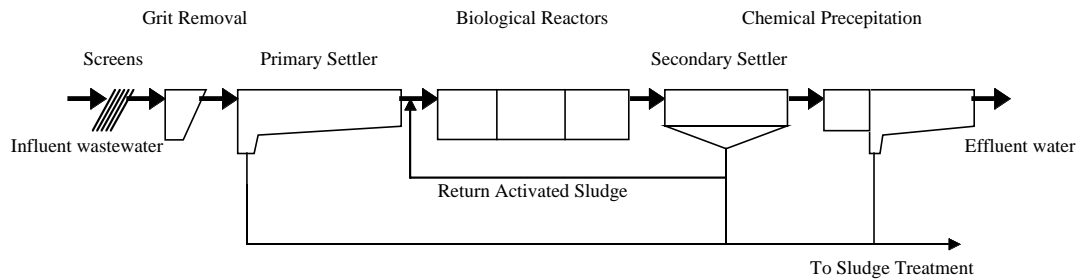
**Figure 2.2**   The basic layout for a typical wastewater treatment plant using physical, biological and chemical treatment.

achieved in many different ways, depending on the characteristics of the wastewater, the desired effluent quality and other environmental and social factors. Traditionally, the wastewater treatment processes are divided into *physical*, *chemical* and *biological* treatment, which are used in many different combinations. Figure 2.2 shows the principal layout of a typical treatment plant with physical, biological and chemical treatment.

Physical treatment involves, for instance, *screens*, *sedimentation*, *flotation*, *filters* and *membrane* techniques. Sedimentation implies that particles heavier than water are settled in tanks and separated from the water phase. In flotation, or *dissolved air flotation* (DAF), particles are separated from the water phase by using dissolved air in pressurised water. When the pressure decreases, the dissolved air is released as small air bubbles, which attach to and lifts the particles to the surface of the tank.

Chemical treatment involves coagulation and flocculation of colloidal and finely suspended matter as well as precipitation of some dissolved matter. Typical chemicals used are ferro, ferri and aluminium salts as well as lime. In order to further increase the efficiency of the process, coagulation aids such as polymeers can be used. The chemical treatment also includes separation of the flocculated matter as a chemical sludge.

Biological processes are based on biological cultures, consisting of bacteria, unicellular life forms and even some multicellular life forms. The organic pollutants in the wastewater serve as food and energy sources

for the microbiological culture as it grows. The microbiological culture can either grow suspended in the water phase or in a fixed position on surfaces as a biofilm. Suspended growth is used in so called *activated sludge* (AS) reactors, while the fixed growth is used in *fixed bed reactors*. A combination thereof is, for instance, *suspended carriers*, where the biofilm grows on small carriers, which are suspended in the water phase. Biological treatment aims at having a certain amount of microbiological culture in the process. In an AS reactor this is achieved by separating the sludge from the water phase in a separation unit and then returning the sludge into the biological reactor. The excess sludge created in the process is removed and treated in sludge treatment processes, which stabilise and dewater the sludge. Stabilisation of sludge makes it biologically safe and often usable as fertiliser. The reduction of organic matter in a biological treatment plant can be 90% or more.

## Automation and Control in Wastewater Treatment

Today, many treatment plants all over the world are equipped with data collecting systems. These systems are used for monitoring, automatic control and as a decision base for operational strategies. The data collecting systems differ from plant to plant and from supplier to supplier but common sampling rates (in Sweden) are 10 and 12 per hour, *i.e.* every sixth and fifth minute, respectively. The sample values are often an average over the sampling period, during which some sensors continuously deliver values and others perhaps only once a minute. All sensors are afflicted with time lags, but normally these are short in comparison with the time constants of the system. Some variables are controlled automatically with controllers. Oxygen level in aerated basins, return and recycling flow rates and adding of chemicals are simple examples of controlled variables. More sophisticated control can be found in some treatment plants, but is still not common. This is due to a number of factors. Since the process is changing slowly it is possible to use manual control. The lack of accurate models of wastewater treatment processes makes it hard to implement model based control, and of course, a conservative attitude towards automatic control also contributes.

**Process Dynamics**

A wastewater treatment process consists of many subprocesses with
dynamics of various time scales. Some variations are slow, for instance
sludge dynamics and temperature, with time scales of days, week and
even months. The daily variation in influent flow rate and substance
concentrations is perhaps the most dominant variation. However,
there are even faster variations present, such as dissolved oxygen (DO)
dynamics and hydraulic shocks.

The different time scales make it difficult to analyse the cause-effect
relationships, especially when recirculation and other feedback loops
are present. Therefore, it is important to establish the dynamic beha-
viour of the process and adapt the analysis methods in accordance to
the dynamics.

## 2.3   Process Descriptions

A process description may appear differently depending on the process
and the method used to describe the process. This thesis focuses on
*input-output* descriptions or models. Input-output models are some-
times called *empirical, statistic* or *external* models. The main feature
of input-output models is that they do not have internal states. In-
stead they are based on empirical relationships between the input and
output variables of the model. However, there are other types of mod-
els structures available. *Mechanistic* (or *internal*) models are based
on fundamental knowledge of mechanisms that affect the modelled
process. When the information of the process is good, models based
on elementary principles are preferable. However, this is not always
the case, and combinations of empirical and mechanistic models are
common. In this thesis, only input-output models are considered.
There are some convenient abbreviations used for input-output mod-
els depending on the structure of the model. *Single input-single output*
(SISO) implies that the model describes a single output variable us-
ing a single input variable. In analogy to this, *multiple input-multiple
output* (MIMO) models describes several output variables based on
several input variables.

A process can either be considered to be *static* or *dynamic*. In a static process description, the process output is only dependent on the present state of the process. However, industrial processes, such as wastewater treatment processes, are normally dynamic processes. As opposed to static process descriptions, the process output of a dynamic process description is dependent not only on the present state of the process, but also on the history of the process. A change of the process conditions cannot be seen immediately, but takes some time.

## Input-Output Processes

As the name suggests, the variables of an input-output system consist of input variables and output variables. Input variables are sometimes called *independent* variables and the output variables are, consequently, sometimes called *dependent* variables. In this thesis independent variables are denoted $X$ and dependent variables are denoted $Y$. The direction of causality is from the independent to the dependent variables. The independent variables decide the outcome of the dependent variables.

The system definition determines which variables are independent and dependant, respectively. For instance, if the aim of a model is to estimate the pH level in the biological reactors, then the variables that describe the influent wastewater characteristics are independent variables. The pH level is the dependent variable in this case. However, if the aim is to estimate the effluent pH level, the variables measured in the biological step (including the pH level) may be added to the influent variables as independent variables. As the system definition changes independent variables may become dependent variables.

## Dependency between Measurements

A measurement is said to be *time independent* if it does not depend on preceding (or successive) measurements. This is seldom true for a process variable. Instead process variables are normally *time dependent* variables. The degree of dependency between the current sample $y(k)$ and a historic sample $y(k - \tau)$ can be expressed as *autocovariance*
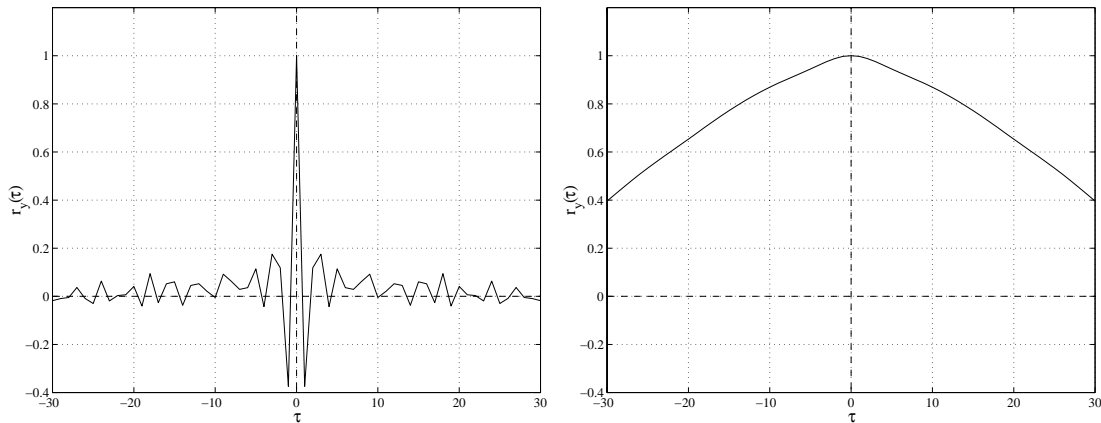
**Figure 2.3**  The autocorrelation function of DO measurements (left) and influent ammonia measurements (right). The time unit is samples, corresponding to 5 minutes.

or *autocorrelation*, which is the normalised autocovariance. In Figure 2.3, the correlation is plotted as a function of $\tau = -30 \ldots 30$ ($\tau$ is in unit samples, which corresponds to 5 minutes in this case). To the left the autocorrelation function of the dissolved oxygen (DO) concentration level is displayed. It can be seen that the correlation is low when $\tau \neq 0$. Thus, the measurement can be considered as independent. The reason for this is that the DO level is controlled to a set point value. The variations in the signal is noise of high frequency, which can be considered independent. To the right, in Figure 2.3 the autocorrelation function of influent ammonia is shown. The covariance is here high even though $\tau$ increases. This implies that the measurements are dependent over a time span of many samples. Dependent measurements indicate that the process they represent is time dependent, *i.e.* dynamic. Most process variables display autocorrelation functions similar to the right function in Figure 2.3.

A characteristic feature of dynamic processes is that the change in an input variable does not influence the output variables immediately. This can be expressed by the cross-covariance or crosscorrelation function. Let $x$ be an input variable and $y$ be an output variable of a process. The crosscorrelation function expresses the dependency between $x(k)$ and $y(k + \tau)$. In Figure 2.4, the crosscorrelation function of the influent flow rate ($x$) and the air valve position of an aerator in a biological reactor ($y$) is plotted.
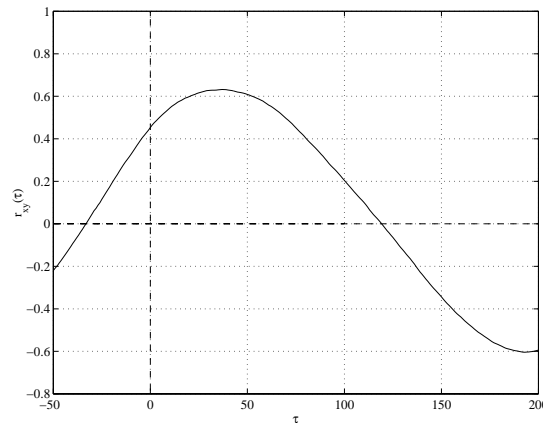
**Figure 2.4**   The crosscorrelation function influent flow rate and air-valve position of the aerator in biological reactor. The time unit is samples, corresponding to 5 minutes.

The maximum correlation is here slightly more than 0.6 at $\tau = 37$. This means that it takes on an average 37 samples ($\approx 3$ hours) for a change in the input to fully propagate to the output. The high crosscorrelation values for $\tau$ close to $\tau = 37$, indicate that the variables are time dependent. If the variables were time independent, but still mutually correlated, the crosscorrelation function would display a peak at $\tau = 37$ and values close to zero for $\tau \neq 37$.

## Static and Dynamic Process Descriptions

In order to describe a process, static and dynamic descriptions can be used. In many cases, it is possible to achieve good results with a static description, even though the true process is dynamic. It is possible to make use of the fact that in certain time scales, a dynamic process may be considered to be *quasi-stationary*. Quasi-stationary means that most variables can be either considered constant, due to slow variations in comparison with the time scale of interest, or equal to their mean if the changes are much faster than the time scale of interest.

Let $X$ be the process input and $Y$ be the process output. A static process description can the be expressed as:

$$Y(k) = f_p(X(k)) \tag{2.1}$$

where $f_p$ is the process function and $k$ is the point in time. If there are time delays between the input and the output variables have been established using, for instance, crosscorrelation analysis, the delays can be incorporated in the process description as:

$$Y(k) = f_p(X(k - d)) \tag{2.2}$$

where $d$ denotes the delay. If a MIMO or MISO system is considered, the delay may be different for the various variables. The description is now dynamic in the sense that a change in the input variable does not immediately yield a change in the output variable. However, since the change is momentary when the time corresponding to the delay has passed, process dynamics is normally not well described by this model description. An exception is the concentration dynamics in a true plug flow process. In this thesis, models of the form expressed by Equation 2.2 are referred to as *static with time lag.*

A better dynamic description of a process take both present and historic measurements into consideration. The process can be expressed:

$$Y(k) = f_p(X(k), X(k - 1), \dots, X(k - l)) \tag{2.3}$$

where $l$ is the time required until the contribution of the historic states to the present state are negligible. As discussed above, time delays may be present. They can be introduced in the description as:

$$Y(k) = f_p(X(k - d), X(k - 1 - d), \dots, X(k - l - d)) \tag{2.4}$$

where $d$ again denotes the delay.

# Chapter 3

# Detection, Diagnosis and Consequence analysis

In this chapter the use of computers to extract information from on-line measurements is discussed. The demands on process knowledge and controllability of processes have increased rapidly over the last few decades. Higher requirements on product quality, production costs, safety and production flexibility are enabled, as the computer control and process knowledge develop. The use of computers for control and process information extraction is today widely spread in all industrial fields.

## 3.1 Why Computer Aided Control and Operation?

A lot of money is being invested into measurement and monitoring systems in most process industries today and the wastewater treatment industry is no exception.

### System Complexity

The operation and control of a modern process industry, such as wastewater treatment plants, is often associated with high complexity. The complexity is caused by, for instance:

- the vast source of disturbances, e.g. changing ambient conditions and mechanical breakdowns;

- the large amount of data collected by the measurement systems;

- dynamic conditions caused by changes in the influent wastewater;

- complex cause-effect relationships caused by, for instance, the use of biological cultures, recirculations and control actions.

Thus, early detection of disturbances, methods to handle large data sets, studies of the dynamic process behaviour and tools for tracking complex cause-effect relationships are important issues in order to operate and control the process in the most efficient manner.

Many of the issues listed above are suitable for computerised investigations and analyses. Some tasks can be more or less fully automated, while others are based on interactions between the operators the computers. To introduce automatic or semi-automatic operation of complex tasks and to present the result in a comprehensible way, may lead to a complexity reduction of the basis for operational decisions.

## Computational Capability

Information extraction often involves intensive calculations. As the amount of available data increases, the computational capability becomes important. Computers are made for numerical computations and are superior to man in that sense. To use computers for information extraction makes it possible to process data in a way that would be impossible if the calculations were to be carried out manually. Usually, a common PC of today is adequate to perform the calculations required.

## Consistent Monitoring

Many of the tasks involved in information extraction of process data ought to be carried out consistently. For instance, monitoring influent wastewater characteristics must be done continuously in order to detect disturbances in the influent wastewater. This cannot be done manually, since the disturbances may occur during times when the plant is unmanned. Monitoring of measurements is also a task that man find monotonous, especially if the disturbances are rare.
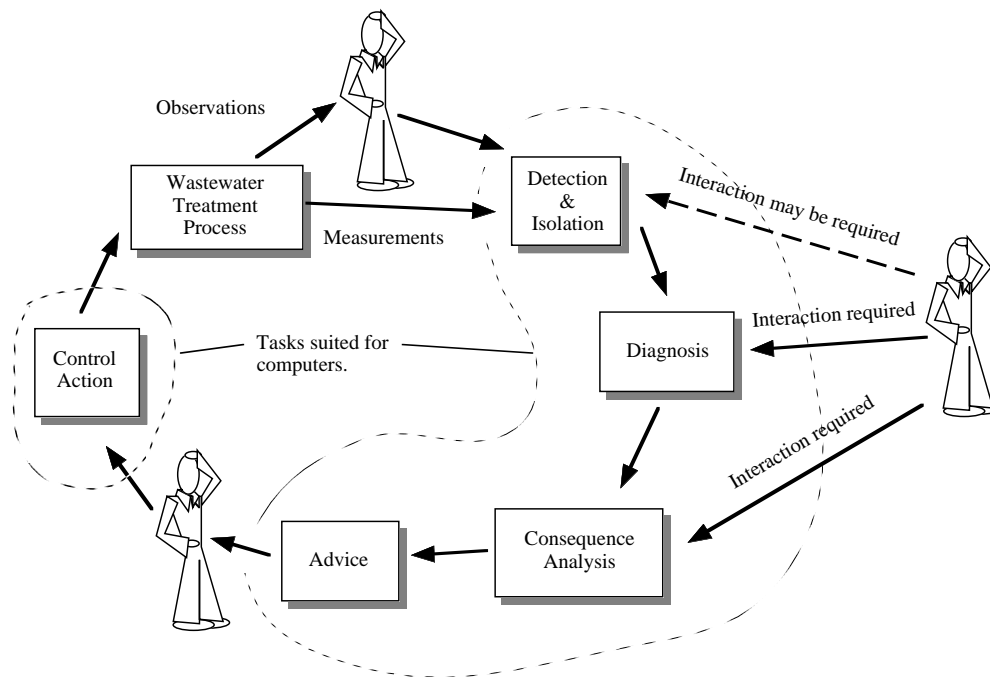
**Figure 3.1**   The information flow and processing in a wastewater treatment plant.

# 3.2   Elements of Information Extraction

If the information available from disturbances is to be taken care of, a strategy for information extraction is needed. There are some elements that have to be included in such a strategy:

- detection and isolation;

- diagnosis;

- consequence analysis.

The elements can be used separately, but in order to extract as much information as possible from, for instance, a disturbance event, they must all be carried out. Figure 3.1 illustrates the information cycle at a wastewater treatment plant. Since the detection, diagnosis and consequence analysis tasks are significantly different by their nature, the methods for achieving the tasks are based on different ideas and methodologies.
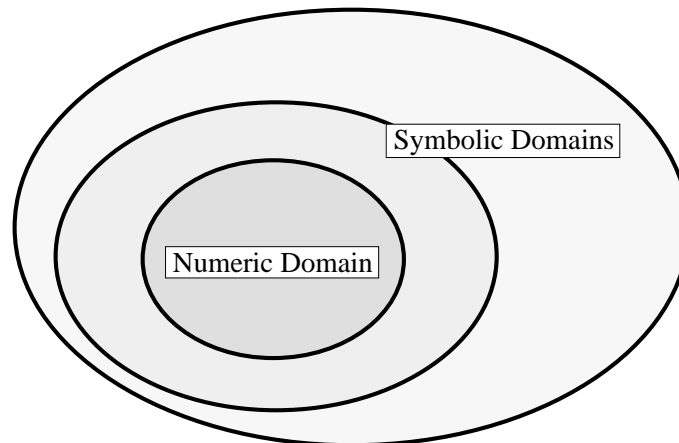
**Figure 3.2**   A principal view of the available information in a system. The numerical domain is the core of the system.  The symbolic domains can be more or less extensive.

## Detection and Isolation

The *detection* part of the information extraction concept involves detecting deviating situations. Detection is thus an important part because if nothing is detected nothing can be learned.  The detection can range from a simple binary information on, for instance, a pump status to more sophisticated information on the current process status, including many variables and estimates of variables.  Whatever the detection task is, the time is important if countermeasures are to be taken.  The faster the operator will be notified, the greater is the chance of saving the process if a serious disturbance hits the process. Thus, the capability to early warn the operator is of highest the priority.

When a disturbance is detected and confirmed, the task of finding the cause begins.  The first step is to isolate what has been detected. To find out what sensor reading or estimate is exceeding its pre-set alarm value or to find out what binary operation that has failed, is called *isolation*[1].  To isolate the fault is to find what triggered the alarm, but not necessarily to determine what caused the alarm.  The isolation task will never exceed the boundaries of the monitoring system. An example is when a pump failure is detected.  The isolation will determine what triggered the detection, which in this case could be

---

[1]In the literature, the term diagnosis is often used synonymously to isolation.

an indicator indicating whether the pump shaft is turning or not. But the status "pump not turning" is not the cause of the problem. The cause may be a loose electrical wire or clogging of the pump. It is the task of diagnosis to determine the cause. Thus, detection is limited to the numerical domain of the process system (see Figure 3.2). A general description of detection and isolation of faults can be found in Kramer and Mah (1994) or Davis *et al.* (1996).

The methods for detection must be able to process large amounts of data, collected as measurements. There are several different steps involved in detection:

- Firstly, the data have to be screened, in order to obtain good data quality. Data screening involves, for instance: noise reduction; detection and correction of outliers, *i.e.* measurements not representative for the physical process; estimation of missing values; trend removal. This is described in Chapter 4.

- Secondly, analysis of individual measurements (single variable detection) can be carried out in order to establish deviations from the normal measurement region. In addition to amplitude, location and spread, the frequency domain of the measurement signal can be analysed. Single variable detection is discussed in Chapter 5.

- Thirdly, the relations between process variables and their influence on the output or quality variables must be investigated. This must be done with methods capable of simultaneously analyse multiple variables. Multivariate analysis is discussed in Chapter 6 and examples of multivariate detection are given in Chapters 7 and 8.

The focus of this thesis is directed towards the third step, that is multivariate methods for detection. However, this does not mean that the first two steps are less important.

# Diagnosis

*Diagnosis* of a disturbance is about finding the cause-effect relationships that lead from the deviation in isolated variable/variables to the mechanism that has caused the change. Consequently, the definition of system boundaries is an important issue. The system boundaries can differ depending on who is carrying out the diagnosis analysis. For instance, if the operator can make a call to a pump repair service, the diagnosis ends at the isolation. The operator does not have know why the pump is not working. However, if the operator has to repair the pump himself, then the diagnosis must be carried a bit further until the cause of the pump breakdown is determined. Thus, the meaning of diagnosis used in this thesis is that it is primarily a qualitative task, carried out outside of the numerical domain defined by the measurement system (see Figure 3.2). This also implies that diagnosis is not suitable for complete automation. Instead the experience and interaction of man are vital for a computerised diagnosis system to perform well. The diagnosis task can be semi-automatic.

An approach to diagnosis analysis that has proven successful is graph-based diagnosis. Graph-based diagnosis implies that the causal relations are described by *nodes* and *connections* in *networks* (see Figure 3.3). A function or entity is described by a node and the mutual relations of nodes are represented by connections. Two different approaches can be distinguished. The *failure space* approach focuses on possible failures or disturbances and their propagation through the process. As the complexity of the process increases, the failure space modelling becomes difficult, as the size of the failure space grows rapidly. This is due to the almost inexhaustible source of failures or disturbances in a complex process. If instead the *success space* is modelled, the number of successful operational modes are limited and often just a few. In success space modelling the desired functions and goals of the process are modelled and every unfulfilled function or goal indicates a failure or disturbance. The success space approach results in less complex and more comprehensive cause-effect relation models of the process (Lind 1990; Larsson 1994).
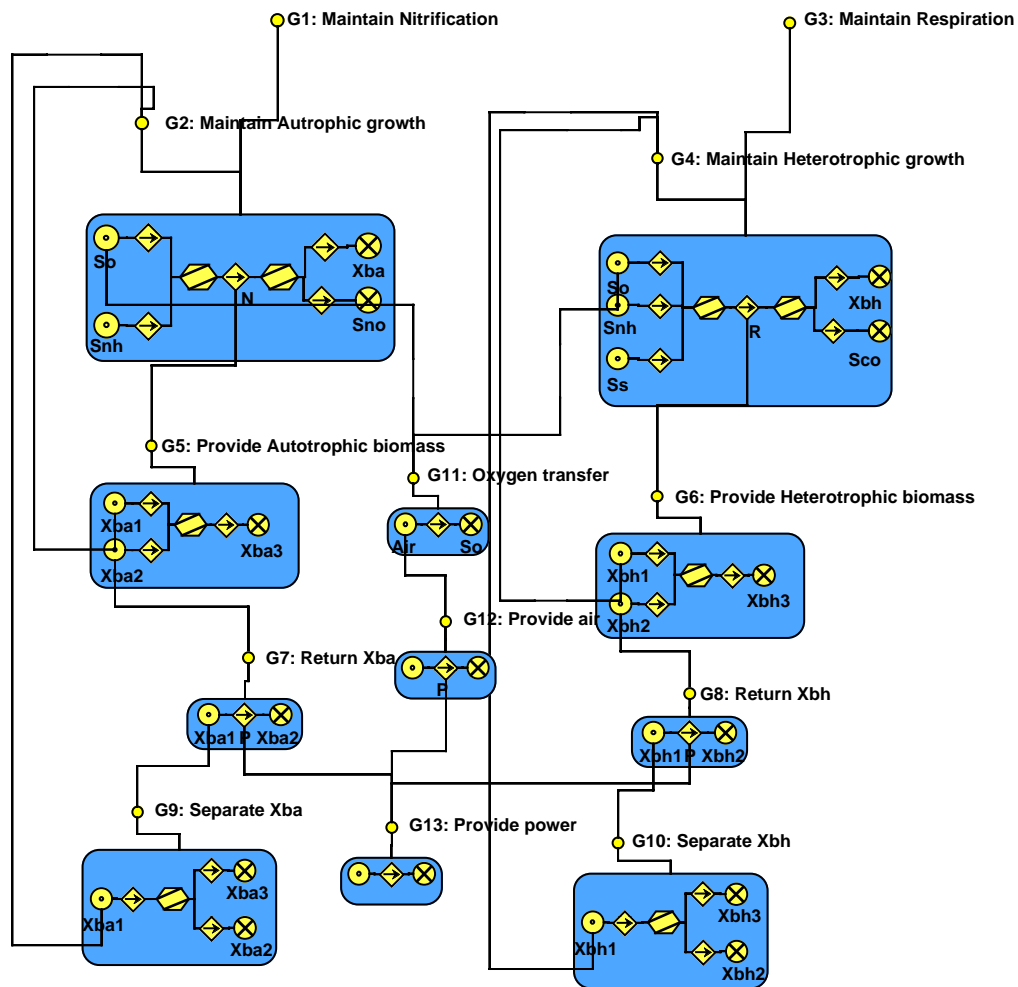
**Figure 3.3**  An example of graph-based diagnosis. A success-space representation of a wastewater treatment process. The components included are: **goals**, **functions** and **connections**. An example: goal G1 (maintain nitrification) is influenced by goal G2 (maintain autotrophic growth). Goal G2 is influenced by, *e.g.*, functions So (DO) and Snh (ammonia). Function So is influenced by goal G11 (oxygen transfer) and so on.

## Consequence Analysis

When a failure or disturbance has been detected and diagnosed, the
consequences for not yet affected parts of the process must be invest-
igated. This is important in order to take the right precautions or
activate the proper countermeasures. Consequence modelling can be
carried out on different abstraction levels. Depending on the nature
of the failure or disturbance, quantitative simulations in the numer-
ical domain can be complemented with qualitative investigations of
the cause-effect relationships. Mechanistic models based on differen-
tial equations can be used for quantitative simulations, or predictions,
whilst qualitative prediction can be achieved by shifting the chrono-
logy and using the diagnosis model "backwards". Consequence ana-
lysis can be carried out in both the symbolical and numerical domain,
depending on the desired granularity of the result.

## $D^2C$

The combination of detection, diagnosis and consequence analysis of
disturbances, faults and other deviating events form a basis for an
information extraction concept, which we call $D^2C$.

# Chapter 4

# Data Screening

This chapter emphasises the task of processing data to establish the validity and quality of data consisting of variable measurements. On-line measurements are difficult. This is due to the almost inexhaustible sources of disturbances. The sources may consist of, for instance, electromagnetic interference, hostile measuring environment, defective installation, insufficient maintenance or erroneous use and handling of the measuring system. Therefore, before any analysis of the measurements can be carried out, data screening is crucial. Corrupt measurements must be found and dealt with, so that false conclusions based on the measurements are avoided. Proper validation of data quality is essential to achieve reliable results. Corrupt data can be found and replaced/removed by different methods depending on the situation and the nature of the disturbance or fault. Computers make it possible to treat large amounts of data digitally and thereby the quality of the data increases. However, one should never forget the device: "garbage in - garbage out". Digital processing of data cannot perform miracles. Therefore, the quality disturbing factors must be kept at a minimum and maintenance and handling be performed professionally. Further reading on data screening within the field of biotechnology can be found in Hellinga *et al.* (1998).

## 4.1   Corrupt Data

In order to achieve good analysis results, the validation of the collected measurements is important. The measurement data must be representative for the investigated process. A continuous critical data validation gives information on the data quality and the condition of the measurement system. There are many different methods for data
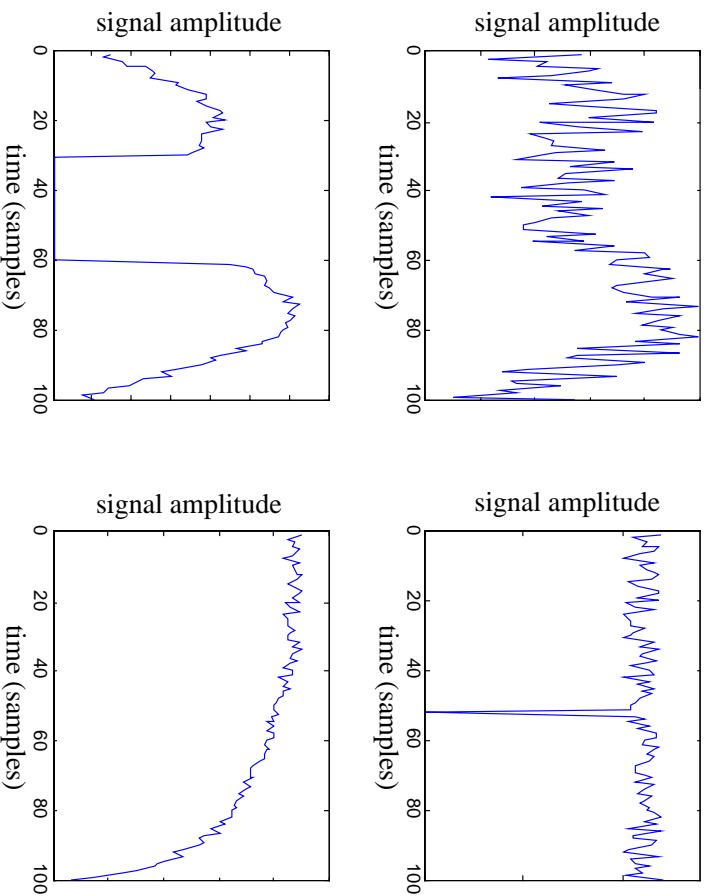
**Figure 4.1** Different types of measuring faults (artificial data). Noisy data (upper left), data with outlier (upper right), data with missing values (lower left) and data with drift (lower right).

validation ranging from logical algorithms testing the reasonableness of the measurement to more sophisticated statistics or model based methods for outlier detection. Almost every measurement series is affected by:

- noise;

- missing values;

- outliers;

- drifting measurements or trends.

Here, some useful methods for handling of corrupt data are presented. Figure 4.1 shows some examples of corrupt data.

# 4.2 Noise Attenuation

Noise - that is disturbances found in the measurement signal that do not have a physical interpretation in the actual process - is a common problem in almost every measurement system. Measurement noise is caused by electromagnetic disturbances, the design of the measuring devices, the methods used and so on, and is hard to avoid. The noise can be further amplified by incorrect installation, poor maintenance and changes in the ambient environment in which the measurement system is located. A typical example of changes in the environment is when temporary mechanical equipment or heavy electrical machinery has been located too close to the measuring device. Cleaning, calibration and exchange of worn parts are also important, in order to keep the noise level on an acceptable level.

Irregularities within the process can also be considered as noise. Process noise is the noise which cannot be explained by variations in the measurement or communication system. Process noise may be caused by inhomogeneous mixing, random variations of, for instance, air bubbles and other non-measurable causes. For noise reduction of measurement data *filters* can be applied. Depending on where in the measurement system the filters are applied, they can be either *analogue* or *digital*. Analogue filtering is commonly used in sensor devices for basic noise reduction, while digital filtering is used to achieve a wide variety of outputs in computers. Digital filters allow for a smart compromise between signal information and noise corruption. Only the basics of digital filtering will be discussed here but further reading on digital filtering can be found in, for instance, Krauss *et al.* (1994) or Proakis and Manolakis (1992).

## Digital Filtering

Digital filtering is a large discipline and only the basics for noise reduction purposes will be discussed. Digital filtering of data is almost exclusively a question of reconstructing or estimating a certain sample value based upon preceding (or succeeding) values in the same data series. As illustrated in Figure 4.2 different filters are used to achieve
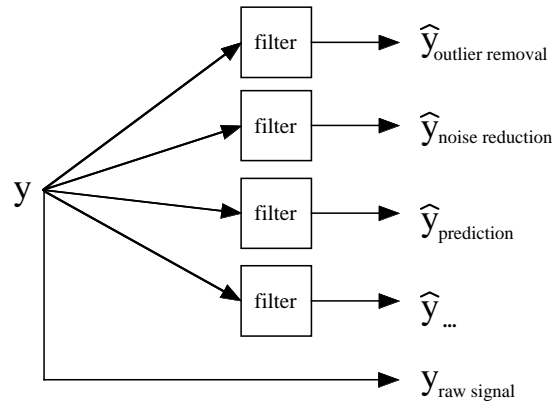
**Figure 4.2**   Different filters are used for different purposes.

signals suitable for different purposes and the resulting signals may
differ significantly depending on the filter characteristics. The digital
filters presented here are simple but effective as they are easy to im-
plement. There are more sophisticated filters, such as adaptive filters
that can be used with good result. A moving average adaptive expo-
nential (MAX) filter for wastewater applications has been proposed
by Bergh (1996). In the applications described in this thesis, median
filters are mostly used, due to their ability to preserve discontinuities
(Piovoso *et al.* 1992).

## Linear Filters

For noise reduction low-pass filters are usually used.  Measurement
noise is normally of much higher frequency than the process variations
themselves and, therefore, it is possible to filter the signal without
losing too much information. Low-pass filters allow, as the name sug-
gests, low frequencies to pass while high frequencies are removed. A
linear causal digital filter (*i.e.* a digital filter using only the present
and historic measurements to calculate the filter output) can be writ-
ten in a general form as (Olsson and Piani 1992):

$$\hat{y}(k) = -a_1\hat{y}(k-1) - a_2\hat{y}(k-2) - \ldots - a_n\hat{y}(k-n)$$
$$+ b_0 y(k) + \ldots + b_m y(k-m) \quad (4.1)$$

where $\hat{y}$ is the filtered signal and $y$ is the measurement signal. De-
pending on the choice of the parameters $a_1, \ldots, a_n, b_1, \ldots, b_m, n$ and
$m$, the filter will be given different characteristics. If at least one of

the $a$ coefficients is non-zero and only $b_0$ is non-zero, it is an autoregressive (AR) filter. This implies that the filter has an infinite impulse response (IIR), i.e. the filter has an infinite "memory". If all $a$ coefficients are equal to zero the filter is a moving average (MA) filter. The impulse response of an MA filter is finite and MA filters are sometimes called finite impulse response (FIR) filters. The combination of AR and MA filters are called ARMA filters.

MA filters are widely used as low-pass filter. The MA filter forms the weighted mean of a certain number of samples within a moving window. It can be written as:

$$\hat{y}(k) = b_0 y(k) + \ldots + b_m y(k - m) \tag{4.2}$$

where $m$ is the number of previous measurements used to calculate the filter output. If the weights (*i.e.* the $b$ parameters) are distributed equally over the samples and the sum of the weights are equal to one, then Equation 4.2 becomes:

$$\hat{y}(k) = \frac{1}{m + 1}(y(k) + \ldots + y(k - m)) \tag{4.3}$$

A major drawback of the MA filter is the delay, which if $m$ becomes large, is considerable. In off-line situations the delay can be compensated for, but in on-line situations the average delay will be $m/2$ samples.

Another simple and widely used low-pass filter is the *exponential* filter. The first-order exponential filter can be expressed as:

$$\hat{y}(k) = \alpha \hat{y}(k - 1) + (1 - \alpha)y(k) \tag{4.4}$$

where $\alpha$ has a value between 0 and 1. When $\alpha$ is close to one, the noise sensitivity of the filter is low at the expense of a large *time constant* and thus poor agreement with the signal variations. The time constant of a signal is defined as the time required to reach approximately two thirds of the final value after a step change in the filter input and is used as a measure of the filter speed. Figure 4.3 shows the effect of different $\alpha$-values on a step change. There is a time delay when using exponential filters as well, and this delay increases and becomes severe when significant noise reduction is desired. Digital filters of higher order, *i.e.* filters using more than one historic estimate to
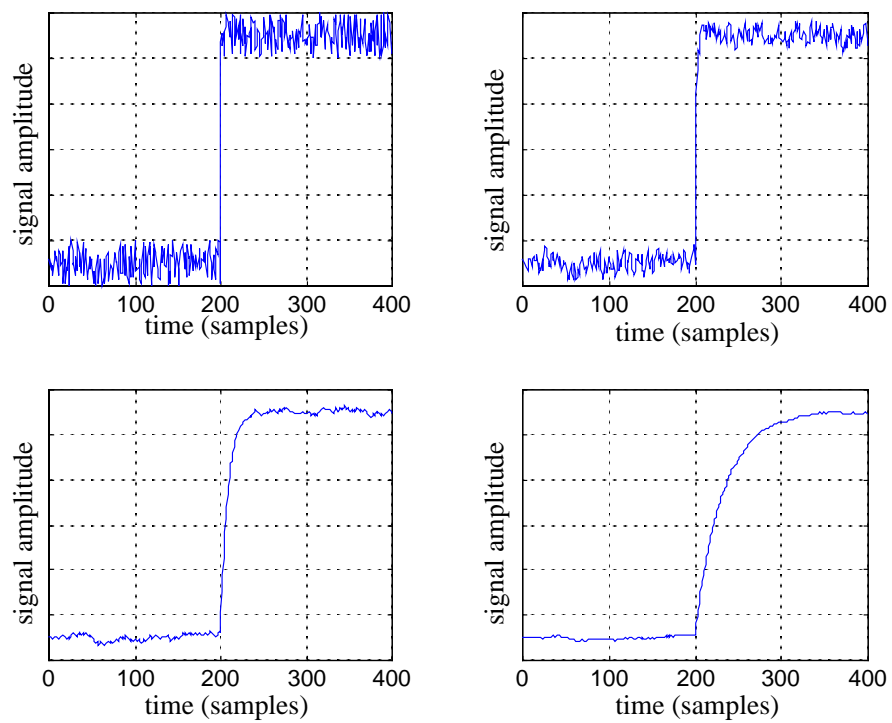
**Figure 4.3**    The effect on the noise using different $\alpha$-values: $\alpha = 0$ (upper
left),$\alpha = 0.5$ (upper right),$\alpha = 0.9$ (lower left) and $\alpha = 0.97$
(lower right) (artificial data).
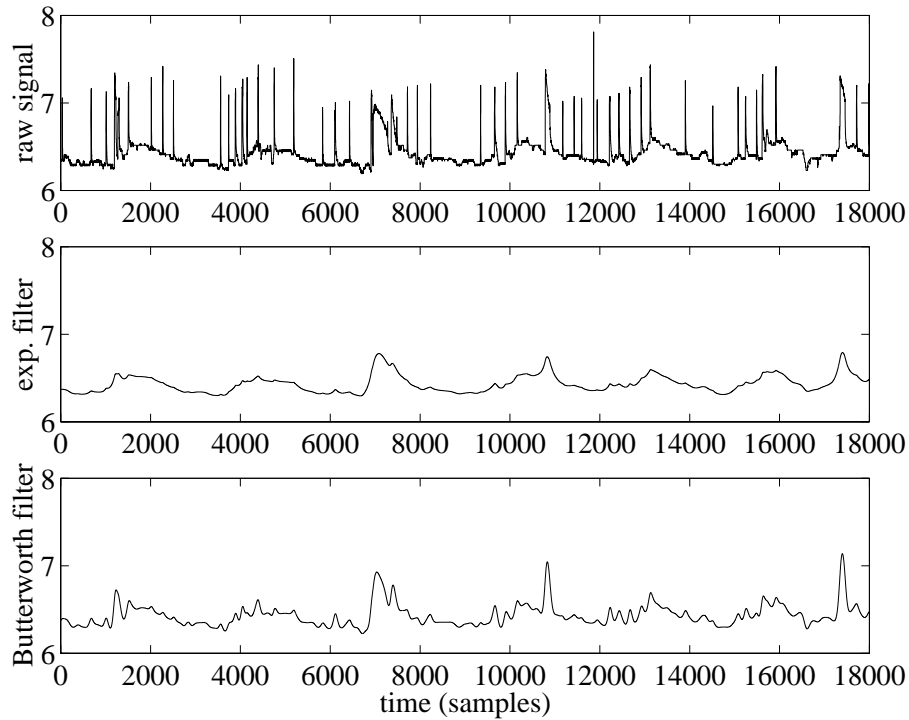
**Figure 4.4**   The original signal and the filter output from an exponential
filter and a Butterworth filter of the eighth order (Real pH
measurements from a direct precipitation plant).

calculate the output, compensate for this to some extent, but there
will always be a compromise between noise reduction and time lag.
In off-line situations, where the filter does not have to be causal, it is
possible to achieve high noise reduction with no time lag. In Figure
4.4, the original signal, the output from a first order exponential filter
and a higher order Butterworth (Krauss *et al.* 1994) filter are shown.
The time constants of the exponential and the Butterworth filters are
approximately the same.

## Median Filters

A completely different filter not based upon Equation 4.1 is the median
filter. A median filter is simply a moving time window in which the
median of the samples is equal to the output.

$$\hat{y}(k) = median(y(k), y(k-1), \ldots, y(k-l)) \qquad (4.5)$$

The median is the middle measurement if the measurements are sorted in descending or ascending order:

$$median(\mathbf{y}) = y(i), \quad i = \frac{1}{2}(m+1) \tag{4.6}$$

if $m$ is an odd number and

$$median(\mathbf{y}) = \frac{y(i) + y(i+1)}{2}, \quad i = \frac{1}{2}m \tag{4.7}$$

if $m$ is an even number. The median filter in Equation 4.5 is causal, but non-causal filters can also be constructed. Median filters can be used for coarse and fast removal of outliers if their duration is shorter that half the filter length (*i.e.* the number of points used to calculate the filter output). Another appealing feature of the median filter is that it does not smooth the shape of a step change. The noise reduction achieved by a median filter is limited, unless a large time window is used and the output is constructed from numerous samples. Causal median filters also introduce a time delay, for which it is possible to compensate in off-line (non-causal) situations. Figure 4.5 shows the output of a median filter when a step change and a few single outliers are introduced. Notice the difference in time lag between the causal 20 samples median filter in (c) and the non-causal 20 samples median filter in (d). An extended form of the median filter is the *FIR Median Hybrid* (FMH) filter. The FMH filter is a filter algorithm for obtaining steady state values from noisy data (Piovoso *et al.* 1992). The FMH filter can be described as:

$$\hat{y}_{FMH,l}(k) = median(\frac{1}{l}\sum_{i=k-l}^{k-1} y(i), \, y(k), \, \frac{1}{l}\sum_{i=k+1}^{k+l} y(i)) \tag{4.8}$$

This means that the filter output is the median of three estimates of $y(k)$: the average of $l$ previous values, $y(k)$ itself and the average of $l$ future values. The filter is obviously not causal and ,therefore, only applicable in off-line situations. The length of $l$ is used to give the filter different characteristics. The filter can be applied iteratively with better noise reduction as a result.

**Figure 4.5** The median filter based on $n$ number of samples, $n = 1$ (upper left),$n = 3$ (upper right),$n = 20$ (lower left) and $n = 20$ (non-causal) (lower right) (artificial data).

# 4.3    Outliers and Missing Values
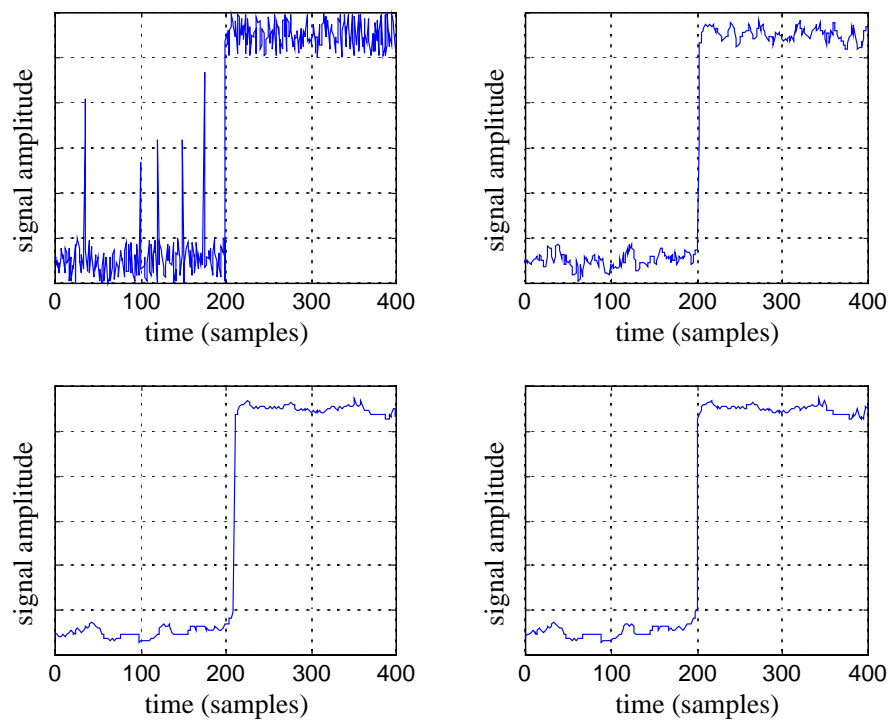
An outlier - that is a sample value that differs notably from the mean of the measurement series - can be caused by many factors. A problem in detecting outliers is to decide whether they represent a true value or whether they are false and, consequently, caused by a disturbance in the measurement system. In order to ensure the validity of data, outliers must be removed or replaced, depending on the requirements of the analysis. Removing the outlier and, consequently, the complete sample is straightforward, but is only recommendable if the amount of data is sufficient and if the analysis does not take dynamics into consideration. On the other hand, replacing outliers is difficult if no redundant information is available.  Removing/replacing outliers is similar to the task of replacing missing values. In static analysis the sample, including all variables, can be removed if no data are available. In dynamic analysis such an approach may distort the dynamic properties of the data.

## Outlier Detection

Algorithms for detection of outliers based on the statistical properties of the measurements can be found in the literature, for instance in Barnett and Lewis (1994). Detection of outliers can also be handled by using redundant sensors or digital filtering (Åström and Wittenmark 1997). However, one must be careful when dealing with outliers. A highly unexpected value may sometimes be both true and significant (Bergh 1996). The difficulties in discerning outliers make it important that the number of outliers caused by poor maintenance of the measurement system is kept at a minimum. The task of detecting outliers has a lot in common with disturbance detection in general, which will be described in Chapters 6, 7 and 8.

### Manual Detection of Outliers

A straightforward method for off-line detection of outliers is to manually remove outliers. In time series, the human eye has a remarkable

ability to pick out outliers with good result. By a careful investigation of the time series in combination with experience of the process, the manual detection and replacement of outliers can be as good as any automatic method. This is, however, a very time consuming task and can only be performed off-line. In on-line situations an automatic algorithm must replace the human eye. When preparing data for model identification or training, manual detection of outliers is sometime preferable. It gives the model builder a sense for the data and also of what can be expected from the model. Manual detection and replacement of outliers involves a great deal of subjectivity and the result will depend on who is performing the task.

## Detection of Outliers Using Redundant Sensors

Redundant sensors are useful for outlier detection. If two redundant sensors are used, then an indication of an outlier is achieved when the sensors do not deliver the same value (within an reasonable margin). An alarm can inform the operators that something is wrong with one of the sensors (not telling which one) and then a calibration procedure can be initiated. The information from the combined sensors is then the measurement value or an alarm. If the measured variable is of high importance, three redundant sensors can be used. The measurement is then considered true when two out of three sensors display the same value. A simple logic algorithm can be applied to supply the measurement system with the accepted value and alarm the operator if none of the sensors display the same value. However, direct redundance is expensive as it demands a large number of sensors and are seldom used unless in situations where extremely high reliability is required, *e.g.* in operation of nuclear power plants. In many wastewater treatment plants, the wastewater is treated in parallel lines, which gives a possibility to use measurements from another line to make a validity check. The conditions are rarely exactly the same but if the configurations do not differ significantly the information from such a validation can be used together with other methods for outlier detection.

**Other Methods for Detection of Outliers**

The effect of an outlier on a time series model can be analysed in order to detect outliers in the data series. Other statistics based detection techniques of outliers can also be used, but are not discussed here. However, some aspects of residual based detection in association with multivariate analysis are discussed in Chapter 6. The reader is referred to, for instance, Johansson (1993) or Söderström and Stoica (1989) for time series analysis and to Barnett and Lewis (1994), for outlier detection in statistical data.

# Missing Values

A missing value is caused by a sensor that does not deliver a measurement value, which makes the sample incomplete. Depending on the measuring equipment, missing values can appear as, for instance, blanks, zeros or negative values for entities limited to positive values. Therefore, missing values are often simple to detect. Some measuring equipments have the capability to perform a test on the reasonableness of the measurement. If the actual value does not pass the test, the result may be a missing value.

Missing values are a serious problem as they distort the dynamic properties of the signal. In order to perform a dynamic analysis the value must be estimated in different ways depending on the signal and the type of analysis. Especially when multivariate analysis is considered, a missing value is problematic, as it makes the complete sample difficult to use. However, when multivariate models are used, there are good possibilities to accurately estimate a missing value from other variables.

Longer time periods of missing values are often impossible to recreate, and this makes the data unusable. Missing values may lead to severe problems, while some dynamic analyses demand long periods of good and reliable data. Therefore, it is important that the number of missing values are kept at a minimum and when the situation occurs, immediate actions are taken to eliminate the problem.

## Replacing Outliers and Missing Values

When the occurrence of an outlier or a missing value has been established, the replacement can be done in many ways. Interpolation can be carried out in an off-line situation and the simplest form of interpolation is:

$$y(k) = 0.5[y(k-1) + y(k+1)] \qquad (4.9)$$

where $y(k)$ is the replacement value for an outlier or a missing value. This is normally sufficient when the problem only occurs during one sample. If there are several successive outliers, the interpolation can be done in a more sophisticated way by using, for example, spline techniques (MathWorks 1996). In on-line situations interpolation is not possible. Extrapolation using the preceding value such as:

$$y(k) = y(k-1) \qquad (4.10)$$

is simple and often accurate enough when the number of succeeding outliers or missing values are few. If there are long periods of missing values or outliers, the difficulty increases and normally the information must be considered lost. Figure 4.6 illustrates the different methods. If a model has been used either to detect the outliers or is run in parallel with the process the estimate from the model can be used, *i.e.*:

$$y(k) = \hat{y}(k|k-1) \qquad (4.11)$$

where $\hat{y}$ is the model output at time $k$, based on measurements up to time $k-1$. If the model is a time series model, the use is limited, but if the model is based upon other measurements than the signal of interest, the estimate can be used for shorter periods. The accuracy of the estimate depends on how good the model is and how long the period of missing values extends.
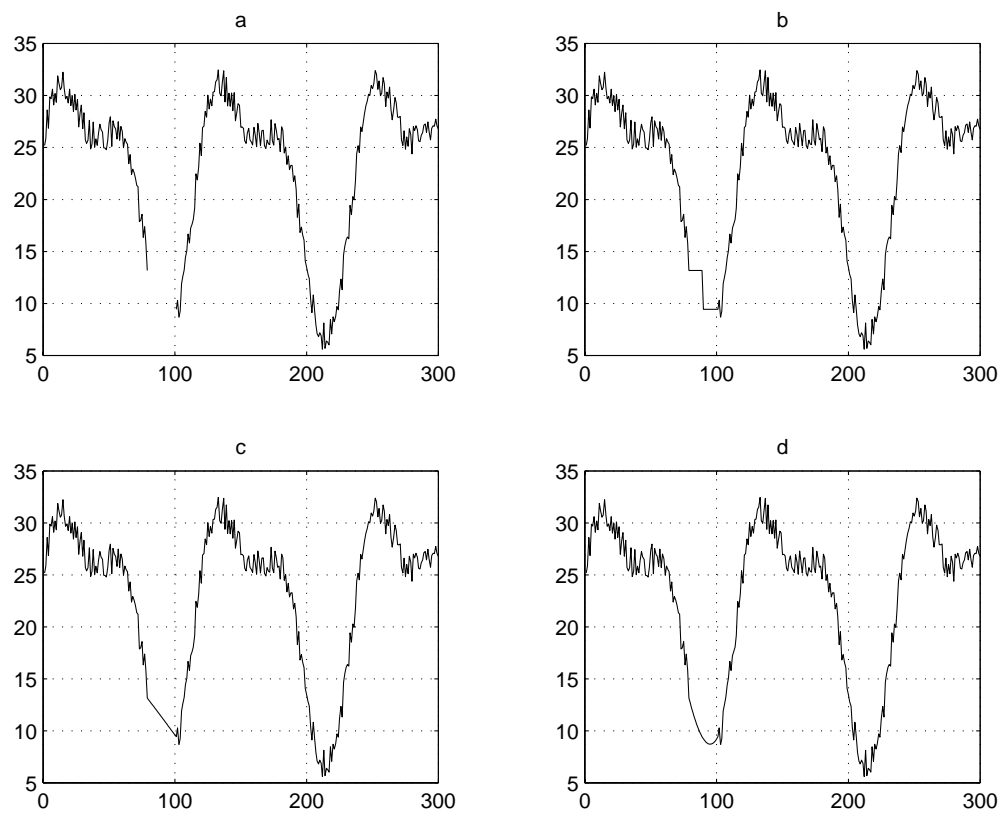
**Figure 4.6**    Original signal(a), interpolation using nearest neighbour (b), linear interpolation (c) and interpolation with splines (d).

# 4.4 Detection of Drifting Measurements

Handling of drifting measurements involves three important elements:

- detecting the slow change;

- establishing whether it is caused by a drifting sensor or if it describes a true change in the variable;

- if necessary make corrections.

In addition to the misleading information, drifting measurements can distort the mutual relations between measurement variables and make multivariate analysis difficult. Therefore, it is important to detect drift in data and to establish whether the drift describes a true variable change or a deteriorating performance of a sensor.

## Detection

Detection of slowly drifting measurement series is basically the same as detecting trends. Consequently, the same techniques can be used and they are discussed in Chapter 5.

## Establishing Cause

It is not possible to establish whether a change is caused by a true process change or a drifting sensor without some additional information. This information can naturally be achieved if redundant sensors are available. When this is not the case, an experienced operator may be able to determine the state of the problem. However, multivariate analysis can be a helpful tool in establishing the cause of a drifting sensor. By looking at other variables and their mutual relationships with regards to the investigated variable, the probable cause may be determined. This is discussed further in Chapters 6, 7 and 8.

## Correcting Data

If a drifting sensor has been detected, the first step is to make corrections of the measurement system, *i.e.* calibration or cleaning of the sensor. However, the data collected can be used if the drift is compensated for. This can be done by simply subtracting (or adding) the slope of the change to the data series. In this way drifting data can still be used for model building or off-line evaluation of the investigated time period.

# 4.5 Preparing Data for Analysis

In addition to the screening mentioned above, different analysis methods may require further preparation of data to be effective. Such preparation may include, for example, mean centring, scaling and weighting of variables. *Mean centring*, *i.e.* subtracting the variable by its average, is a way to make calculations easier and is useful in both single and multivariate analyses. Scaling is important to obtain comparable variables, especially when the analysis is based on comparison of variables. In single variable analysis, the scaling becomes less important.

## Standard Manipulation

Standard manipulation is performed to make it possible to compare variables with different amplitudes and variances. It normally involves scaling and mean centring of the data. Scaling is done to ensure that the variables are comparable, independently of the absolute value of the variable. For example, if one variable is varying between 0.1 and 1 and another one is varying between 100 and 110, then the second variable would be much more influential than the first one if they were not scaled properly. The information content of changes in the second variable is not evidently greater than the information content of the first variable. A rule of thumb in this matter is to scale each variable to unit variance, that is divide each variable data by its standard deviation value. Autoscaling is a simple way to scale the data. It implies
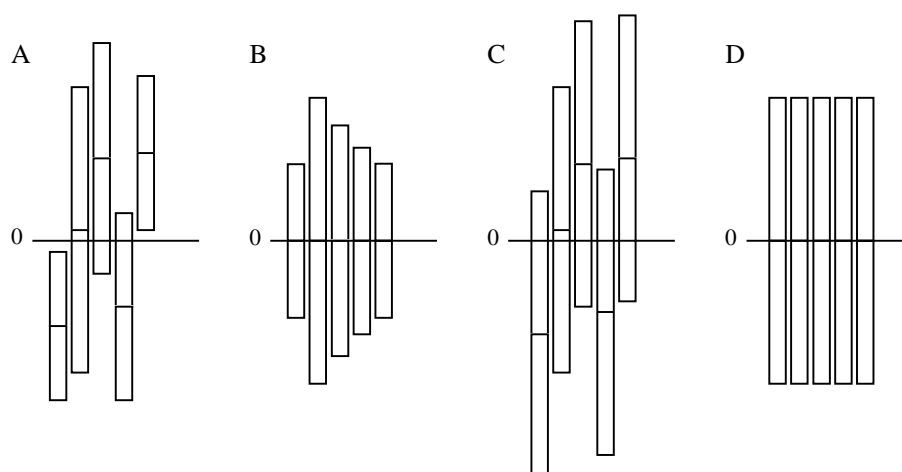
**Figure 4.7**   Data pre-processing. The data for each variable are represented
by a variance bar and its center. Unmanipulated data (A),
mean centred data (B), variance scaled data (C) and mean
centred and variance scaled data, *i.e.* autoscaling (D) (Geladi
and Kowalski 1986).

unit variance and mean centring, *i.e.* the data is adjusted to have zero
mean by subtracting the mean value from the variable data. Figure
4.7 illustrates some of the differences in scaling and centring. How-
ever, a word of caution is justified when dealing with almost constant
variables with a low signal-to-noise ratio. If such a signal is scaled
to unit variance, the noise contribution to the variability will be high
(Kresta *et al.* 1991). The problem can be reduced by digital filtering
before scaling or by a different scaling method.

## Non-linear Manipulation of Data

There are situations where it may be wise to scale the variables in a
different manner. A typical situation is when the variable is gener-
ated by highly non-linear devices. For example, valve measurements
are often expressed in percentage opening. This is a non-linear meas-
urement, as the flow rate through the valve does not depend linearly
on the percentage opening. Changes in a valve position close to fully
open will generate smaller changes in the flow rate than a change by
the same amount in a position, for instance, at half closed. The non-
linearity of a device can be partly compensated for by simply raising
the variable to a desired power. The manipulation, *e.g.* $y_{new} = y^2$ or

$y_{new} = y^{\frac{1}{2}}$, is done prior to scaling and mean centring.

A second situation where it can be useful not to use standard scaling is when it has been empirically or theoretically established that a certain variable has a significant influence on the process. In this case it is possible to scale this variable in such a way that its variance is slightly greater than unit variance and, consequently, the variable will have a stronger influence on a model describing the process.

# Chapter 5

# Single Variable Detection

In this chapter methods to extract information from single measurement variables are presented. Detection of deviations in single measurements time series can be carried out both in the time domain and the frequency domain. Time domain detection involves signal amplitude, mean and variance. Frequency domain detection is based on changes in the measurement signal frequency.

## 5.1 Monitoring Measurement Variables

Monitoring single variables is perhaps the most basic way to obtain information from measurements. The monitoring can be performed at various complexity levels, but all monitoring normally utilise basic statistical features such as location and spread.

### Basic Statistical Features

In order to extract information from measurement signals the basic properties of the signal must be recognised. Each individual signal can be analysed with respect to a number of characteristic features:

- amplitude;

- center of location;

- spread.

## Amplitude

The amplitude is the basic information content of the measurement. Usually, a normal range with high and low limits is defined in order to make qualitative comparisons.

## Mean and Median

The *arithmetic mean* or just *mean* is the most basic statistical feature of a signal. The mean is used in many statistical analyses and is expressed by:

$$mean(\mathbf{y}) = \frac{1}{m} \sum_{k=1}^{m} y(k) \tag{5.1}$$

A second useful measure of the center of location is the *median*. As described in Chapter 4, the median is the middle measurement if the measurements are sorted in descending or ascending order:

$$median(\mathbf{y}) = y_i, \quad i = \frac{1}{2}(m+1) \tag{5.2}$$

if $m$ is a odd number and:

$$median(\mathbf{y}) = \frac{y(i) + y(i+1)}{2}, \quad i = \frac{1}{2}m \tag{5.3}$$

if $m$ is an even number of measurements in the data set. If the measurements are symmetrically spread and there are no outliers, the mean and the median agree well. However, if there are outliers present the results can differ significantly. The median is unaffected by single outlying values and, thus, a more robust measure of the center of location. In order to make the mean measurement more robust, the *trimmed mean* can be used. As the denotation indicates, trimmed mean implies that some of the largest and smallest measurements are removed prior to the calculation (Chapman 1992).

## Spread Measures

The variability of a measurement series can be expressed by its *standard deviation*. The standard deviation of $m$ independent samples is

estimated by:

$$\sigma = \sqrt{\sum_{k=1}^{m} \frac{(y(k) - mean(\mathbf{y}))^2}{m-1}} \qquad (5.4)$$

Sometimes it is more convenient to use the square of $\sigma$. This gives the estimated variance: the *variance*.

$$\sigma^2 = \sum_{k=1}^{m} \frac{(y(k) - mean(\mathbf{y}))^2}{m-1} \qquad (5.5)$$

Standard deviation as presented above can be used as a measure on the spread if the measurements are normally distributed. If this is not the case, other measures can be used to describe the spread.

A simple and intuitive measure of spread is the *range* (R). This is simply the distance between the largest and smallest value in the data set. The range can also be calculated as the *interquartile range* (IQR). The IQR is the distance between the 0.75 and 0.25 *quantile*. A quantile corresponds to the value below which a certain percentage of the data set is located. Thus, the 0.90 quantile is larger than 90 percent of the data. This implies that the 0.50 quantile is the same as the median, *i.e.* the middle value in a data series. The calculation of quantiles is based on the rank of the measurements, that is the measurements are sorted in ascending order. The smallest value gets rank $r = 1$ and the largest value gets rank $r = m$ ($m$ is the number of values in the data series). The corresponding fracture can be calculated as (Chapman 1992):

$$f_i = \frac{r - \frac{1}{2}}{m} \qquad (5.6)$$

From the fractures quantiles can be calculated. Range and quantile are often referred to as *non-parametric* measures.

# Charts and Plots

The most straightforward type of plot technique is time series plots. In time series plots the individual measurement is plotted on the y-axis and time on the x-axis. This is an intuitive way of presenting the variable state and an example of *time series plots* has already been shown in Figure 4.4. Typical ways to present different aspects of the measurement signal are, for instance:

- raw measurement signal;

- filtered measurement signal;

- cumulative sum of the measurement signal.

The evaluation of the measurements is done by using control and alarm limits, indicating normal and abnormal ranges for the measurement variable.

## Alarm Limits

In order to decide when a variable is inside its normal range, adequate limits must be determined. In the process industry it is common with two types of limits: *warning limits* and *actions limits*. Warning limits do not call for immediate action. Instead the purpose is to warn the operator that the measurement variable may be drifting away. If a variable exceeds an action limit, there is need for action in order to bring the variable back into the normal range. For the detection purposes, *alarm limits* are used. A violation of an alarm limit triggers a detection alarm. The limits may be derived from a previous period when the process is operating in a desired manner or when the product quality is acceptable. They can also be derived from a desired target value, from which the process variable should not deviate significantly. If the measurements are normally distributed, the measurement mean plus two and three standard deviations are a common choice for upper warning and action limits, respectively, while the mean minus two and three standard deviations define the lower limits.

However, if the normal distribution is not applicable, there may be ways around this problem by transformation of data to an approxim-

ately normal distribution. A usable transformation for this purpose is the logarithm of the measurement. Measurements from wastewater treatment plants not seldom tend to be more log-normal than normal distributed (Chapman 1992). If a transformation is not possible then the normal distribution constraint can be avoided by using non-parametric methods. Non-parametric methods do not make any assumptions about the shape of the distribution from which the data are taken (Miller and Miller 1993).

In some cases the limits can be derived from physical limitations. For example, the upper level of a tank is limited by its height (and a safety margin). Empirical information and desired targets may also be the basis for decision of limits.

## Alarm and Detection Rules

When a limit is exceeded, it must be decided whether it is a true disturbance situation or simply a false alarm. To determine this, a set of rules can be worked out. Depending on the monitored variable and the use of limits, the rules will have different appearances. In addition to violation of the action or detection limit, rules for more than one consecutive sample above (or below) the warning limit can trigger an alarm or detection. More sophisticated rules, such as more than a certain number of consecutive samples on the same side of the target value or more than a certain number of samples above (or below) the warning limits within a specified time range (or sample range), is discussed by Bissel (1994).

## Statistical Process Control

Monitoring process operation in time series is often referred to as *statistical process control* (SPC). The first ideas of SPC for quality improvement go back as far as to the beginning of the century when, for instance, Vilfredo Pareto and Walter Shewart made some important contributions to SPC (Thompson and Koronacki 1993). The ideas were further developed during the 1950s, but it is not until the 1970s that SPC has become a standard tool for quality improvement in the

process industry. SPC involves many methods for monitoring and presenting measurement variables, but perhaps the most common ones are:

- 'x'-charts, that is measurement values plotted against the time;

- MA charts, *i.e.* a moving average of the measurement series plotted against time;

- EWMA charts, that is exponentially weighted moving average filtered measurements;

- CUSUM charts, cumulative sum of the difference between the measurement and a target value.

These methods have great similarities to conventional signal processing techniques. There are many references to SPC in the literature, such as Bissel (1994), Thompson and Koronacki (1993) and Box and Luceno (1997). SPC in wastewater treatment applications is described in Chapman (1992). In this thesis, only some basic aspects of SPC is discussed.

# 5.2  Detection in the Time Domain

Feature extraction in the time domain can be carried out in many ways, but the most basic information can be found by analysing a signal with respect to location, spread, rate of change and slow variations or trends.

## Monitoring the Value

As mentioned earlier in this chapter, the actual value must be compared with a reference value to be informative. Ideally, the limits can be defined by an experienced operator. However, this is a time consuming effort since it implies a continuous update of every measured variable as the conditions in the process change. One method is to use constant limits calculated from the spread of the measurement variable during a period of normal operation. A second way is
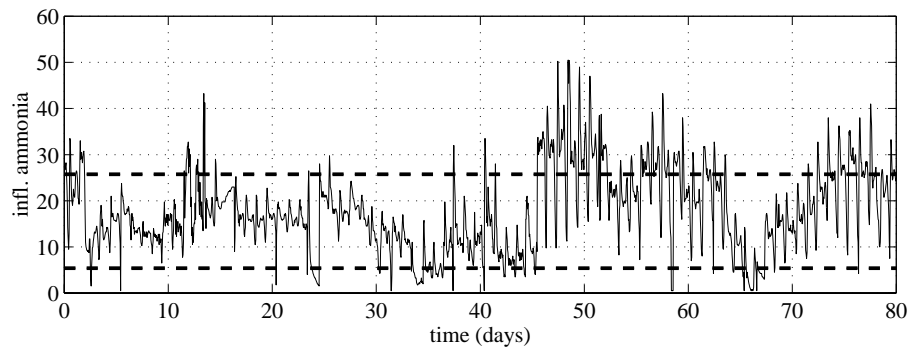
**Figure 5.1** Monitoring the location of influent ammonia concentration with constant limits based on the 0.01 and 0.99 quantiles of normal operating conditions, respectively (real data from the Ronneby wastewater treatment plant).

to let the computer calculate limits from a historic moving window. The limits are continuously updated and thus adapted to the actual situation. Depending on the purpose of the detection, the adequate choice of detection limits may differ. If the main objective is to keep the level below or within specific limits, constant limits based upon desired levels are used. On the other hand, if the purpose is to detect relative changes then adapting limits are normally more efficient. Influent ammonia measurements from the Ronneby wastewater plant are investigated. It is established that the data cannot be considered as normally distributed. In Figure 5.1, a constant limit, based on 3 weeks of normal operation, is used as the detection limit for influent ammonia. Peaks in the influent ammonia concentration are easily detected and so are major decreases. However, the number of triggered detections are increasing when the process conditions change. From day 45 and onwards deviating measurements are constantly detected. Figure 5.2 shows monitoring of influent ammonia concentration with adapting limits. Even though the limits adapt to the changing conditions, major increases or decreases are detected. But instead of continuously triggering the detection, the limits adapt to the new situation. The detection limits are based on the 0.01 and 0.99 quantiles of the previous 14 days of data.

Instead of using the 0.01 and 0.99 quantiles, the IQR of previous data can be used. The limits are then calculated as the $median \pm f\,IQR$ where $f$ is typically in the range of 2 to 3. When the distribution
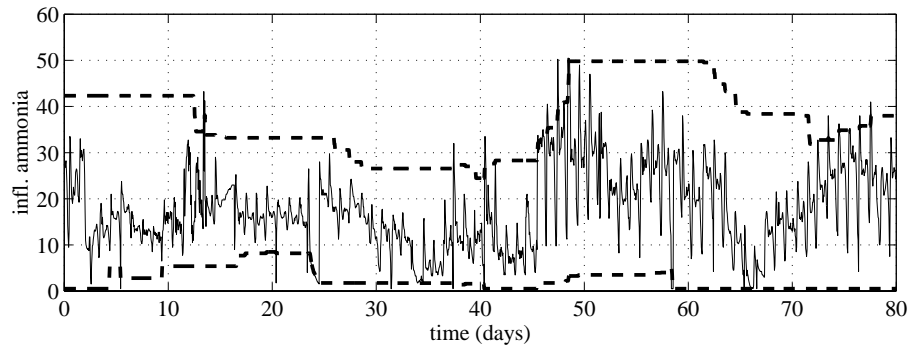
**Figure 5.2**    Monitoring the location of influent ammonia concentration
with adapting detection limits based on 0.01 and 0.99 quantiles
of the last 14 days of data (real data from the Ronneby
wastewater treatment plant).

of deviating values are distorted, the direction of detection may be
taken into consideration.  Kanaya *et al.* (1996) use a factor times
the difference between the 0.75 and 0.50 quantiles of a previous day's
data to calculate the upper limit.  The lower limit is, consequently,
calculated as a factor times the difference between the 0.50 and 0.25
quantiles of the same previous data.

## Monitoring the Spread

The spread or variability of a signal may reveal information on process
stability or sensor performance.  A sensor exposed to a disturbance
may show an increase of the noise level of the measurement signal.
An increase of the noise level will add variance to the signal in the
frequencies dominated by the noise. By monitoring the signal variance,
a disturbance of this type can be detected. One way of monitoring the
measurement signal variance is to calculate the variance of a moving
window from a certain number of measurement samples.  However,
it may be necessary to high-pass filter the signal before the variance
calculation can be performed.  This is done in order to remove the
slow variations (in comparison with the noise variation) caused by
process changes, since this will distort the variance calculations.  In
Figure 5.3 (top) a measurement signal is displayed. It can be observed
that the noise level increases significantly at sample 480. This may be
an indication that something has happened to the measuring device.
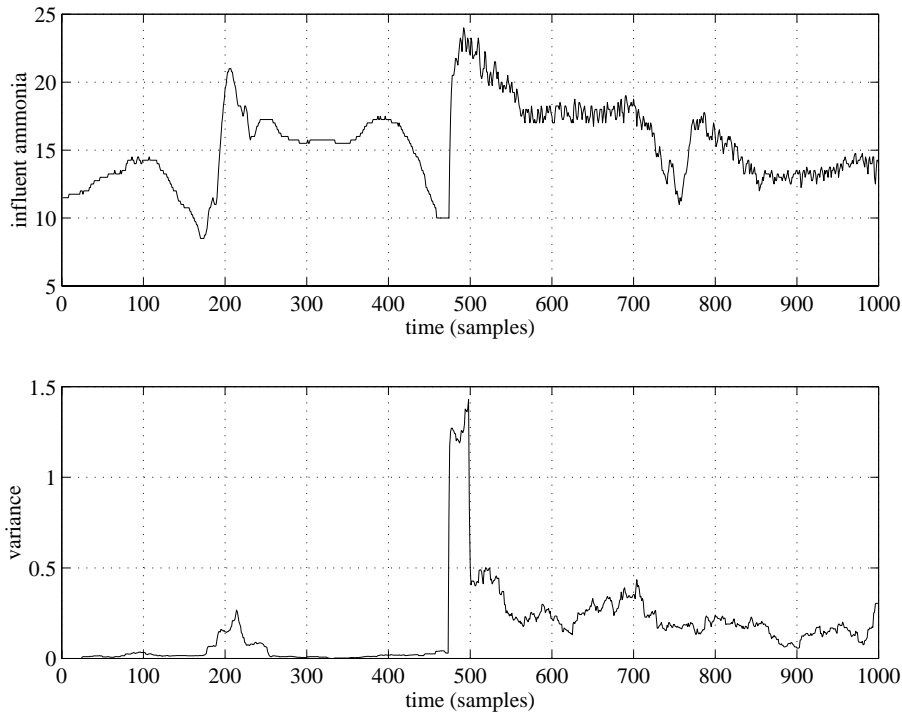
**Figure 5.3**  Influent ammonia measurement signal (top) and the variance of the high-pass filtered measurement signal (bottom).

A moving window of 24 samples is used to calculate the variance. Here, 24 samples correspond to 2 hours of continuous sampling. The variance of the inter-sample difference (a difference builder used as high-pass filter) is calculated for every sample and can be viewed in Figure 5.3 (bottom). There is a sudden increase in the variance at sample 480. The peak is caused by the large intersample distance when the amplitude increases quickly, but the variance level is kept at a high level and is easily detected.

In order to detect changes in the variance, the noise of the measurement must not be removed during the data screening phase, since it is the noise that is the important information. However, outliers and missing values must still be dealt with. This emphasises the need for different data-screening methods for different types of analyses.

## Rate of Change Monitoring

The rate of change or the derivative of a measurement signal will provide information on some of the dynamic properties of the signal.

The rate of change is calculated in its simplest way with a difference builder expressed by (Olsson and Piani 1992):

$$\hat{y}(k) = \Delta y(k) = y(k) - y(k-1) \tag{5.7}$$

which is a special case of the general high-pass filter.

## Trend Detection

Recognising trends in data series is important to understand the long term variations or tendencies of the process. By trends we mean signal changes with time constants in the range of days, or more likely weeks, months and even years. Trends are normally not recognisable if only a day or a few days are considered in the analysis or monitoring task.

Trends in time series do not display a specific point in the time series that is easily detected. This makes it hard to detect drifting measurements and, consequently, a drift may continue for a long time before it is detected. For this reason the damage may become severe and be costly in terms of quality and economics. In varying conditions, a limit of the amplitude of the signal is not applicable. Instead, the long-term trend must be addressed. Two ways of accomplishing this are slope fitting and cumulative residuals.

### Slope Fitting

By identifying the slope of the long-term changes in measurements, trends can be detected. For mean-centred data the slope can be found by the *least squares method*, that is:

$$\mathbf{y} = b\mathbf{x} \tag{5.8}$$

where $b$ is defined by

$$b = (\mathbf{x}^T\mathbf{x})^{-1}\mathbf{x}^T\mathbf{y} \tag{5.9}$$

This can be done on not mean-centred data as well, but since we are only interested in the slope, mean centring is convenient. Monitoring the slope of a signal over a longer period of time can give us some indication of how the variable changes. Deviating slope values can be
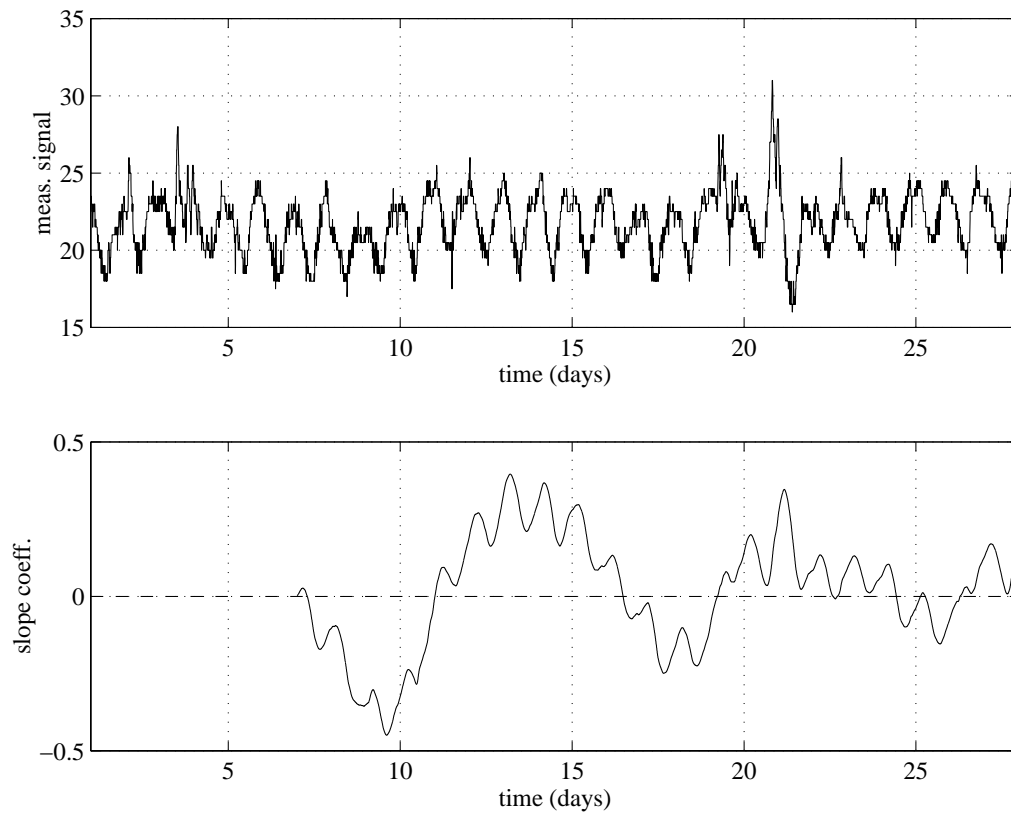
**Figure 5.4** A measurement signal (top) and the slope coefficient of the last week's data.

a criterion for detection. Figure 5.4 (top) shows a signal which varies slowly during 28 days. Below, the slope of the preceding week's data is shown. This means that the slope $b$ is calculated from a moving window of a length of one week. As a new sample is obtained, the slope is calculated again and the result can be plotted as a time series. It is clear that the data display some slow variations or trends.
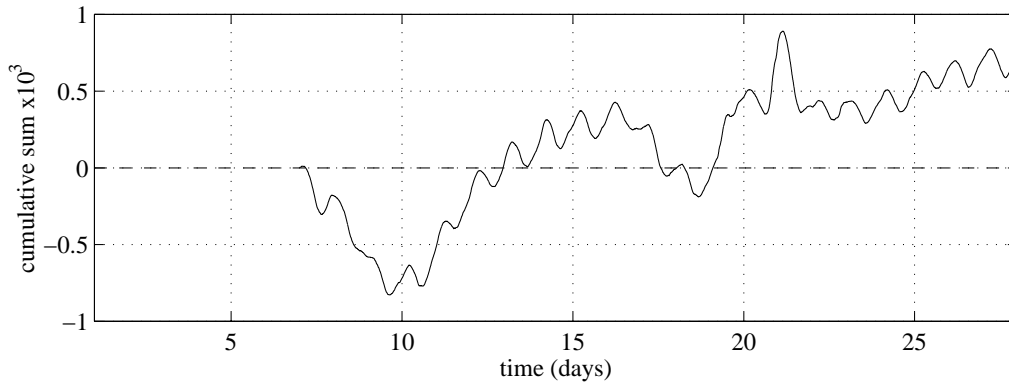
**Figure 5.5**   Cumulative residual between the present sample and a mean
of the preceding week.

## Cumulative Residuals

Plotting the cumulative residual between the measurement and a target value, may reveal a long-term trend in the signal, which is difficult to detect manually. The target value can be one out of several choices. Some examples are:

- set-point value where the process is known to perform well;

- long-term mean of the signal;

- predicted or forecasted value of the signal.

The absolute value depends on when the summation was started and may, therefore, look completely different depending on the start time. Instead, the important criterion for detection in a cumulative residual plot is the change within a certain time window. In Figure 5.5, the cumulative sum of the residual between the signal, shown in Figure 5.4 (top), and a mean of the preceding week (2016 samples), is presented. It can be seen that there is an increasing trend and especially the period between day 10 and 14 displays a significant increase.

# 5.3   Feature Extraction in the Frequency Domain

In this section, a few examples of how information can be obtained by investigating the frequency domain, are shown.  The intention is not to provide an exhaustive discussion about frequency analysis but rather to show that there may be potential tools for disturbance or fault detection purposes.

## Spectral Analysis

The underlying theory of frequency analysis is beyond the scope of this thesis, but a short description of the basic components are described below.  Estimation of the frequency content of digital signals is based on the *discrete Fourier transform* (DFT). DFT is defined as (Johansson 1993):

$$Y(f) = \sum_{k=0}^{m-1} y(k)e^{-i2\pi f k} \tag{5.10}$$

where $m$ is the number of samples in the data series and the frequency $f$ is:

$$f = -\frac{1}{2}f_s, \ \ldots, \ \frac{1}{2}f_s \tag{5.11}$$

The frequency $f_s$ corresponds to the sampling frequency.  The estimated *spectral density* of a signal can expressed by the *periodogram*:

$$R_{per}^* = \frac{1}{m}\left|Y(f)\right|^2 \tag{5.12}$$

There are ways to improve the estimated spectral density.  One way is to divide the time series into several time intervals and then calculate the mean of all periodograms.  The length of the time interval determines the resolution in frequencies.  Thus, if high resolution is needed, then the time series must be long.  There are more sophisticated ways to improve the estimate but the reader is referred to text books in the field.  However, methods for frequency analysis are available in most computer packages for numerical computing and the study presented below is based on functions available in MATLAB.
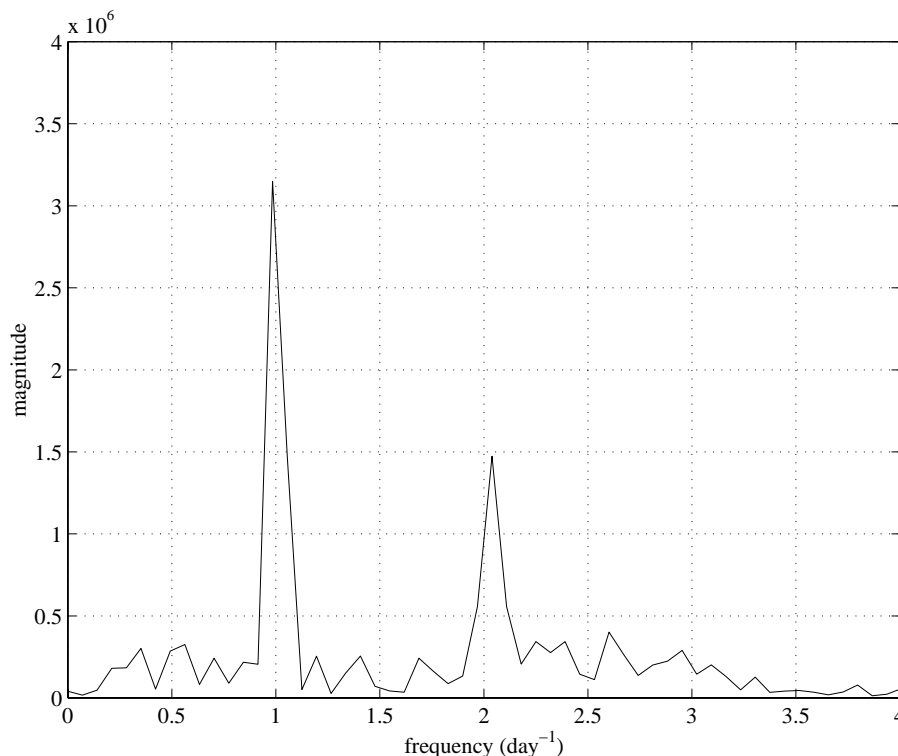
**Figure 5.6**   The periodogram for influent flow rate measurements. Two dominant frequencies can be discerned at one and two per day.

## Off-line Frequency Analysis

Most signals display more or less periodic variations. However it is not always obvious to determine the frequencies of the variations, especially not when there are many frequencies present. This is due to the fact that some frequencies tend to "drown" in the most dominant frequency of the signal. A useful tool for periodic variation detection is spectral analysis. This is mostly done in off-line situations in order to gain information on the process. In Figure 5.6 the periodogram of a measurement is shown. It can be seen that the most dominant frequencies are in the order of one and two per day. This is not surprising as the analysed signal is the influent flow rate. Flow rates typically display dominant frequencies of one or two per day.

In Figure 5.7 (top), a measurement signal displaying the DO level is shown. The DO concentration is controlled with a setpoint value of 3.0. No obvious frequencies can be discerned. The periodogram of the signal is shown below in the figure. It confirms that there are no significantly dominant frequencies. The DO control system is performing
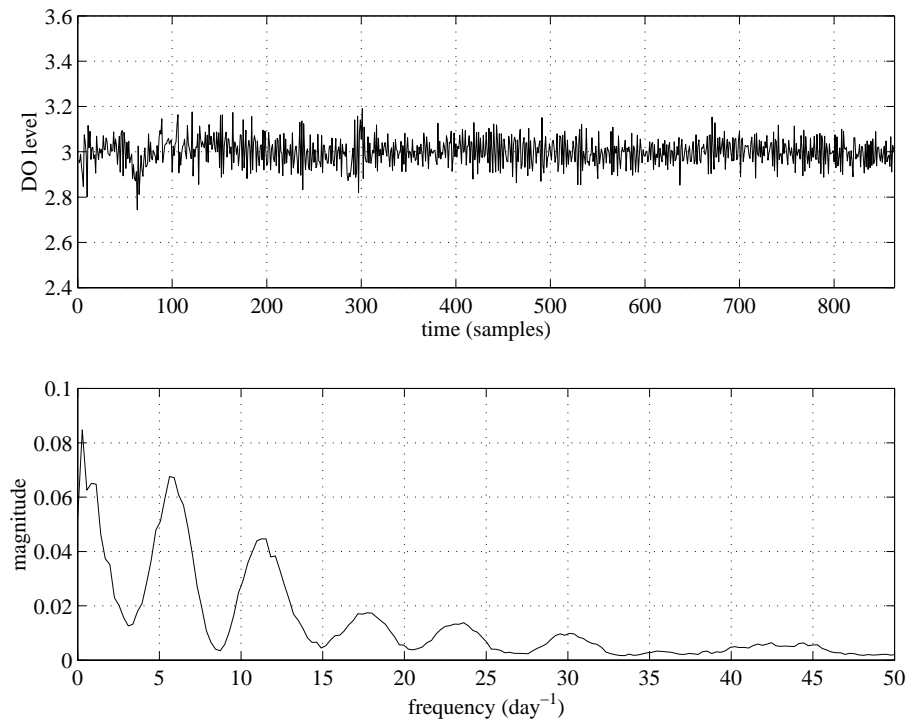
**Figure 5.7** The DO concentration measurements (top), and the periodogram of the measurements (bottom). No dominant frequencies of significant magnitude can be discerned. (Note that more than the measurements shown in the figure are used to calculate the periodogram.)

well. However, in Figure 5.8 (top), another DO signal is displayed (also three days, but with slightly different sampling frequency). Here, some dominant frequencies can be discerned. Looking at the periodogram of this signal reveals that there is a diurnal variation but also a variation of $\approx 22$ per day (Figure 5.8, bottom). The higher frequency can be an indication of an oscillating control system. There are no indications that the higher frequency is caused by influent variations. Instead, there are suspicions that the control system is incorrectly tuned. The DO data of Figure 5.8 are not from the Ronneby wastewater treatment plant.
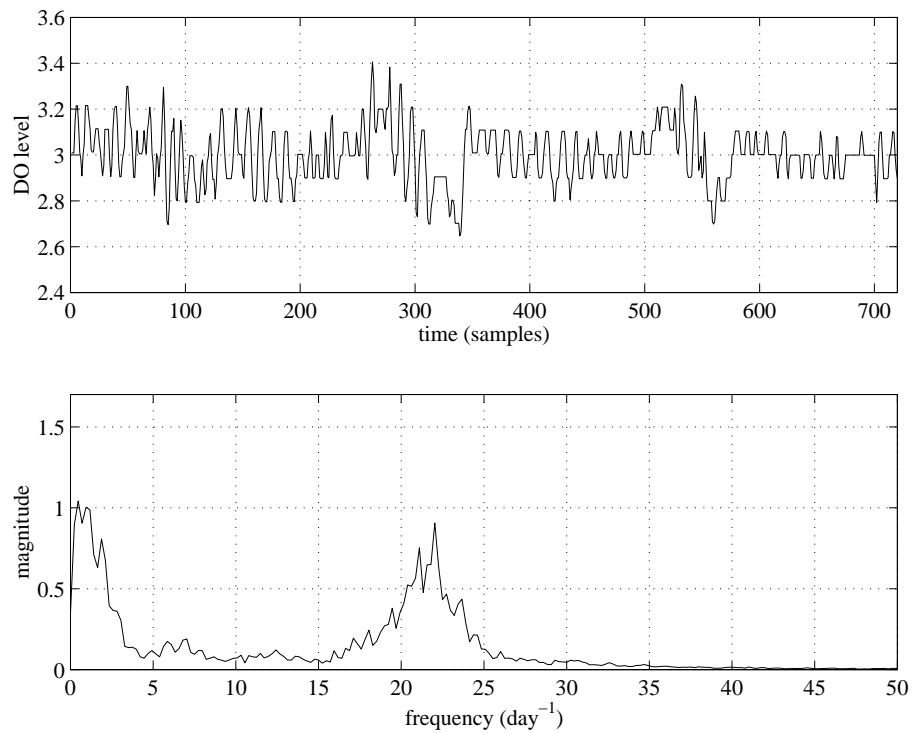
**Figure 5.8**   The DO concentration measurements (top), and the period-
ogram of the measurements (bottom).  The periodogram re-
veals a dominant frequency at 22 per day, possibly caused by
oscillations in the control system.  (Note that more than the
measurements shown in the figure are used to calculate the
periodogram.)

# Detection of Frequency Content Changes

High frequencies in a measurement signal with normally only low frequencies present may indicate that the signal is subjected to disturbances. The disturbances may originate, for instance, from electromagnetic sources, but it may also be an indication that the sensor device is defective. Whatever the cause is, it is important to quickly detect and correct the problem.

In Figure 5.9 (top), the original measurement signal is shown. This is the same signal that was investigated with respect to variance (see page 51). It is clear that the latter part of the signal contains high frequencies. This may be an indication of an imminent sensor breakdown. Is it possible to detect this by looking at the frequency content of the signal? A moving time window of a certain number of samples, $y(k), y(k-1), \ldots, y(k-l)$, is investigated with respect to its frequency content. The periodogram is calculated for the time window and the result is denoted $R^*_{per}(k)$. The sum of the frequency magnitudes between a threshold and the *Nyquist frequency* (half the sampling frequency), constitute the measure used for the detection. The sum for time $k$:

$$E_f(k) = \sum_{j}^{k-l} R^*_{per}(k) \tag{5.13}$$

where $j$ is the element in $R^*_{per}(k)$ that corresponds to the threshold frequency. The threshold frequency used here is 0.2 of the sampling frequency. The accuracy of $E_f$ depends on the length of the time window. There is a tradeoff between fast detection and accuracy. The present situation determines the appropriate window length. It is possible to extend the time window when there is an indication of a change in the frequency content. In Figure 5.9 (bottom) a moving time window of 48 samples has been used to estimate the high frequency content of the influent ammonia concentration signal. It can be seen that there is a significant increase of high frequency components after sample 480. This may be an indication that a more thorough investigation of the signal frequencies is needed and that corrections must be made.
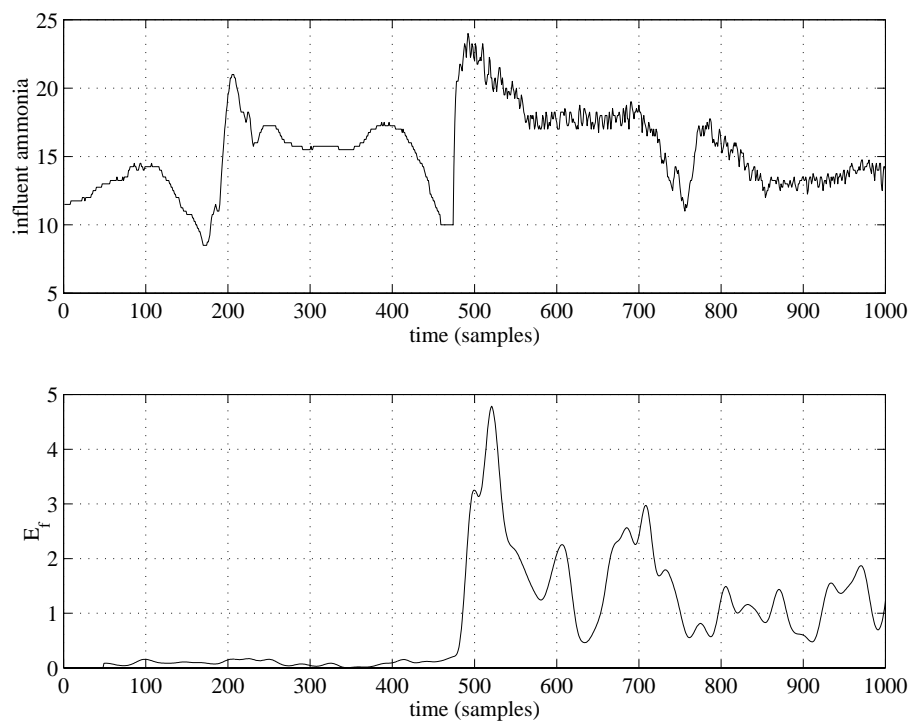
**Figure 5.9**   Influent ammonia concentration measurement signal (top) and
the sum of the frequency magnitudes between $f = 0.2$ and
$f = f_s/2$ of the corresponding periodogram calculated from a
48 samples time window.

# Chapter 6

# Detection Using Multivariate Statistics

In this chapter methods for *multivariate statistical* (MVS) analysis and monitoring are discussed. Kresta *et al.* (1991) list some challenges for any statistical monitoring method:

1. The method must be able to deal with collinear data of high dimension, in both the independent and the dependent variables.

2. The method must reduce the dimension of the problem substantially and allow for simple graphical interpretations of the results.

3. If both process and quality variables are present, it must be able to provide good predictions of the dependent variables.

The challenges listed above will be discussed and some simple examples will be given to illuminate the discussion. The examples in this chapter are based on real wastewater treatment plant data from the Ronneby wastewater treatment plant in Sweden. In the following chapters monitoring is applied to data from a simulation model (Chapter 7) and from the Ronneby plant (Chapter 8) to exemplify the methods described here.

Multivariate statistics or MVS is a group of methods for investigation of large data sets with many variables. Often, several variables are highly correlated, since most variables only reflect a few underlying mechanisms that drive the process in different ways (Kourti and MacGregor 1994). The "true" dimension of the process space is often a lot smaller than the dimension of the variable matrix space (Davis *et al.* 1996). The aim is to project the high-dimensional process space into a more visual low-dimensional space and by doing so identifying

key variables and important features of the data. This is achieved by transforming the measurements of the original coordinate system in such a way that a maximum of the variability[1] of the process variables is described by a new coordinate system. Thus, there will be a number of new variables, so called *latent variables* (LVs) or *principal components* (PCs), which describe most of the process variability in a space of fewer dimensions than the original space.

There are many available multivariate statistics methods but here only the most classical approaches, such as *principal component analysis* (PCA), *principal component regression* (PCR) and *projection to latent structures* (PLS), are discussed. Descriptions of multivariate analysis in process monitoring and control can be found in the literature, *e.g.* Geladi and Kowalski (1986), Kresta *et al.* (1991), MacGregor *et al.* (1994). In the discussion below, the nomenclature of Wise and Gallagher (1996) is mostly used. Further reading on multivariate analysis in wastewater treatment systems can be found in, for instance, Mossberg (1995), Krofta *et al.* (1995), Champely and Doledec (1997). Piovoso and Kosanovich (1994) is a good reference on multivariate statistical methods in control applications and Wold (1987) and Höskuldsson (1988) thoroughly describe the theoretical basis of PCA and PLS, respectively.

In order to fully appreciate the theory behind PCA, PCR and PLS, basic knowledge in linear algebra is required. This information can be found in most textbooks in mathematics today and will not be presented here. However, the intention is that the uninitiated reader should be able to appreciate the basic ideas behind the methods.

# 6.1   MVS Methods

In this section the basic theory of PCA, PCR and PLS is presented. Appendix B provides supplementary details on the calculations of PLS, but is not needed for the basic understanding of the method.

---

[1]In this context, variability or variance can be seen as the information content of the data.
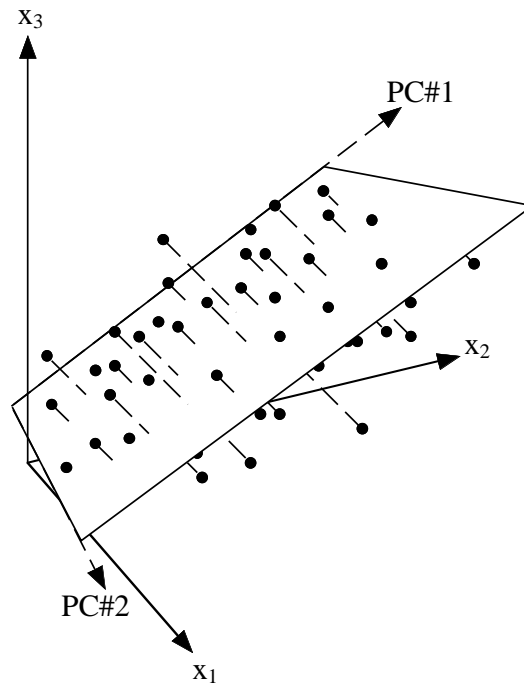
**Figure 6.1**   Reducing process space from three to two dimensions. The new space is defined by *principal components.*

## Principal Component Analysis

Principal component analysis (PCA) is one of the most basic MVS methods. In PCA the process variable space is projected to a space with less dimensionality, described by the principal components (PCs). Such a projection is illustrated in Figure 6.1. Even though there are only three dimensions in the figure, there are no difficulties to extend the methodology to an arbitrary number of dimension. The complexity of the mathematics behind PCA will not increase as the number of dimensions is extended.

### The PCA Algorithm

Let $\mathbf{X}$ be an autoscaled (*i.e.* mean centred and scaled to unit variance) $[m \times n]$ matrix of measurement values for $n$ variables at $m$ number of samples defining a variable space of $r$ dimensions. This means that $\mathbf{X}$ is of rank[2] $r$. $\mathbf{X}$ can be expressed as a sum of matrices $\mathbf{M}_i$ of the

---

[2]Here, the term rank refers to the matrix rank.

same size as $\mathbf{X}$ but of rank 1:

$$\mathbf{X} = \mathbf{M}_1 + \mathbf{M}_2 + \ldots + \mathbf{M}_a + \mathbf{E} \qquad (6.1)$$

where $\mathbf{E}$ is the residual (or error) matrix and $a \leq r$. If $a = r$ then $\mathbf{E} = 0$, as all the variability directions are described. However, if $a < r$, that is, less principal components than original variables are retained, then $\mathbf{E}$ describes the variability not described by the sum of the $\mathbf{M}$-matrices .

The matrix $\mathbf{M}_i$ can be written as the outer product of two vectors $\mathbf{t}_i$ and $\mathbf{p}_i^T$. Thus:

$$\mathbf{X} = \mathbf{t}_1\mathbf{p}_1^T + \mathbf{t}_2\mathbf{p}_2^T + \ldots + \mathbf{t}_a\mathbf{p}_a^T + \mathbf{E} \qquad (6.2)$$

or

$$\mathbf{X} = \mathbf{T}\mathbf{P}^T + \mathbf{E} \qquad (6.3)$$

The vectors of $\mathbf{T}$ ($\mathbf{t}_i$) are called the *score* vectors or *scores* and the vectors of $\mathbf{P}$ ($\mathbf{p}_i$) are the *loading* vectors or *loadings*. The matrix $\mathbf{P}$ can be determined by *singular value decomposition* (SVD) of the covariance matrix of $\mathbf{X}$:

$$cov(\mathbf{X}) = \mathbf{P}\Lambda\mathbf{P}^T \qquad (6.4)$$

where $\Lambda$ is the diagonal matrix of the eigenvalues $\lambda$. A column vector $\mathbf{p}_i$ of $\mathbf{P}$ is the $i$th eigenvector of $cov(\mathbf{X})$, such that:

$$cov(\mathbf{X})\mathbf{p}_i = \lambda_i\mathbf{p}_i \qquad (6.5)$$

where $\lambda_i$ is the eigenvalue associated with $\mathbf{p}_i$. The covariance matrix of $\mathbf{X}$ is estimated by:

$$cov(\mathbf{X}) = \frac{\mathbf{X}^T\mathbf{X}}{m-1} \qquad (6.6)$$

The orthogonal loading matrix $\mathbf{P}$ is a so called *unitary* matrix. Important properties of unitary matrices are that $\mathbf{P}^T\mathbf{P} = \mathbf{I}$, $\mathbf{P}\mathbf{P}^T = \mathbf{I}$ and $\mathbf{P}^T = \mathbf{P}^{-1}$, where $\mathbf{I}$ is the identity matrix.

The first pair of $\mathbf{t}_i$ and $\mathbf{p}_i$ captures the largest amount of variation possible to capture by a linear factor in matrix $\mathbf{X}$. Consequently, the subsequent pair will captures the largest amount of variation left in

$\mathbf{X}$ when $\mathbf{t}_i \mathbf{p}_i^T$ is subtracted from $\mathbf{X}$. The score vectors are the original data projected in the new coordinate system defined by the principal components. When the model is subjected to new data the scores are calculated as:

$$\hat{\mathbf{T}} = \mathbf{X}_{new}\mathbf{P} \qquad (6.7)$$

The new scores can be visualised in different ways, which will be discussed later.

# Principal Component Regression

In many processes there are key quality variables that are of higher interest than others, *e.g.* output or effluent quality variables. It would be convenient to build a model that especially considers the variables influencing the quality variables of interest. The characteristics of the process variables must be linked to the quality variables so that the features affecting the variables of interest can be emphasised. Regression techniques provide us with methods for this.

## The PCR Algorithm

In *multiple linear regression* (MLR), the quality variables are regressed onto to the process variables. In matrix form MLR is:

$$\mathbf{Y} = \mathbf{X}\mathbf{B} + \mathbf{E} \qquad (6.8)$$

where $\mathbf{Y}$ is the *dependent* variable matrix, $\mathbf{X}$ the *independent*[3] variable matrix, $\mathbf{B}$ the regression matrix and $\mathbf{E}$ the residual matrix. Using a set of training data, $\mathbf{B}$ is calculated by minimising $\mathbf{E}$. A popular method for this is the *least-squares method* (Söderström and Stoica 1989). The regression matrix is calculated as:

$$\mathbf{B} = (\mathbf{X}^T\mathbf{X})^{-1}\mathbf{X}^T\mathbf{Y} \qquad (6.9)$$

However, MLR is not always applicable since the inverse of $\mathbf{X}^T\mathbf{X}$ may not exist, which is due to collinearity of $\mathbf{X}$. A combination of PCA,

---

[3]The term *independent* is here used in the meaning that the state of the $X$-block variables do not depend on any other variables included in the analysis. The measurements of the $X$-variables are normally not *time independent*.

which produces a matrix of orthogonal variables, and MLR may then be a successful way to proceed. *Principal component regression* (PCR) is an extension of PCA where the independent variables of $\mathbf{X}$ are linked to the dependent variables of $\mathbf{Y}$, that is the process variables are linked to the quality variables. In PCR, the system properties are regressed onto the principal component scores instead of onto the original measurement variables as in MLR. The scores are better suited for regression as the scores are orthogonal. This solves the collinearity problem often encountered in process monitoring. The MLR equations become:

$$\mathbf{Y} = \mathbf{TB} + \mathbf{E} \tag{6.10}$$

which has the solution:

$$\mathbf{B} = (\mathbf{T}^T\mathbf{T})^{-1}\mathbf{T}^T\mathbf{Y} \tag{6.11}$$

with $\mathbf{T}$ and $\mathbf{E}$ defined by Equation 6.3.

In MLR, the aim is to capture the correlation between dependent and independent variables and the internal structure of the input or independent block is not considered. PCR, on the other hand, only considers the internal structure of the input block in order to maximise the capture of input block variance. *Projection to latent structures* (PLS) could be said to be a combination of these two extremes. As a matter of fact, there are ways of uniting all three methods in a continuum regression (Wise 1991), but this will not be discussed here.

## Projection to Latent Structures

Projection to latent structures or *partial least squares* is also a MVS method. In PLS the *latent variables* (LVs) of the $X$ space are calculated to maximise the correlation between an input matrix $\mathbf{X}$ and an output matrix $\mathbf{Y}$. In this way the detection effort can be applied to the variables that have the most influence on one or several specific quality variables.

## The PLS Algorithm

Building a PLS model involves creating the outer relation for the independent variables ($X$-block) and the dependent variables ($Y$-block), separately. The inner relation linking the two blocks is then established. The outer relation for the independent block is the same as in Equation 6.3, *i.e.*:

$$\mathbf{X} = \mathbf{t}_1 \mathbf{p}_1^T + \mathbf{t}_2 \mathbf{p}_2^T + \ldots + \mathbf{t}_a \mathbf{p}_a^T + \mathbf{E} \tag{6.12}$$

or

$$\mathbf{X} = \mathbf{T}\mathbf{P}^T + \mathbf{E} \tag{6.13}$$

In the same way, the outer relation for the dependent block is arranged as:

$$\mathbf{Y} = \mathbf{u}_1 \mathbf{q}_1^T + \mathbf{u}_2 \mathbf{q}_2^T + \ldots + \mathbf{u}_a \mathbf{q}_a^T + \mathbf{F} \tag{6.14}$$

or

$$\mathbf{Y} = \mathbf{U}\mathbf{Q}^T + \mathbf{F} \tag{6.15}$$

where $\mathbf{U}$ and $\mathbf{Q}$ corresponds to $\mathbf{T}$ and $\mathbf{P}$, respectively. The inner relation can be expressed in different ways depending on the relation between the input and output blocks. The simplest form is a linear relation:

$$\mathbf{u}_j = b_j \mathbf{t}_j \tag{6.16}$$

where $\mathbf{u}_j$ and $\mathbf{t}_j$ are the $j$th columns of $\mathbf{U}$ and $\mathbf{T}$, respectively. $b_j$ is estimated with the least-squares method as:

$$b_j = \frac{\mathbf{t}_j^T \mathbf{u}_j}{\mathbf{t}_j^T \mathbf{t}_j} \tag{6.17}$$

The mixed relation becomes:

$$\mathbf{Y} = \mathbf{T}\mathbf{B}\mathbf{Q}^T + \mathbf{F} \tag{6.18}$$

where $\mathbf{B}$ is the diagonal matrix of the regression vector $\mathbf{b}$.

To calculate the mixed relation in Equation 6.18, the iterative *nonlinear iterative partial least squares* (NIPALS) algorithm can be used.

The algorithm is described in Appendix B. However, an important remark is that in order to obtain an orthogonal loading matrix for the $X$-block, a weight matrix ($\mathbf{W}$) must be introduced to replace $\mathbf{P}$.

When the PLS model is identified, the new latent variable projections are given by:

$$\hat{\mathbf{T}} = \mathbf{X}_{new}\mathbf{W}(\mathbf{P}^T\mathbf{W})^{-1} \tag{6.19}$$

## MVS and Prediction

PCR and PLS can be used for prediction[4] of the $Y$-block. In the PCR case the predicted $Y$-block is:

$$\hat{\mathbf{Y}} = \hat{\mathbf{T}}\mathbf{B} \tag{6.20}$$

with $\hat{\mathbf{T}}$ defined by Equation 6.7 and $\mathbf{B}$ by Equation 6.9. Since $\hat{\mathbf{T}} = \mathbf{X}_{new}\mathbf{P}$, Equation 6.20 can be written as:

$$\hat{\mathbf{Y}} = \mathbf{X}_{new}\mathbf{P}\mathbf{B} \tag{6.21}$$

In the PLS case the predictor equation becomes:

$$\hat{\mathbf{Y}} = \hat{\mathbf{T}}\mathbf{B}\mathbf{Q}^T \tag{6.22}$$

where $\hat{\mathbf{T}}$ is given in Equation 6.19, $\mathbf{B}$ is the diagonal matrix of the regression vector $\mathbf{b}$ and $\mathbf{Q}$ is the loading matrix for the $Y$-block ($\mathbf{b}$ and $\mathbf{Q}$ found iteratively by the PLS algorithm). Equation 6.22 can also be written as:

$$\hat{\mathbf{Y}} = \mathbf{X}_{new}\mathbf{W}(\mathbf{P}^T\mathbf{W})^{-1}\mathbf{B}\mathbf{Q}^T \tag{6.23}$$

if Equations 6.19 and 6.22 are combined. For both PCR and PLS predictions, it is important that the input data are scaled in the same manner as when the model was built.

## Statistical Properties of MVS

MVS methods are useful tools to detect disturbances in measurement data. An MVS model can be combined with techniques from statistical process control. If the scores are normally distributed, the $i$th

---

[4]The term prediction is used even though the implication in some cases is filtering.

confidence limit $(t_{i,\alpha})$ of scores for the $i$th principal component is calculated as (Wise and Gallagher 1996):

$$t_{i,\alpha} = \sqrt{\lambda_i}\, t_{m-1,\alpha/2} \qquad (6.24)$$

where $t_{m-1,\alpha/2}$ corresponds to the probability point on the single sided t-distribution and $\lambda_i$ is the the eigenvalue associated with the $i$th loading vector. The assumption that the scores are normally distributed is not always true, even if the number of samples is large enough, according to the central limit theorem. The theorem states that the sampling distribution of the mean tends to the normal distribution when the number of independent observations increases (Miller and Miller 1993). Firstly, the observations (samples) can seldom be considered time independent. Secondly there may be situations when the distribution is severely distorted by, for instance, control actions or saturation.

The *squared prediction error* ($SPE$) of a sample and its projection into the new space (defined by the principal components) indicates how well the model fits the data set. The residual variable can be visualised in a chart with confidence limits. The residual at time $k$ is calculated as (Kresta *et al.* 1991):

$$SPE_X(k) = \sum_{j=1}^{n} \left( x_j(k) - \hat{x}_j(k) \right)^2 \qquad (6.25)$$

for the $X$-block. $n$ is the number of variables of the $X$-block and $\hat{x}_j(k)$ is the model prediction. If PLS is considered, the residual of the $Y$-block becomes:

$$SPE_Y(k) = \sum_{j=1}^{n} \left( y_j(k) - \hat{y}_j(k) \right)^2 \qquad (6.26)$$

where $n$ is the number of variables in the $Y$-block and $\hat{y}_j(k)$ is the model prediction at time $k$. For detection purposes, the $SPE_X$ is mostly used and from now on the term $SPE$ refers to $SPE_X$ if nothing else is stated. $SPE$ can also be written in matrix form as:

$$SPE(k) = \mathbf{e}(k)\mathbf{e}^T(k) \qquad (6.27)$$

where $\mathbf{e}(k)$ is the $k$th row of $\mathbf{E}$. In PCA modelling Equation 6.25

becomes:

$$SPE(k) = \sum_{j=1}^{n} \left(x_j(k) - \mathbf{t}(k)\mathbf{p}_j^T\right)^2 = \sum_{j=1}^{n} \left(x_j(k) - \mathbf{x}(k)\mathbf{P}\mathbf{p}_j^T\right)^2 \quad (6.28)$$

as $\mathbf{t}(k)$ is substituted by $\mathbf{x}(k)\mathbf{P}$ (Equation 6.7). $\mathbf{p}_j$ is the $j$th row of $\mathbf{P}$. In PLS modelling the $SPE$ is calculated as:

$$SPE(k) = \sum_{j=1}^{n} \left(x_j(k) - \mathbf{t}(k)\mathbf{p}_j^T\right)^2 = \sum_{j=1}^{n} \left(x_j(k) - \mathbf{x}(k)\mathbf{W}(\mathbf{P}^T\mathbf{W})^{-1}\mathbf{p}_j^T\right)^2$$
$$(6.29)$$

where $\mathbf{t}(k)$ is substituted by $\mathbf{x}(k)\mathbf{W}(\mathbf{P}^T\mathbf{W})^{-1}$ (Equation 6.19). According to Wise (1991) the confidence limit for $SPE$ from a PCA model is:

$$SPE_\alpha = \Theta_1 \left[ \frac{c_\alpha \sqrt{2\Theta_2 h_0^2}}{\Theta_1} + 1 + \frac{\Theta_2 h_0(h_0 - 1)}{\Theta_1^2} \right]^{\frac{1}{h_0}} \quad (6.30)$$

where

$$\Theta_i = \sum_{j=a+1}^{n} \lambda_j^i \quad (6.31)$$

for $i = 1$, 2, 3 and

$$h_0 = 1 - \frac{2\Theta_1\Theta_3}{3\Theta_2^2} \quad (6.32)$$

$c_\alpha$ in Equation 6.30 is the standard normal deviate corresponding to the upper (1-$\alpha$) percentile and $a$ in Equation 6.31 is the number of principal components retained in the model. However, the SPE statistic of PLS is often not well behaved, which shows itself in a not normally distributed $SPE$ measure. Wise and Gallagher (1996) use an empirical form of calculation used for PCA as an approximation. Here Equation 6.31 is replaced by:

$$\Theta_1 = \frac{1}{m - 1} \sum_{k=1}^{m} SPE(k) \quad (6.33)$$

$$\Theta_2 = (n - a) \left( \frac{\Theta_1(n - a)}{n - a} \right)^2 \quad (6.34)$$

$$\Theta_3 = (n - a)\left(\frac{\Theta_1(n - a)}{n - a}\right)^3 \tag{6.35}$$

where $a$ is the number of components or latent variables retained in the model and $n$ is the number of variables in the $X$-block. However, this results in an underestimation of the confidence limit, but it is compensated for by choosing a higher value of $c_\alpha$. Non-parametric measures to determine appropriate detection limits, such as the quantile discussed in Chapter 5, can also be used to avoid that false conclusions are drawn.

Another measure used to validate the model is Hotelling's $T^2$ statistics, which is the normalised sum of scores. The $T^2$ at time $k$ is calculated as (Wise and Gallagher 1996):

$$T^2(k) = \mathbf{t}(k)\Lambda^{-1}\mathbf{t}^T(k) = \mathbf{x}(k)\mathbf{P}\Lambda^{-1}\mathbf{P}^T\mathbf{x}^T(k) \tag{6.36}$$

where $\mathbf{t}(k)$ is the scores at time $k$ and $\Lambda^{-1}$ is the diagonal matrix of the inverse of the eigenvalues associated with the retained principal components (see Equation 6.4). The confidence limits for $T^2$ are obtained using the F-distribution (Wise 1991; MacGregor *et al.* 1994):

$$T^2_{a, m, \alpha} = \frac{a(m - 1)}{m - a}F_{k, m-a, \alpha} \tag{6.37}$$

where $m$ is the number of samples in the model and $a$ is the number of principal components.

What do $SPE$ and $T^2$ tell us and how can they be used? $SPE$ is the Euclidian distance from a sample to the hyperplane defined by the principal components. If the model is valid, the distance from the sample to the model plane has to be small, since this is a direction not included in the model. Thus, $SPE$ is a measure of how the data characteristics vary orthogonally to the model plane. The $T^2$ measure describes how the data vary within the plane of the model. Consequently, $T^2$ is a measure of how far a sample is from the intersection of the principal components (origin, if the variable matrix is mean centred). The geometrical interpretation of $SPE$ and $T^2$ is visualised in Figure 6.2. Both $SPE$ and $T^2$ plots can be used to monitor the statistical fit of a model to real data. Plotting the $SPE$ and $T^2$ measures as time series with the confidence limits from Equations 6.30 and 6.37 are a condensed way of monitoring the process. However, the
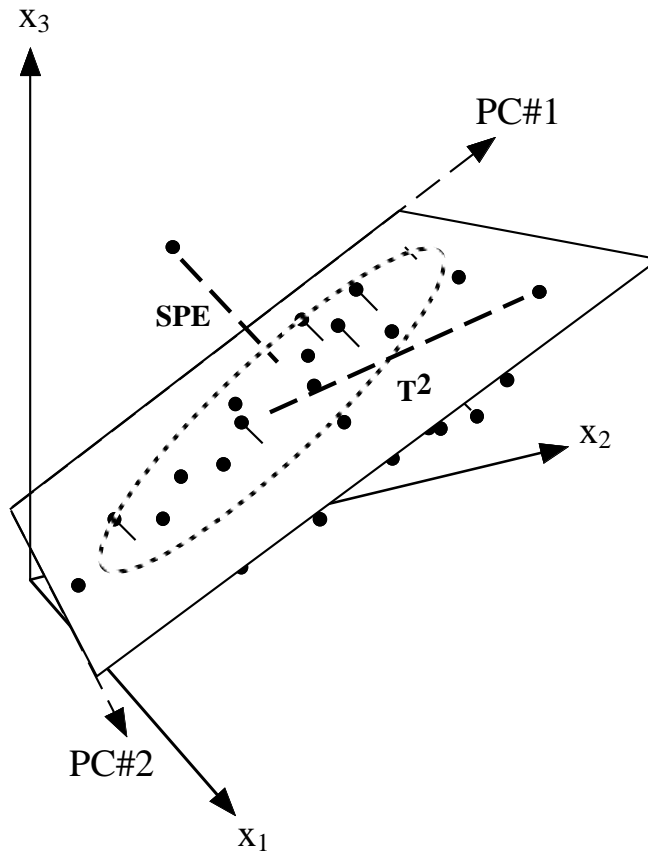
**Figure 6.2**   The geometrical interpretation of the $SPE$ and $T^2$ measures, respectively.

$SPE$ measure, as stated before, is a measure of the distance between a sample and the model plane. The implication of this is that when all possible principal components are retained in the PCA or PLS model (*i.e.* as many PCs or LVs as original variables), the $SPE$ residual will be zero. This is because the model in this case contains components to model all the directions present in the original data set. Thus no sample can be positioned outside the model plane.

## 6.2   Building Multivariate Models

In this section the first step of multivariate monitoring is described. Before the on-line monitoring task can be initiated, the model development must be carried out. Model building involves pre-processing of data and model identification.

# Preparing Data for Multivariate Analysis

Pre-processing of data is described in Chapter 4 and processing needed for data used to identify MVS models may include:

- outlier reduction and replacement of missing data;

- noise reduction by digital filters;

- mean centring, *i.e.* subtracting the variable mean value from the variable value;

- variance scaling, *i.e.*dividing each variable value by the variable standard deviation;

- auto scaling, *i.e.* mean centring and variance scaling.

Noise reduction is especially important in the model building phase in order to obtain a model, based on the key features of the process. Centring and scaling can be used to level the various variables and to make the calculations easier. As a rule of thumb, autoscaling is a good start when the information on the data is limited. Autoscaling has been used in all examples in this thesis.

However, other manipulations may be called for. In order to increase the information content of the $X$-block, new variables can be created from combinations of the original variables of the $X$-block. All combinations are not increasing the information content. Linear operations on a variable will not increase the information. Typical linear operations are:

- scaling and centring of variables;

- subtraction and addition of different variables of the $X$-block.

Linear combinations of variables do not increase the dimensionality of the process space, as the linear combinations are captured by the plane defined by a combination of the original variables. Consequently, in a PCA model of three variables, where the third is a linear combination of the first two variables, two principal components will cover 100 % of the variability. On the other hand, non-linear operations on

the variables *may* increase the information content. The variability
of the process will increase, but this does not mean that the usable
information content increases. Typical non-linear operations are:

- exponential and logarithmic operations;

- product of and ratio between different variables of the $X$-block.

However, it is important to validate the increased content of inform-
ation, so that a new variable does not only add random noise. In
diagnosis it is an advantage if the new variable has some physical
interpretation, in order to quickly determine ways to handle a dis-
turbance. Typical non-linear combinations of process variables are
mass transport, which is a combination of a flow rate and a substance
concentration or loads, which may be the ratio of two substance con-
centration variables. In some cases it may be a good idea to replace
variables by linear combinations. For instance, if the concentration
level is less important, but the difference between two concentration
levels are crucial, the difference between the two variables can be used
instead.

## Non-linearities

In most processes the relations between variables are not linear. PLS,
as discussed above, does not take this into consideration. However,
there are ways to introduce non-linearities. Scaling of data, as men-
tioned earlier, can be used but extensions to the PLS algorithm are
also possible.

In linear PLS modelling the scalar $b$ relates the $X$-block score vector
($\mathbf{t}$) to the $Y$-block score vector ($\mathbf{u}$). However, the relation between
$\mathbf{t}$ and $\mathbf{u}$ is sometimes better described in a non-linear way. A more
sophisticated representation of the inner relation is when the scalar
$b_i$ in Equations 6.16 and 6.17 is replaced by a vector of polynomial
coefficients. The inner relation is then expressed as:

$$\mathbf{u}_j = \mathbf{b}_{2,j}\mathbf{t}_j^2 + \mathbf{b}_{1,j}\mathbf{t}_j + \mathbf{b}_{0,j} \qquad (6.38)$$

if a second-order polynomial is used. Note that $\mathbf{t}_j^2$ is $\mathbf{t}$ squared element
by element. Thus, $\mathbf{t}_j^2$ is of the same size as $\mathbf{t}$. In Figure 6.3, a non-
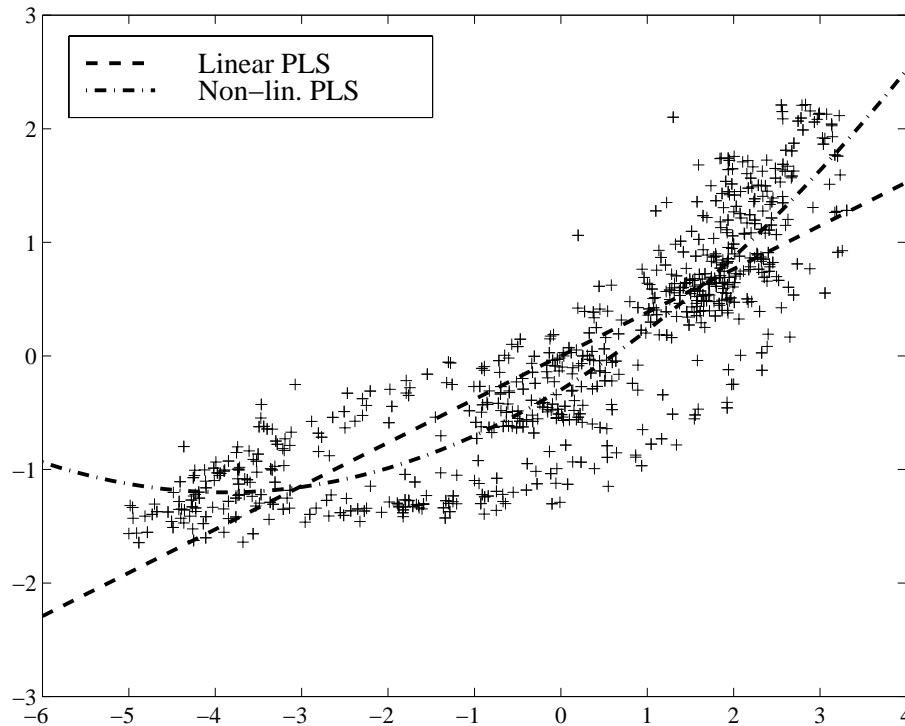
**Figure 6.3**  The relation between **t** and **u** described by a scalar and a second-order polynomial.

linear relation between **t** and **u** is shown. When linear PLS is used, the relation between **t** and **u** is described by the dashed line. A second-order polynomial PLS model describes the relation as the dash-dotted line. It is obvious that the second line describes the relation better. However, one must use non-linear relations with caution as the model becomes more sensitive to extrapolation as the order of the polynomial increases.

There are other methods to introduce non-linearities. Spline techniques and neural networks are two examples that can be found in the literature, for example Qin and McAvoy (1991) and Wise and Gallagher (1996).

## Representing Dynamics

In their basic configuration the MVS based methods are static, and the dynamics of the system is not represented. The static methods can be used for monitoring with good results, but when the goal is to estimate,

and especially predict, variable values, dynamics must be taken into consideration. Here, extensions to MVS aiming at representing the dynamics of the process, are presented.

## Time Lags

In all dynamic processes *time lags* are present. By time lag we mean the time it takes for a change in the $X$-block to propagate to the $Y$-block. In basic MVS the time lag between the $X$-block and the $Y$-block is not addressed. One way of dealing with this, if there is just one quality variable in the $Y$-block, is to investigate the cross-covariance function between every input variable and the output variable and calculate the suitable lag (Åström and Wittenmark 1997; Wise and Gallagher 1996). A second way is to use an *a priori* model for the time lag of every relation, for example, depending on the retention time. By doing so the time lag between each process variable and the quality variable will change dynamically as the flow rate changes and we will have a quasi-dynamic representation of the flow dynamics.

## FIR and IIR Models

A distinguishing feature of dynamic processes is that the present state is a result of its history. Therefore, it is desirable to take the history into consideration. This can be achieved by applying the ideas behind time series modelling and *finite impulse response* (FIR) models (or MA models). Consider Equation 4.1. A FIR filter is obtained if all $a$ coefficients are equal to zero. Let the estimate $\hat{y}$ be based on $x(k), x(k-1), \ldots, x(k-l)$ ($m$ in Equation 4.1 is replaced by $l$ to avoid ambiguity) and let the prediction error be $e$. This is the same case as in Equation 4.2. The equation expresses a *single input-single output* (SISO) model. However, the equation can be extended to comprise multiple inputs and multiple outputs, *i.e.* a MIMO model. The MIMO form of Equation 4.2 is expressed as:

$$\hat{\mathbf{y}}(k) = \mathbf{B}_0 \mathbf{x}(k) + \mathbf{B}_1 \mathbf{x}(k-1) + \ldots + \mathbf{B}_l \mathbf{x}(k-l) + \mathbf{e}(k) \qquad (6.39)$$

where $\hat{\mathbf{y}}(k)$ is a column vector of a length corresponding to the number of variables in the $Y$-block ($n_y$). The $\mathbf{B}$ matrices are of size $[n_y \times n_x]$

and the $\mathbf{x}$:s are column vectors of size $[n_x \times 1]$. This can also be expressed as:

$$\hat{\mathbf{y}}(k) = \begin{bmatrix} \mathbf{B}_0 & \mathbf{B}_1 & \ldots & \mathbf{B}_l \end{bmatrix} \begin{bmatrix} \mathbf{x}(k) \\ \mathbf{x}(k-1) \\ \vdots \\ \mathbf{x}(k-l) \end{bmatrix} + \mathbf{e}(k) \tag{6.40}$$

In order to obtain the above matrices in the format used earlier in this thesis, let:

$$\hat{\mathbf{y}}(k) = \hat{\mathbf{y}}^T(k) \tag{6.41}$$

$$\mathbf{x}_{FIR}(k) = \begin{bmatrix} \mathbf{x}(k) \\ \mathbf{x}(k-1) \\ \vdots \\ \mathbf{x}(k-l) \end{bmatrix}^T \tag{6.42}$$

and

$$\mathbf{B}_{FIR} = \begin{bmatrix} \mathbf{B}_0 & \mathbf{B}_1 & \ldots & \mathbf{B}_l \end{bmatrix}^T \tag{6.43}$$

Then the estimate for a certain time $k$ is:

$$\hat{\mathbf{y}}(k) = \mathbf{x}_{FIR}(k)\mathbf{B}_{FIR} + \mathbf{e}(k) \tag{6.44}$$

and the estimate for all samples is:

$$\hat{\mathbf{Y}} = \mathbf{X}_{FIR}\mathbf{B}_{FIR} + \mathbf{E} \tag{6.45}$$

where $\hat{\mathbf{Y}}$ is of size $[m \times n_y]$, $\hat{\mathbf{X}}_{FIR}$ is of size $[m \times n_x l]$, $\mathbf{B}_{FIR}$ is of size $[n_x l \times n_y]$ and $\mathbf{E}$ is of size $[m \times n_y]$. The identification of the FIR coefficients in $\mathbf{B}_{FIR}$ can be carried out with MVS. Let the training $Y$-block be $\hat{\mathbf{Y}}$ and the training $X$-block be $\mathbf{X}_{FIR}$ from a historic period of known $\hat{\mathbf{Y}}$ and $\mathbf{X}_{FIR}$. The FIR coefficients, $\mathbf{B}_{FIR}$, can then be identified by (compare with Equation 6.23):

$$\mathbf{B}_{FIR} = \mathbf{W}(\mathbf{P}^T\mathbf{W})^{-1}\mathbf{B}\mathbf{Q}^T \tag{6.46}$$

where $\mathbf{W}$, $\mathbf{P}$, $\mathbf{T}$, $\mathbf{B}$ and $\mathbf{Q}$ are determined by the PLS algorithm.

The same approach as used for FIR model identification is applicable if *infinite impulse response* (IIR) model (or AR model) is desired. In

an IIR model the $a$ coefficients in Equation 4.1 are not equal to zero. Consequently, Equation 6.39 must be rewritten:

$$\hat{\mathbf{y}}(k) = -\mathbf{A}_1\hat{\mathbf{y}}(k-1) - \mathbf{A}_2\hat{\mathbf{y}}(k-2) - \ldots - \mathbf{A}_{l_y}\hat{\mathbf{y}}(k-l_y)$$
$$\mathbf{B}_0\mathbf{x}(k) + \ldots + \mathbf{B}_{l_x}\mathbf{x}(k-l_x) + \mathbf{e}(k) \quad (6.47)$$

Analogous to the FIR model, the IIR model can be written as:

$$\hat{\mathbf{y}}(k) = \mathbf{x}_{IIR}(k)\mathbf{B}_{IIR} + \mathbf{e}(k) \quad\quad\quad (6.48)$$

where

$$\mathbf{x}_{IIR}(k) = \begin{bmatrix} \hat{\mathbf{y}}(k-1) \\ \hat{\mathbf{y}}(k-2) \\ \vdots \\ \hat{\mathbf{y}}(k-l_y) \\ \mathbf{x}(k) \\ \mathbf{x}(k-1) \\ \vdots \\ \mathbf{x}(k-l_x) \end{bmatrix}^T \quad\quad\quad (6.49)$$

and

$$\mathbf{B}_{IIR} = \begin{bmatrix} \mathbf{A}_1 & \mathbf{A}_2 & \ldots & \mathbf{A}_{l_y} & \mathbf{B}_0 & \mathbf{B}_1 & \ldots & \mathbf{B}_{l_x} \end{bmatrix}^T \quad\quad (6.50)$$

The estimate for all samples is:

$$\hat{\mathbf{Y}} = \mathbf{X}_{IIR}\mathbf{B}_{IIR} + \mathbf{E}_i \quad\quad\quad (6.51)$$

Thus, the identification of a PLS model with $Y$ and $X$-blocks from Equations 6.45 and 6.51 is also an identification of the FIR and IIR coefficients, respectively. However, identification of the coefficient matrices $\mathbf{B}_{IIR}$ is done based on one important assumption. The equation errors $\mathbf{e}(k)$ are assumed to be uncorrelated. In this way, the identification is kept linear.

There are two reasons to use PLS (or PCR) in order to identify the FIR and IIR coefficient matrices, instead of direct identification with the least-squares method (see Equation 6.9). Firstly, the inverse of $\mathbf{X}^T\mathbf{X}$ may be ill-conditioned or may not exist at all due to collinearities. Secondly, the primary goal is not to identify the best possible

model. Instead, the goal is to obtain key variables for detection and visualisation with consideration taken to the dynamics of the process.

A problem with FIR and IIR models is the increased number of variables. The number of variables is now the original number of values multiplied by the length of the finite time window. If the computational power is limited, this may be a problem. The problem can partly be solved by not using every sample in the range $k$ to $k - l$. Instead, every $j$th sample can be used. The data preparation becomes somewhat more complicated, but is solved by a simple computer algorithm.

## Number of Components

A crucial question when building MVS models is the number of components to use. If too many components are retained in the model, the dimensionality of the process has not been reduced and the only gain is the orthogonality of the new variables. On the other hand, if too few variables are retained, information will be lost as the variability captured by the model decreases with the number of components.

For PCR and PLS a decision criterion, the total $SPE_Y$, can be used. If the model is built for prediction, the $SPE_Y$ is a natural choice, as $SPE_Y$ measures the prediction error of the model. Cross-validation techniques can then be applied in order to find the optimal number of components. Cross-validation implies that a part of the data set is kept out of the model development. This data are then compared with predictions made by the model and the total $SPE_Y$ is calculated. The number of components used is altered and the number of components resulting in the smallest total $SPE_Y$ is chosen. The procedure is repeated keeping different parts of data out of the development. A more thorough description of cross-validation can be found in (Wold 1978).

For PCA, it is not possible to use the $SPE_Y$ as a criterion. Neither is it possible to use $SPE_X$, since it decreases as the number of components increases. Instead an investigation of the eigenvalues associated with the model can be used. Figure 6.4 shows the eigenvalues versus the number of components of a PCA model. If there is a "knee" in the
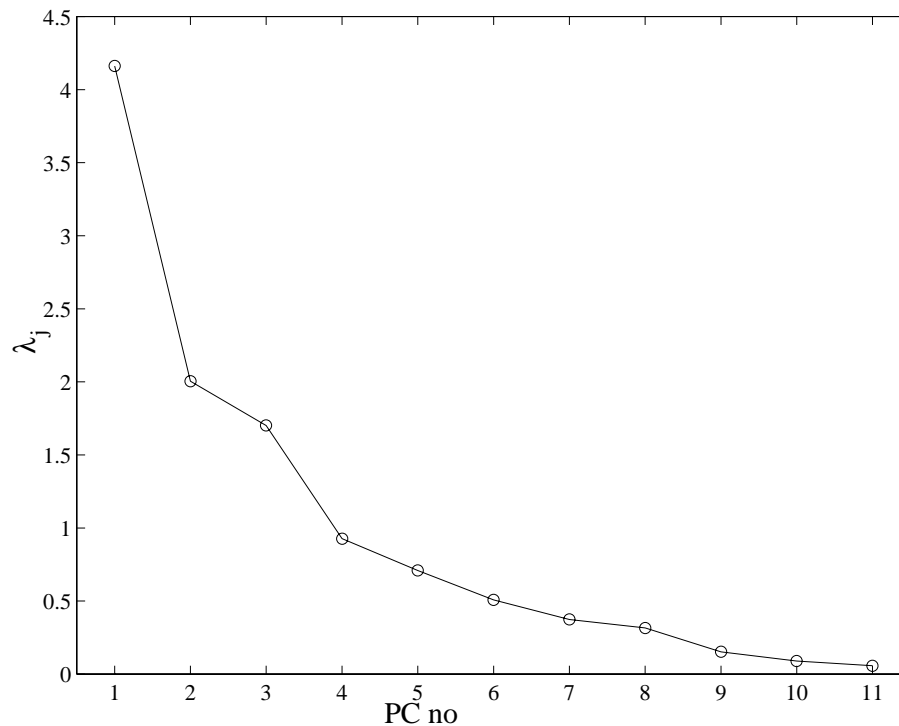
**Figure 6.4**   The eigenvalues associated with the principal components in a PCA model.

plot, this may indicate a good choice of the number of components (Wise and Gallagher 1996). In this case, a reasonable choice of the number of components retained in the model may be 4. Knees in the eigenvalue plot can be further accentuated if the squares of the eigenvalues are plotted.

## Outliers in Training Data

Once a model has been built, there may be sample values not consistent with the model behaviour. There are various techniques available to decide whether a sample is in agreement with the model or not (Wise and Gallagher 1996). The $SPE$ and $T^2$ measures of the training data can be used to decide whether a sample is representative for the process mode or not. Caution must be taken though, when using the confidence limits as limits for outliers. Firstly, the limits are calculated based on the assumption of normally distributed variables, and secondly, if the amount of training data is great, representative samples will exceed the limits. In Figure 6.5, the $SPE$ (top) and $T^2$
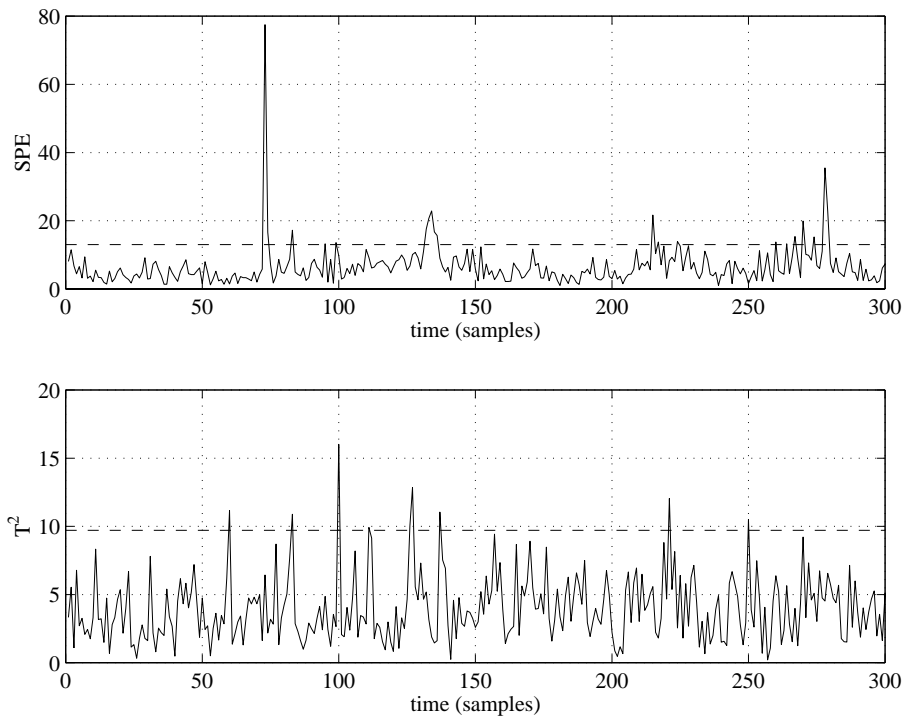
**Figure 6.5**   The $SPE$ (top) and $T^2$ (bottom) residuals with approximate
95 % limit.  Probable outliers can be seen at sample 72 and
100.

(bottom) measures are plotted. At least sample 72 in the top figure
and sample 100 in the bottom figure ought to be further investigated.
If the deviating samples are believed to represent a true event in the
process, they should be kept. A similar situation may occur in the
future, and the information is then critical for predictive performance.
If the samples are believed to be outliers and thus not representing a
true deviation of the process, they ought to be removed in order to ob-
tain a good model. However, depending on the model, the method to
treat outliers differ. In a static model, erroneous samples can simply
be removed. No consideration to the history is taken, and the order of
the samples is not important. If the model is dynamic, that is a FIR
or IIR model has been developed, the time is important. Therefore, it
is not possible to simply remove a sample. Instead, the sample must
be replaced with an estimated value as discussed in Chapter 4.

# 6.3   On-line Monitoring

On-line monitoring of measurement variables aim at continuously ana-
lyse and interpret the measurements in order to detect and isolate
disturbances and faults. MVS provide us with tools for analysis and
interpretation. An important part of the analysis and interpretation
is visualisation of the measures and variables.

## Visualisation

In order to present variables and measures discussed in this chapter,
different methods for visualisation can be used. The visualisation
methods must be easily interpretable and comprehensible, so that the
key features of the present situation can easily be extracted. If a
disturbance or failure occurs, the operator should not have to spend
precious time to interpret the information presented.

### SPE and $T^2$ plots

The most basic way to present the results from a PCA monitoring
model is to monitor each principal component individually in a time
series plot. The number of principal components is hopefully fewer
than the original number of variables, but there may still be a con-
siderable number of variables to view. The $SPE$ and $T^2$ measures,
however, describe the statistical fit of the model. This means that if
one or a few variables are deviating from the normal model area, the
$SPE$ and/or $T^2$ measures will increase. $SPE$ and $T^2$ plots with con-
fidence or alarm limits are very effective for the initial detection task.
When the measure exceeds a certain threshold, an alarm or detection
is triggered. Figure 6.6 shows how a large disturbance at sample 230
affects $SPE$. The effect on $T^2$ is shown i Figure 6.7.

### Score Plot

Monitoring of the $SPE$ and $T^2$ residuals is effective, but not partic-
ularly transparent. The dimension reduction capability of MVS can
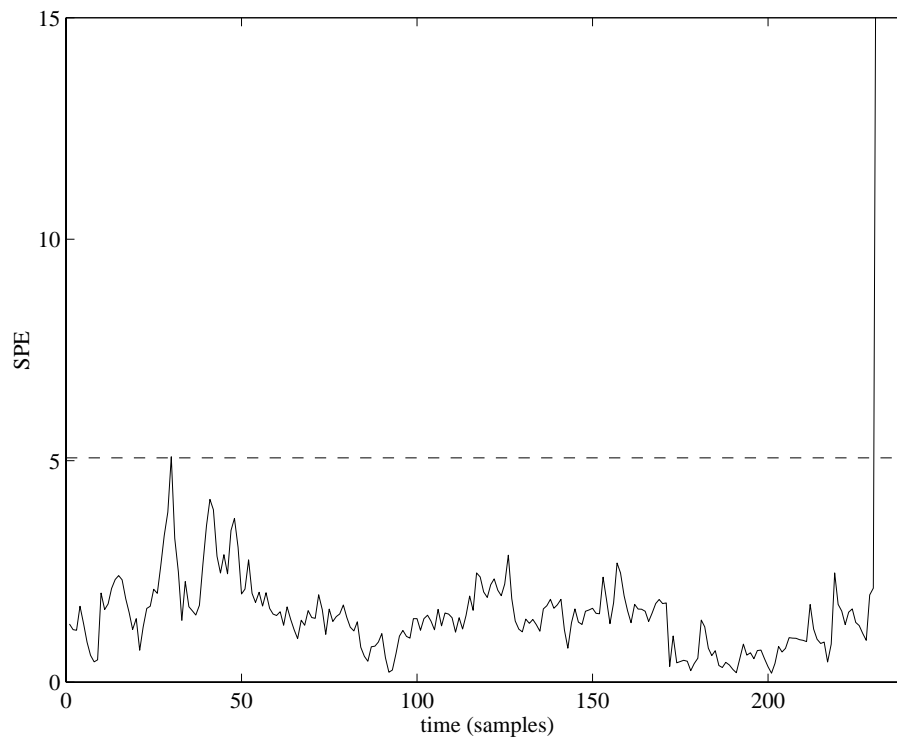
**Figure 6.6**   The $SPE$ residual with the approximate 95 % confidence limit. A disturbance is visible at sample 230.
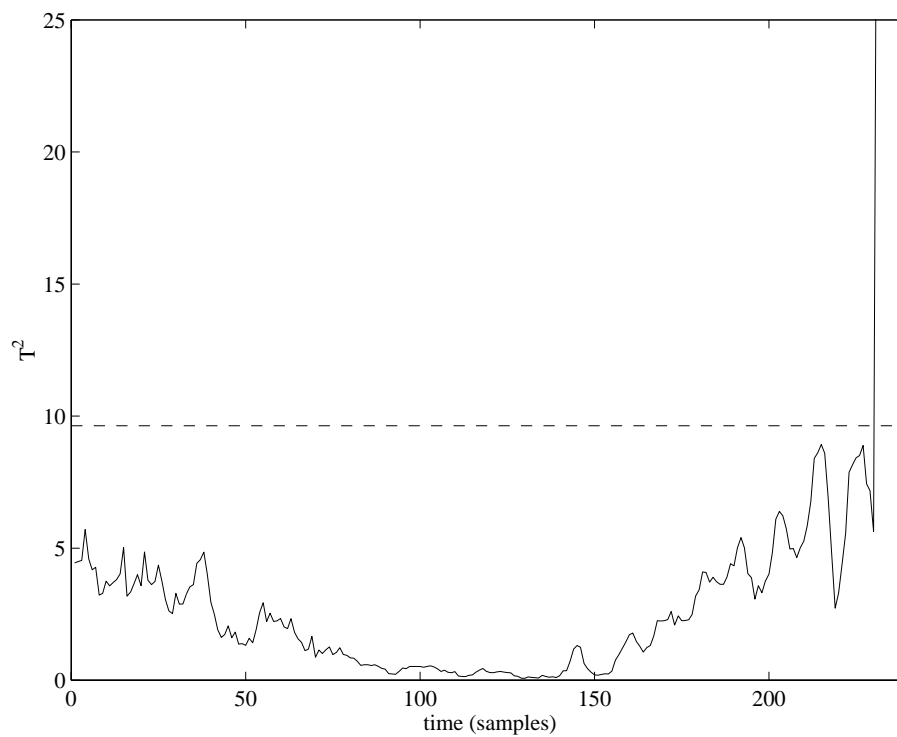


**Figure 6.7**   $T^2$ residual with 95 % confidence limits. A disturbance is visible at sample 230.
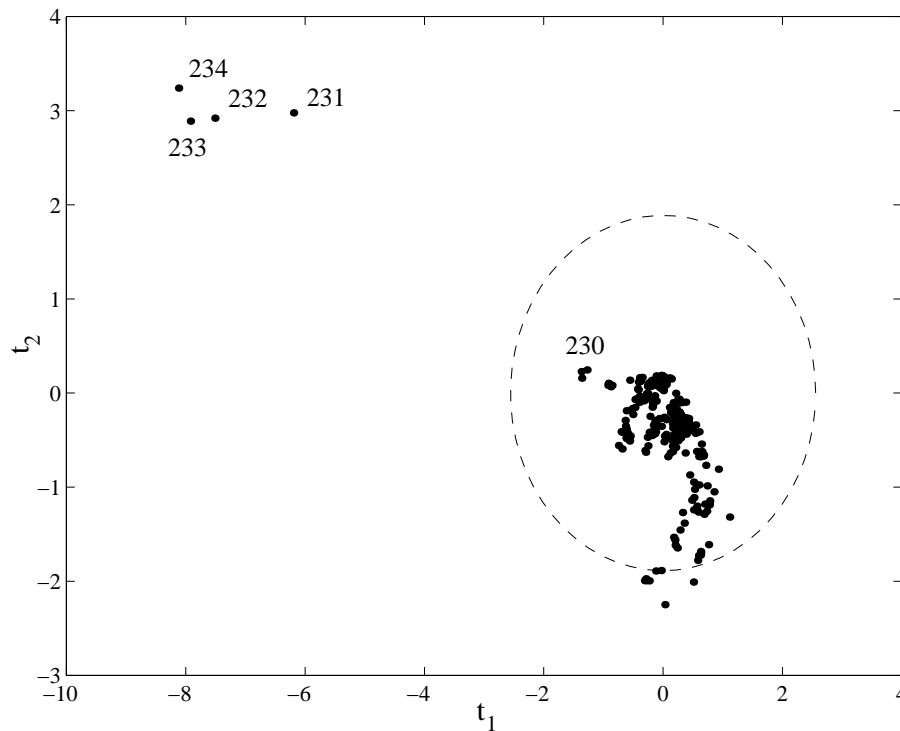
**Figure 6.8**  The scores of the first and second principal component with approximate 95 % confidence limits.

be used to visualise the process status changes in a two- (or perhaps, three-) dimensional plot. As mentioned before, the nature of most industrial processes implies that just a few latent variables or principal components will cover most of the variability in the process space. The MVS algorithms give us the principal components or latent variables which describe the variability in descending order, and the first few variables cover a great part of the total variability of the process. By plotting, for instance, the first score vector against the second score vector, the process changes can be viewed as a point moving around in the plane as new samples are added. Points that cluster represent similar process behaviour and, consequently, deviating points indicate process changes. This makes the score plot comprehensible and usable for classification purposes. In Figure 6.8, such a plot is shown. The data are the same as in Figure 6.6 and 6.7. Every dot represents the values of the first and second scores at a point in time. Under normal operating conditions the centre of gravity of the points ought to be close to the origin, due to the mean centring of data. Points far from the origin indicate a disturbance and, consequently, the operational mode is not longer classified as normal. To be able to differ between
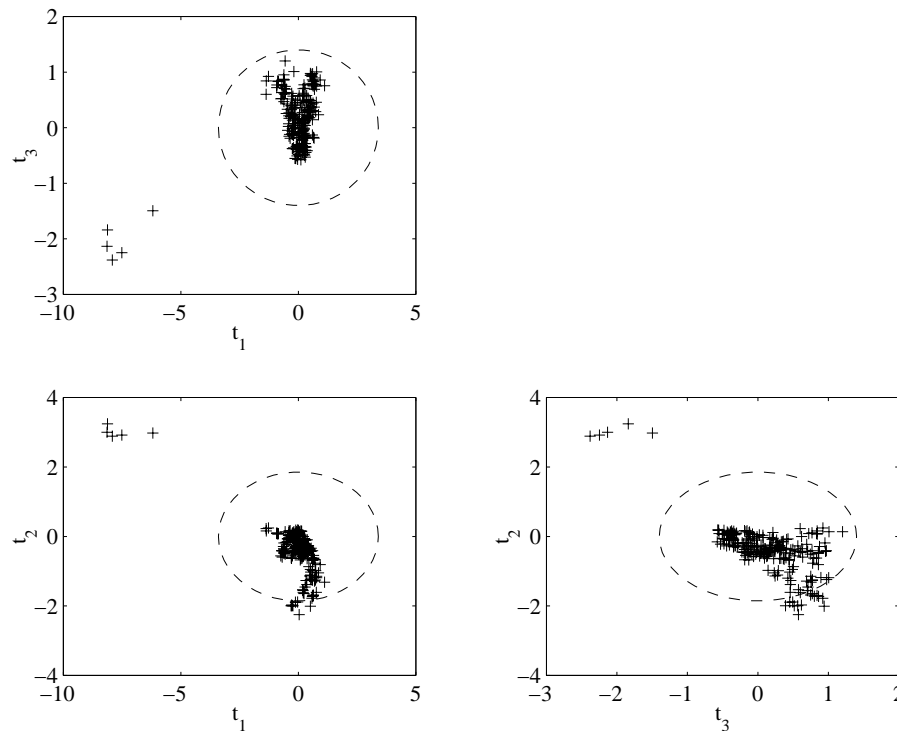
**Figure 6.9**   The scores on the first, second and third principal component
with 95 % confidence limits.

*in-control* variations (that is variations within the normal operation)
and disturbances, control limits can be used. The ellipse in Figure 6.8
represents the 95 % confidence limits of the first and second training
data score vectors. These limits are calculated using Equation 6.24.
Other limits, such as limits based on quantiles or strictly empirical lim-
its, can be used to indicate whether the process is in control or not.
The disturbance indicated by the $SPE$ and $T^2$ plots, can here be seen
as a significant deviation from the origin, far outside the confidence
limit.

It is not always sufficient to monitor the first and second PC (or LVs).
When it is established that only two PCs do not cover enough vari-
ability of the process, three dimensions can be used. There are little
use to visualise all three dimensions in one figure. Instead the result
can be presented as shown in Figure 6.9. Here the axes are defined by
$\mathbf{t}_1, \mathbf{t}_2$ and $\mathbf{t}_3$. It is not as comprehensive as a score plot with $\mathbf{t}_1$ and
$\mathbf{t}_2$, but it is still an improvement compared to monitoring all original
variables.

## Rate of Change

The process status changes within the PC space may reveal interesting information. Fast changes in the process, even though they are inside the defined normal region indicate that the process is not stable (according to the measurements). The Euclidian distance between every sample in the PC space is:

$$d_e(k) = \sqrt{\sum_{j=1}^{a} \Delta t_j^2(k)} \tag{6.52}$$

where $a$ is the number of components retained in the model

$$\Delta t_j^2(k) = (t_j(k) - t_j(k-1))^2 \tag{6.53}$$

The intersample distance $\mathbf{d}_e$ normally changes with high frequency. A single large change is perhaps not interesting. Instead, if there are several consecutive samples with great intersample distance this may be valuable information. Therefore, it is sometimes convenient to filter $\mathbf{d}_e$ with, for instance, a median filter prior to using it for detection.

## Isolation

The monitoring charts described above are efficient to detect deviations from the normal situation, but the reasons for the deviations are not indicated. The process location in two- (or three-) dimensional score plots provide information that can be linked to specific events by experience. An expert system, based on historic data and experience, may then be used to derive the possible causes for a disturbance. Classification algorithms, using the tendency of data to gather in clusters in the process space are also a possible way forward. However, there is more information to gain from a deeper investigation of the PCA model. When a disturbance is detected in score plots or $SPE$ and $T^2$ plots, a physical interpretation can be found by transforming the model output to the original process space. So called *contribution plots* can isolate the variable/variables that has/have caused the deviation.
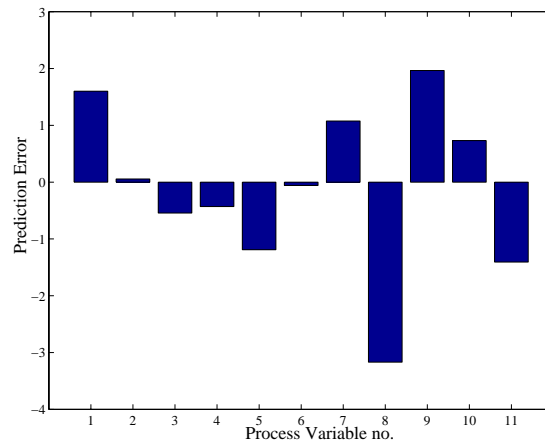
**Figure 6.10**   The contribution of every variable to the prediction error at sample 243.

## Prediction Error Contribution

In Equation 6.27, $SPE(k)$ is defined as the sum of squares of $\mathbf{e}(k)$. Thus, the vector $\mathbf{e}(k)$ contains information on the individual prediction errors of each process variable at sample $k$. By plotting $\mathbf{e}(k)$ as a bar graph, the contributions to $SPE(k)$ can be viewed (Figure 6.10). The relative size of the bars indicates the contribution from each variable to the prediction error, or lack of fit of a sample to the model. In some situations, when the $SPE$ measure is varying, it is a good idea to use a mean of the contribution to $SPE$. This is done by replacing the vector $\mathbf{e}(k)$ by a vector expressing the mean error over a period of length $l$. The delay introduced by the mean filtering makes this less applicable in on-line situations.

## Score Contribution

When $T^2$ exceeds it limits, the contribution to the $T^2$ measure is of interest. In Equation 6.36, $T^2$ is defined as the normalised sum of scores. Another way of expressing Equation 6.36 is:

$$T^2(k) = \frac{t_1^2(k)}{\lambda_1} + \frac{t_2^2(k)}{\lambda_2} + \ldots + \frac{t_a^2(k)}{\lambda_a} \qquad (6.54)$$

where $t_j(k)$ is the score and $\lambda_j$ is the eigenvalue associated with the $j$th principal component. The score,which gives the largest contribution to $T^2$, is the score associated with the largest term in Equation 6.54. The
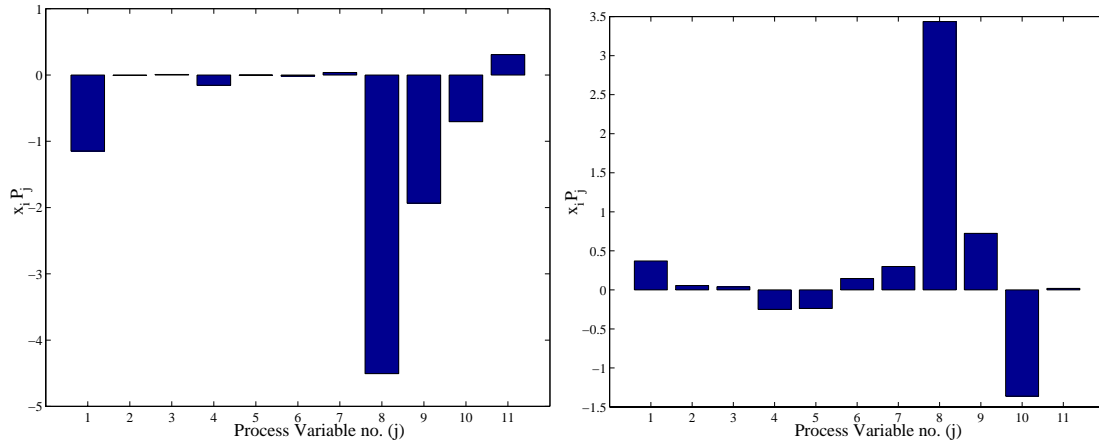
**Figure 6.11**   Variables contributing to the deviation from origin along PC
no 1 (left) and PC no 2 (right) at sample 234.

next step is to find which physical process variables have contributed
to the score deviation. If the data are mean centred, it can be seen
from Equation 6.54 that $T^2$ becomes large when the scores are far
from zero. The variables that have forced the score away from zero
along the $j$th PC can be found by:

$$\mathbf{c}(k) = \mathbf{x}(k)\mathbf{P}_j \qquad (6.55)$$

where $\mathbf{c}(k)$ is a vector with the contributions from each process vari-
able at time $k$. $\mathbf{P}_j$ is the diagonal matrix of the row vector $\mathbf{p}_j$. If PLS
is used the $\mathbf{P}_j$ can be exchanged by $\mathbf{W}_j$ (MacGregor *et al.* 1994). A
bar graph of the contribution to the score changes along the first and
second PCs is shown in Figure 6.11.

A second way to isolate deviating variables is to investigate the *change*
of the score from a sample when the score was inside its limits to a
sample outside the limits, *i.e.*:

$$\Delta\mathbf{x}(k) = \mathbf{x}(k) - \mathbf{x}(k - l) \qquad (6.56)$$

where $\mathbf{x}(k - l)$ represents a sample with normal process behaviour.
When this method is used, $\mathbf{x}(k)$ in Equation 6.55 is replaced by $\Delta\mathbf{x}(k)$.
It is often necessary to look at the movement along more than just
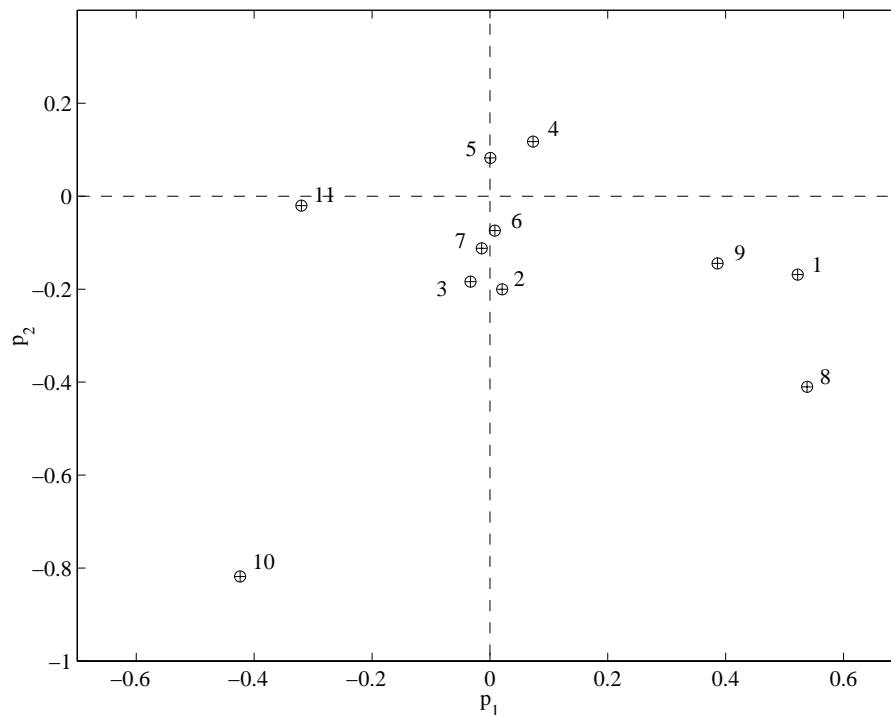one PC and score plots suggest along which PC the deviation is large.

**Figure 6.12**   A load plot indicates variables that have similar impact on the process. The plot also shows how the process status moves when a variable is changed. This can be used to determine possible counteractions.

## Counteractions

The score plot forms a composite representation of the process status changes in the space defined by the principal components. Plotting the loads instead, a picture of the relations between the original variables appears. Clustering points in such a plot, indicate variables that affect the process in a similar way. A score plot can be used to gain information on how changes in original variables move the process point in the PC space. In Figure 6.12, the first and second loading vectors from the previous example are plotted against each other. Variables near each other influence the process in a similar way and the distance from the origin depicts the relative force of the influence in the PC plane. By looking at the load plot, variables that drive the process back to the origin can be established for each disturbance event. In this way, if some of the variables are controlled, it is possible to determine variables that will drive the process back to the normal region. The plot can be used as control strategy advise for the operators.

## Monitoring Slowly Changing Conditions

MVS based methods are sensitive to long-term trends in one or several of the independent variables. For instance, the centre of the samples in the score plot will slowly change, and the boundaries defining the normal region or other classification regions, will not be correctly located. The simplest way to solve this problem is to exclude variables that show indications of long-term trends. However, exclusion is not always feasible as it will lead to information loss. If information on the long-term trends is available, it can be compensated for.

It is difficult to find a model that covers all the situations occurring in a process. A model performing satisfactory during certain operating conditions, may be far from usable during other conditions. Radically changed conditions sometimes call for different control strategies and, consequently, different monitoring models. It is, therefore, sometimes necessary to have several models to choose from, all adapted to specific operating conditions. During transition periods several models can be run in parallel. The model showing the best fit is then used.

Slow variations in the surrounding conditions could possibly also be addressed by updating the detection model. New models can be continuously built from a certain number of historical data. The performance of a new model is compared with the performance of the model which is currently used, and if the new model performs better, the old model is exchanged. In this way slow variations are taken into consideration but there is a risk that the model will not detect other, undesirable, slow variations as it adapts to these as well.

## 6.4   Classification of Operational Modes

Since we are able to analyse many variables simultaneously, MVS provides us with tools for describing the process conditions, or the *operational mode* of the process. Descriptions of operational modes can be divided into two groups depending on what they are aiming at describing. *General* operational modes indicate the general conditions of the process and are described by as many information contributing variables as available. From the general mode description an overall

evaluation of the process can be made. A possible tool for describing the general operational mode is principal component analysis (PCA). In PCA, the analysis emphasises the description of the variability of the process variables (the $X$-block) with no regard to any specific target variable. However, it is sometimes convenient to define modes based upon a specific variable, for instance, an effluent quality variable of great interest. In this case the specific mode is described by the variables most influential to the effluent quality variable. For instance, projection to latent structures (PLS) provides us with a way of doing this, as PLS aims at describing the variability of the process variables (the $X$-block) influencing one or several quality variables (the $Y$-block).

## Qualitative and Quantitative Definitions of Modes

There are two ways to define an operational mode. Firstly, the mode can be defined as a mode with a physical interpretation. Such modes may typically be night, rain, winter and so on. The mode is then linked to the numerical characteristics of the measurement data during such operational periods. Thus, the mode is pre-defined and defined qualitatively and then characterised by the numerics. However, this approach yields overlapping modes, which may result in misclassifications or ambiguous classification of the mode. When a specific operational mode is defined, the qualitative criteria for different modes can be linked to the quality variable ($Y$-block). For instance, the modes can be chosen in such a way that there is a mode for high, normal and low level of a certain quality variable.

Secondly, the mode can be defined directly from the numerical characteristics of the measurement data and then labelled in a suitable way. Consequently, the mode is defined quantitatively and then addressed by a qualitative label. Typical examples of numerical modes are normal, abnormal, upper right corner (in a two-dimensional process variable or latent variable space) and so on. The quantitative modes can sometimes be linked to more interpretable and qualitative labels, but this is not true for all modes. However, the classification is reduced to the location in a space and is not ambiguous. A quantitative description of specific operational modes gives some qualitative
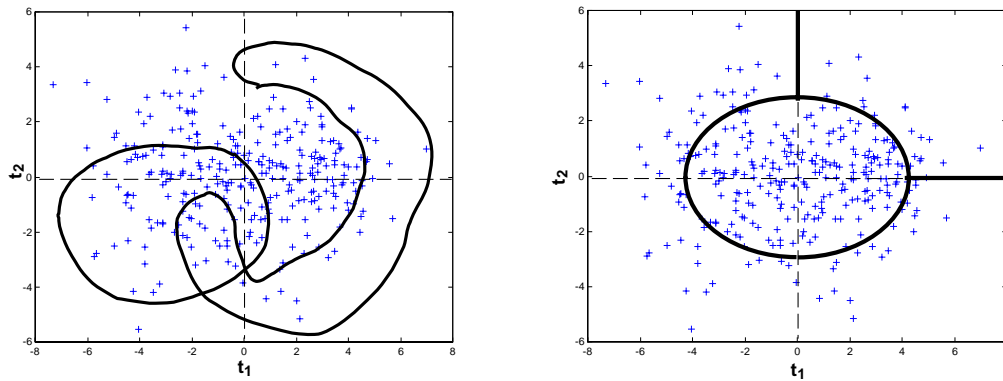
**Figure 6.13**   The mapping of two qualitative operational mode definitions (left) and two quantitative mode definitions (right) into a numerical space.

interpretation of the modes, since the modes are defined with a specific quality variable in mind. However, it may not be possible to link the modes directly to a variable level.

What type of mode definition to use, depends on the aim of the detection task. Under some conditions, qualitative and quantitative definitions may coincide, and that makes the choice easy. However, the quantitative approach is more suitable for the methods presented in this thesis, since it is based on the numerical characteristics of data. Figure 6.13 shows an attempt to illustrate the difference between qualitative and quantitative mode definitions.

## Detection of Operational Modes

The ability to detect and determine the present operational mode is useful in many ways. The most obvious reason for detecting a change in operational modes is to inform the operators and process engineers that something is happening with the process. Secondly, a new operational mode may demand a different control strategy. The goals of the control system during normal conditions may differ significantly from the goals during, for instance, rain events or toxic shocks. Thirdly, it is sometimes wise to have several models for different situations, as a general model often becomes too general and, therefore, not informative. Detection of new operational modes may then be used to trigger

a change of models.

Detection of different operational modes is a task of classifying the present mode as one of the modes available or by defining a new class if no mode covers the current situation. The classification can be carried out in different ways. In the case when there are normal and abnormal modes, the classification is reduced to determine whether the present operational mode is within the limits for normal operation (binary classification) or not. In the case where there are many modes available, the classification is straightforward if the modes are defined as quantitative modes since the mode is directly determined from the process location in the PC space. However, if the modes are defined qualitatively, the class membership may be ambiguous and an evaluation of the class membership must be carried out.

## Binary Classification

If the aim of the classification is to determine whether the process is in a normal operating mode or not, the $SPE$ and $T^2$ measures provide us with information on this. Limits can be imposed on these measures. Exceeded limits indicate an abnormal mode (see Figures 6.6 and 6.7). Classification can also be done with the use of score plots, *i.e.* by using the ellipse defining the normal region (see Figure 6.8). The limits can be statistical confidence limits, empirically established limits or limits corresponding to physical conditions. Due to not evenly distributed measurements, the use of ellipses as class boundaries is not always suitable. The process representation may very well move along a path with little resemblance to an ellipse. Instead, empirically found boundaries can be defined. It is important that the model represents the mode that is normal or desired, and that it is not too sensitive to minor faults that do not influence the product quality or endanger the safety of the process.

## Multiple Classes

To take full advantage of the capability of MVS, more classes than normal and abnormal can be defined as regions in the PC space. As we have seen before, different disturbances will locate the process in

different regions in the PC space. By linking these regions to different disturbance types it is possible to quickly establish the present operational mode and decide upon appropriate counteractions. The task of defining the regions can be carried out both off-line and on-line. When classes are defined off-line, the training data must contain data from all the operational modes that the model is designed to classify. Using PCA, general mode regions can be determined by looking at the data in a score plot and manually define different operational modes based on the process location in the PC space. When PLS is used, restrictions on the $Y$-block can be used to define regions in the PC space, *i.e.* specific operational mode regions.

When the classes are defined on-line, the model is built from normal operating data. When disturbances occur, the regions into which the process representation moves, can be determined and linked to the present disturbance. In this way, normal data will fit the model well, but when disturbances arise, the fit may decrease significantly. The way to accomplish this depends on the use of the model and the desired sensitivity.

**Cluster Classification**

When the class regions are determined (or rather the class membership for the instances in the training set), the *k-nearest neighbours* algorithm can be used in order to automatically find the class of a new sample. In $k$-nearest neighbours, a new point in the $a$-dimensional PC space is simply assigned the most frequent class of the $k$-nearest neighbours. Thus, the training set in the $k$-nearest neighbours method is here the score matrix ($\mathbf{T}$) with classes assigned to every row. When new data are applied, the distance between the new point ($\mathbf{t}_{new}$) and every point in PC space corresponding to the training set is calculated as the Euclidian distance:

$$d(\mathbf{t}_{new}, \mathbf{t}_i) = \sqrt{\sum_{r=1}^{a} (t_{new,r} - t_{i,r})^2} \qquad (6.57)$$

where $\mathbf{t}_i$ is the $i$th row in $\mathbf{T}$ used as training data. The class membership of the $k$-nearest training points are investigated and the most common class is assigned to $\mathbf{t}_{new}$. In this way every new sample of $\mathbf{T}$
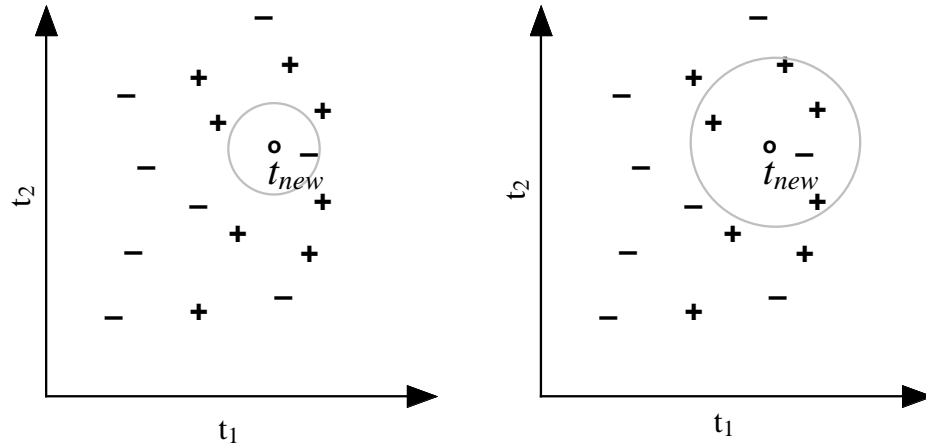
**Figure 6.14**   A 1-nearest neighbour algorithm classifies $\mathbf{t}_{new}$ as negative (left) whereas a 5-nearest neighbour algorithm classifies $\mathbf{t}_{new}$ as positive.

can be assigned a class. In Figure 6.14, a set of training points can be viewed along with their values (or classes) in a two-dimensional space. A new instance $t_{new}$ is located in the space as well. Let $\mathbf{t}_1$ to $\mathbf{t}_k$ be the $k$-nearest neighbours from the training examples. If a 1-nearest neighbour algorithm is used the classification of $\mathbf{t}_{new}$ is negative. However, looking at the training data it is more likely that $\mathbf{t}_{new}$ is positive and a 5-nearest neighbour algorithm classifies $\mathbf{t}_{new}$ as positive. The procedure can be extended to handle continuous outcomes. Instead of assigning the most frequent outcome of the $k$-nearest neighbours, a mean of the outcomes can be assigned.

## 6.5   Other Detection Techniques

This thesis focuses on MVS based methods for detection or classification of operational modes. The examples in Chapters 7 and 8 are, consequently, based on MVS methods. However, there are many other alternatives available for analysis of multivariate data and a short description of some groups of methods is appropriate. The practicability of different methods depends on data and the aim of the analysis. In Figure 6.15, a unifying perspective of available methods is shown. Es-
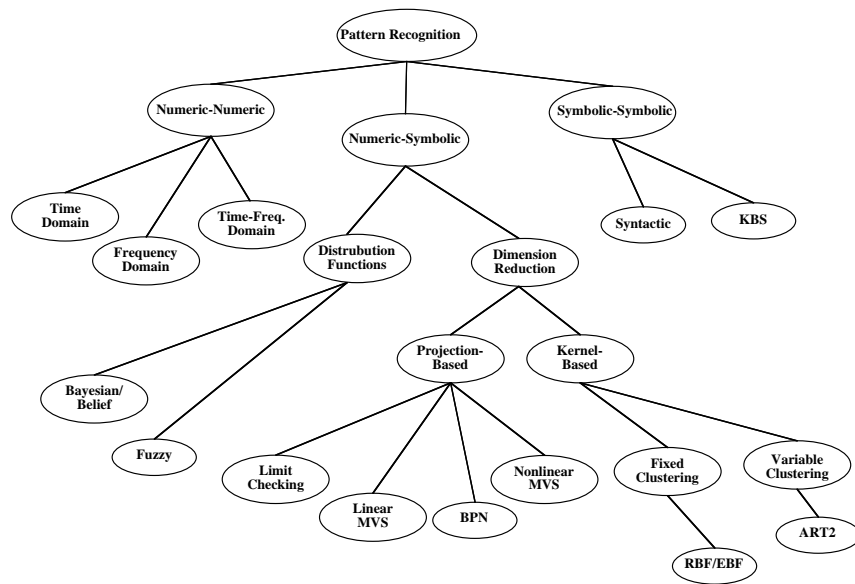
**Figure 6.15**   Unifying view of methods for data analysis usable for operational mode classification (Davis *et al.* 1996).

tablishing the operational mode is, as mentioned before, a task of recognising specific process fingerprints or patterns, characteristic of different operational modes. According to Davis *et al.* (1996), there are three distinct components involved in pattern recognition:

1. *numeric-numeric* analysis or pre-processing of data;

2. *numeric-symbolic* analysis, which constitutes the core of process monitoring techniques;

3. *symbolic-symbolic* analysis, which typically consists of knowledge-based systems.

In order to extract the maximal amount of information from on-line data, combinations of the above listed components may prove successful and comply well with the idea of $D^2C$ described in Chapter 3.

## Numeric-numeric

Numeric-numeric methods for feature extraction is basically what has been discussed in Chapters 4 and 5.

## Symbolic-symbolic

Knowledge-based systems (KBS) belong to this group of analysis methods. KBS can be developed using expert knowledge, as in expert systems, or from different kinds of inductive inference engines applied directly to data. KBS is often used on a higher abstraction level, not directly linked to measurements. Due to the extensive knowledge required for building, KBS is normally not used in monitoring applications. However, KBS can be effective as an advisory tool for operators in abnormal situations.

## Numeric-symbolic

This group of methods comprises *distribution-function* based as well as *dimension-reduction* based methods. MVS based methods are considered as dimension-reduction methods together with, for instance, *artificial neural networks* (ANN). A combination of MVS and ANN is proposed by Qin and McAvoy (1991). However, a few words about distribution-function based techniques are appropriate. These techniques are based on calculation of the class membership probabilities or possibilities. In *Bayesian decision theory*, a decision on class membership is made upon calculations of the probability that a particular pattern can be associated with a specific class or label. A problem with Bayesian decision theory is that it requires a great deal of information on *a priori* probabilities, which is often not available in many possible applications. *Fuzzy-set theory* describes numerical data qualitatively by specifying how well data satisfy qualitative descriptions of the measured feature.

A guide to available methods in the field of process monitoring can be found in Kramer and Mah (1994) or Davis *et al.* (1996).

# Chapter 7

# MVS Applied to Simulated Data

In this chapter, monitoring of simulated data is discussed. There are
mainly two reasons for using simulated instead of real data. Firstly,
available data may have low quality, which makes it hard to isolate
the process disturbances from other disturbances related to the meas-
urement system. Secondly, the desired excitation of the system does
not appear. The question is then: what is the use of the models if
they do not work in real situations? On the other hand, in order to
develop adequate methods, which may work in real situations, simu-
lations are a useful method for evaluation and validation. If a method
does not work with simulated data, it will certainly not work in reality.
Studying simulated data enable us to mimic failures and disturbances,
occurring rarely in reality, and test the methods in situations not rep-
resented in available real data. As the next logical step, it is necessary
to validate the methods in real situations to be able to really speak of
their applicability.

## 7.1   Creating Simulated Data

It is important that the model used to produce data, is adequate and
has demonstrated its ability to mimic the behaviour of the true pro-
cess. The IAWQ Activated Sludge model No.1, or ASM1, (Henze, *et
al.* 1987) was developed by a task group appointed by the *Interna-
tional Association on Water Quality* (IAWQ) and models biological
carbon and nitrogen removal. The ASM1 has been used in many ap-
plications during the last decade, and many references can be found
in the literature on its performance and validity (Dold and Marais
1986; Dold *et al.* 1991). ASM1, or derivatives thereof, is used in
most commercial simulation packages for wastewater treatment avail-

able today.  Since the ASM1 only describes the biological reactions, the model must be supplemented by a settling model. In this chapter, only the biological reactions are taken into account and, consequently, a fairly simple settler model is adequate.

## Ensuring the Credibility

When simulation models are used to produce wastewater treatment data, the credibility of the experiment is inevitably decreasing. However, there are a several ways to make the simulations more realistic:

- *Choice of model* - the model used must be adequate for the purpose and the model parameters must have reasonable values. In this work, the ASM1 model is used with default parameter values (if nothing else is indicated).

- *Influent data* - the input (influent) data to the model must be as realistic as possible. This implies variations, noise and disturbances. The influent files used here are hybrids of real and manipulated data. The data are developed by a working group on operation of wastewater treatment plants within the European scientific research exchange programme COST 682 (Vanhooren and Nguyen 1996).

- *Noise* - applying noise to the variables assumed to be measured mimics the disturbances of a real measurement system. The applied noise contains both high frequency noise and outliers.

- *Variables* - only the variables possible to measure should be used. Thus, no information not readily available at a plant can be used for detection purposes.

### Choice of Model

The ASM1 is today probably the most widely used model for describing the kinetics of activated sludge systems, including organic carbon and nitrogen removal. The model chosen here for creating simulated

data is based on a study currently undertaken within the earlier mentioned COST group. The model is implemented in Simulink, which is a simulation package for MATLAB users.

**Influent Data**

The development of the influent data is described by Vanhooren and Nguyen (1996). However, a short description is appropriate. Influent data have been constructed for a period of 7 days. There are three separate influent data series representing dry weather, dry weather with two different storm events and dry weather with a longer continuous rain. The data series can be used repeatedly to simulate longer periods of time. Influent flow rate data are based on data from a large activated sludge plant. However, some modifications have been performed, based on available information on influent flow characteristics. The data have been scaled from an average of $\approx 75.000 \ m^3/$day to $\approx 18.400 \ m^3/$day to suit the size of the modelled plant.

**Noise**

To mimic the presence of measurement and random high frequency process disturbances, a filter adding noise to every measured variable is applied. This can be done by just adding a mean centred normally distributed white noise with appropriate variance. However, such an approach will not mimic true disturbances especially well. Instead, a filter creating noise with significant "outliers" is used. The filter model can be expressed as:

$$e(k) = 0.4e(k-1) + 0.8e(k-1)z(k-1) + z(k) \qquad (7.1)$$

where $e(k)$ is the noise at time $k$ and $z(k)$ is normally distributed white noise. The new "distorted" signal is then:

$$y_n(k) = max(0, y(k) + e_a(k)) \qquad (7.2)$$

where $e_a$ is the result of mean centring and scaling to an appropriate variance of $e$. The limitation is due to the fact that most measurement systems do not produce negative values. The filter produces an output with good resemblance to noise found in real measurements. In Figure

7.1, an output of the model can be seen before and after applying the filter discussed above.
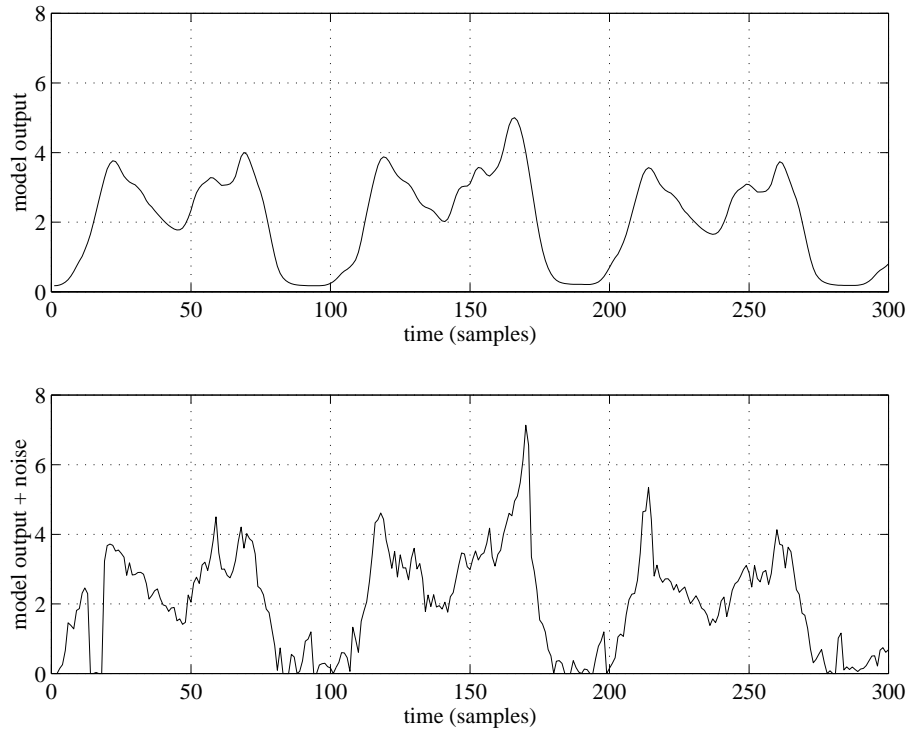


**Figure 7.1**   Model output (top) and model output with noise added (bottom).

## Variables

No variables not available with today's measurement technology should be used. This implies that many of the state variables in the ASM1 remain unknown for the user of the simulated data. This approach ensures that the internal structure of the model is not used to derive states, that cannot possibly be known at a real plant.

## The Activated Sludge Model No.1

A brief presentation of the the Activated Sludge Model No.1 (ASM1) model is given here. The model state variables, dynamics and parameters are discussed.

## State Variables

The state variables included in the ASM1 are listed in Table 7.1. The state variables differ somewhat from the ones we normally measure and observe at a plant and so do the units. Organic matter and dissolved oxygen have the unit mg COD/l. The nitrogen fractions have the unit mg N/l, and the unit for alkalinity is moles $HCO_3^-/m^3$.

| Symbol | Variable |
|--------|----------|
| $S_I$ | Inert organic matter |
| $S_S$ | Readily biodegradable substrate |
| $X_I$ | Particulate inert organic matter |
| $X_S$ | Slowly biodegradable substrate |
| $X_{B,H}$ | Active heterotrophic biomass |
| $X_{B,A}$ | Active autotrophic biomass |
| $X_P$ | Particulate product from biomass decay |
| $S_O$ | Dissolved oxygen |
| $S_{NO}$ | Nitrate and nitrite nitrogen |
| $S_{NH}$ | Ammonia nitrogen |
| $S_{ND}$ | Biodegradable organic nitrogen |
| $X_{ND}$ | Particulate biodegradable organic nitrogen |
| $S_{ALK}$ | Alkalinity |

**Table 7.1** The states of ASM1 model.

At the plant the total suspended solids (TSS) is normally measured. Therefore, the particulate matter must be converted to $TSS$. Henze *et al.* (1995b) proposed following conversion:

$$TSS = 0.75(X_I + X_P + X_S) + 0.9(X_{B,H} + X_{B,A}) \qquad (7.3)$$

## Dynamic Processes

There are eight different dynamic processes in the ASM1 model describing the dynamics.

- *Aerobic growth* of heterotrophs - readily biodegradable substrate, dissolved oxygen, ammonia and alkalinity are consumed and heterotrophic biomass is produced. The growth is modelled by a Monod expression.

- *Anoxic growth of heterotrophs* - readily biodegradable substrate, nitrate (nitrite) and ammonia are consumed and heterotrophic biomass and alkalinity are produced. The growth is modelled by a Monod expression.

- *Aerobic growth of autotrophs* - dissolved oxygen, ammonia and alkalinity are consumed and autotrophic biomass and nitrate (nitrite) are produced. The growth is modelled by a Monod expression.

- *Decay of heterotrophs* - heterotrophic biomass is decomposed into slowly biodegradable substrate and other particulate products.

- *Decay of autotrophs* - autotrophic biomass is decomposed into slowly biodegradable substrate and other particulate products.

- *Ammonification of soluble organic nitrogen* - biodegradable organic nitrogen is transformed to ammonia. Alkalinity is produced.

- *Hydrolysis of entrapped organics* - slowly biodegradable substrate is transformed to readily biodegradable substrate.

- *Hydrolysis of entrapped organic nitrogen* - particulate biodegradable organic nitrogen is transformed to biodegradable organic nitrogen.

The processes are also included in the matrix describing the ASM1 model in presented Appendix C.

## Parameters

The kinetic and stoichiometric coefficients of the ASM1 model must be given values. The task of determining these values is known as model calibration. If the model is used to simulate a specific plant, the calibration must be carried out for this plant. This implies long experiments at pilot and bench-scale plants. In Appendix C, the parameter values suggested by the IAWQ task group are presented. The values can be used when no further information is available, or when the task is to model a plant in general.

# Settler Model

The settler model used in the simulation model is known as a *one-dimensional layer model*. One-dimensional models only describe the settling process along the vertical axis, leaving only cross-sectional area and depth as design parameters. The one-dimensional layer model is thoroughly described in, for instance, Jeppsson (1996) and only the basic ideas behind the model will be presented here.

## Layers

The idea behind one-dimensional layer models is that the settler is divided into a number of layers. The mass balance for each layer is calculated, assuming complete mixing within each layer. The sludge transport between the layers is assumed to depend on two mechanisms; *bulk movement* and *gravity settling*. The bulk movement is caused by the hydraulic flow and can thus be directed both upwards and downwards. A feed layer must be determined. Above the feed layer the bulk flow is directed upwards, corresponding to the effluent flow ($Q_e$). Consequently, below the feed layer the bulk flow is directed downwards, corresponding to the underflow ($Q_u$). However, the gravity settling is always directed downwards due to the gravity action on the sludge. In Figure 7.2, the principle of the one-dimensional layer model is shown.

## Settling Velocity Functions

Many different settling velocity functions can be found in the literature. Traditionally, the settling velocity function is based either on an *exponential* or a *power* function, where the settling velocity only depends on the local concentration. In the model used in this study, the *double-exponential* settling velocity function is used. In this function, consideration is taken to the fact that low concentrations result in a low settling velocity. The function is defined as (Takács *et al.* 1991):

$$v_s = max\left(0, \, min\left(v_0', \, v_0\left(e^{-r_h(X-X_{min})} - e^{-r_p(X-X_{min})}\right)\right)\right) \qquad (7.4)$$
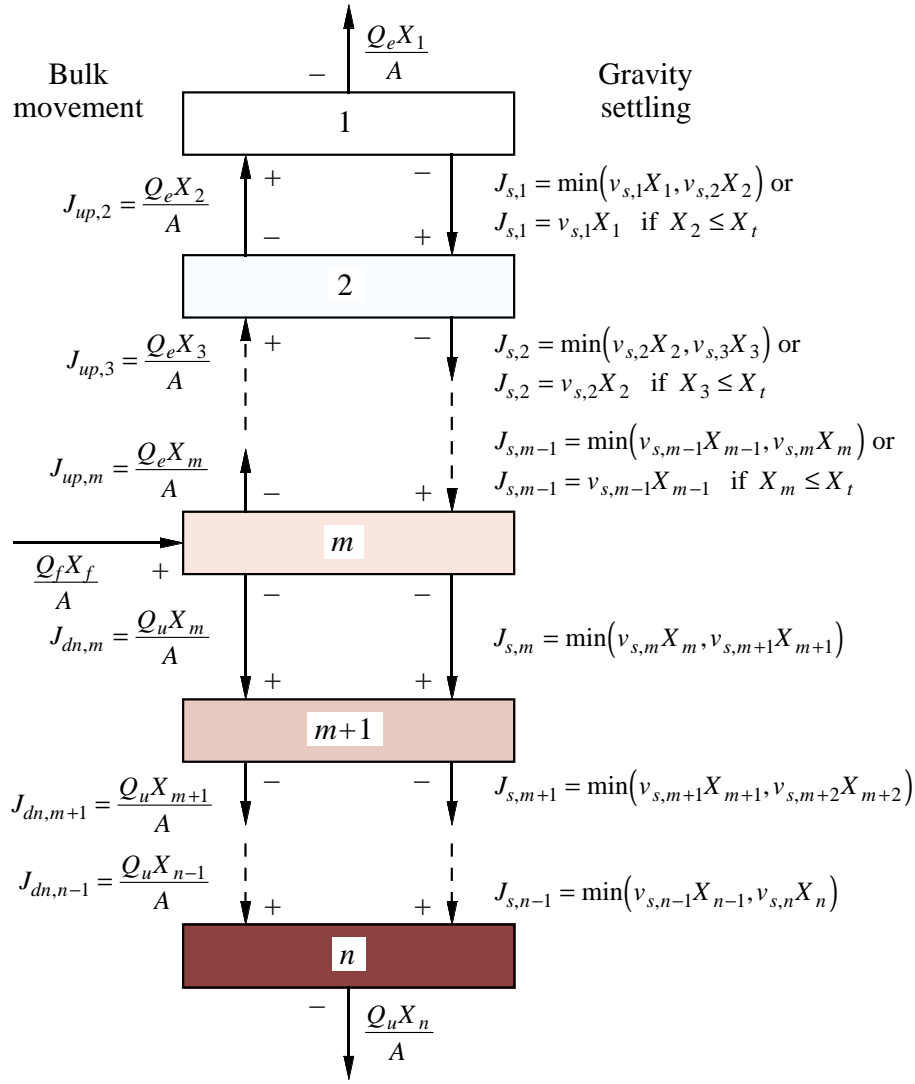
**Figure 7.2**    General description of the traditional one-dimensional layer set-
tler model (Jeppsson 1996).

where $v_0'$ and $v_0$ is the maximum practical and theoretical settling
velocity, respectively. $r_h$ is a settling parameter characterising the
hindered settling zone and $r_p$ is a parameter associated with the set-
tling behaviour at low solids concentrations. $X_{min}$ is calculated as a
fraction of $X$:

$$X_{min} = f_{ns}X_f \tag{7.5}$$

where $X_f$ is the concentration into the feed layer. Figure 7.3 shows
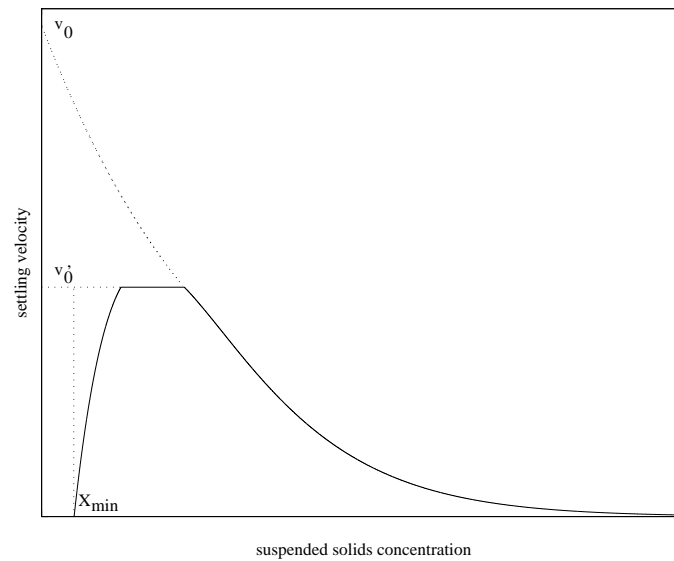the double-exponential settling function.

**Figure 7.3** Schematic description of the double-exponential settling velocity model at a constant $X_f$ (Jeppsson 1996).

## Simulation Model in Simulink

The ASM1 model is implemented in MATLAB as a Simulink model. Simulink is a package used in MATLAB for mathematical modelling, simulation and analysis of dynamical systems. Simulink is capable of handling both continuous and discrete systems as well as combinations thereof. Models are built as block diagrams, which make Simulink models easy to use and comprehend.

### Model Structure

The structure of the model is shown in Figure 7.4. The structure basically consists of six bioreactors, a flow splitter, a settler unit and a flow combiner. There are two recirculations present; return sludge flow and the internal recirculation flow. The DO concentration is controlled in bioreactor 6 and the internal recirculation flow rate is controlled based on an $S_{NO}$ setpoint in reactor 2. The bioreactor and the settler blocks are implemented as C MEX S-functions. This means that the blocks are programmed in C, instead of using graphic blocks or M-files. This has been done to increase the performance of the simulation, reducing the simulation times by a factor of ten.
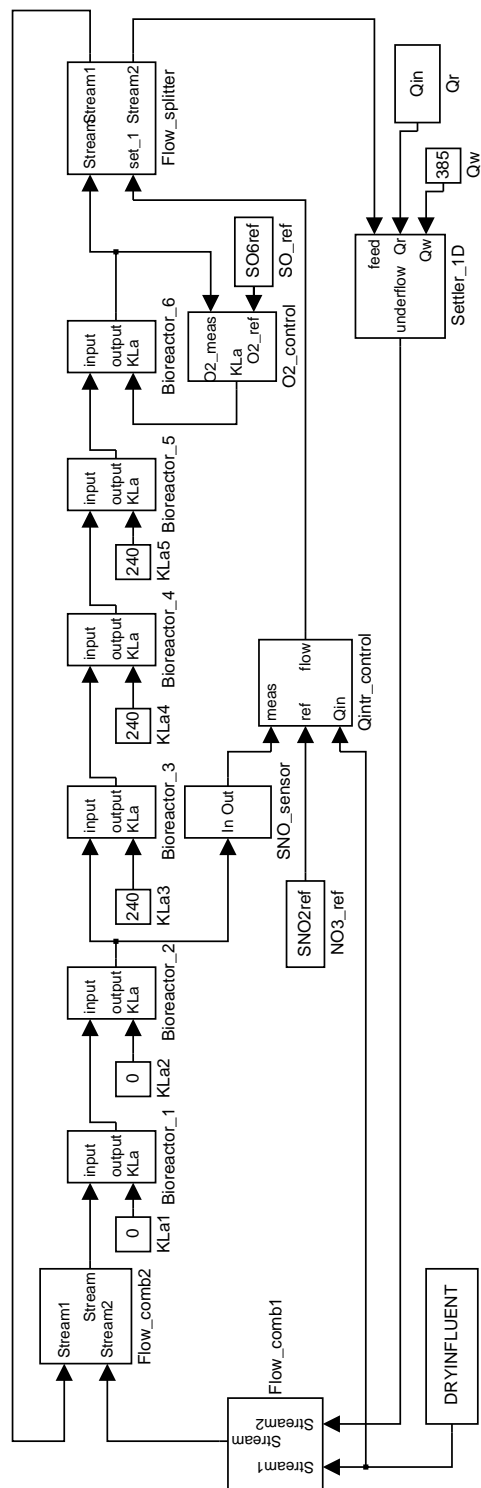
**Figure 7.4**    The plant model implemented as blocks and functions in Simulink.

## Model Parameter Values

In the simulation model, the parameter values decided by the COST group are used (Table 7.2). The chosen parameter values for the settler model are listed in Table 7.3.

|  | Symbol | Unit | Value |
|---|---|---|---|
| Heterotrophs | $\mu_H$ | 1/day | 4 |
|  | $b_H$ | 1/day | 0.3 |
|  | $\eta_h$ | - | 0.5 |
| Hydrolysis | $\eta_g$ | - | 0.8 |
|  | $k_h$ | 1/day | 3.0 |
| Ammonification | $k_a$ | - | 0.05 |
| Autotrophs | $\mu_A$ | 1/day | 0.5 |
|  | $b_A$ | 1/day | 0.05 |
| Half-saturation | $K_{OH}$ | mg/l | 0.2 |
| coefficients | $K_S$ | mg/l | 10 |
|  | $K_X$ | - | 0.1 |
|  | $K_{NH}$ | mg/l | 1.0 |
|  | $K_{OA}$ | mg/l | 0.4 |
|  | $K_{NO}$ | mg/l | 0.5 |
| Stoichiometry | $Y_H$ | gCOD/gCOD | 0.67 |
|  | $Y_A$ | gCOD/gN | 0.24 |
|  | $i_{XB}$ | gN/gCOD | 0.08 |
|  | $i_{XP}$ | gN/gCOD | 0.06 |
|  | $f_P$ | - | 0.08 |

**Table 7.2**  The parameters of the ASM1 model.

## Design and Operational Parameters

The principal layout of the simulated plant is shown in Figure 7.5. The volume of each biological reactor is 1000 m$^3$, which yields a total volume of 6000 m$^3$. The return sludge flow rate is set to 100% of the influent flow rate, while the internal recirculation is controlled, using a setpoint of 1.0 mg N/l for the nitrate concentration $S_{NO}$ in bioreactor

| Parameter | Unit | Value |
|-----------|------|-------|
| $v_0'$ | m/day | 250 |
| $v_0'$ | m/day | 474 |
| $r_h$ | l/(mg $TSS$) | 0.000576 |
| $r_p$ | l/(mg $TSS$) | 0.00286 |
| $f_{ns}$ | - | 0.00288 |

**Table 7.3**   Settler model parameter values.
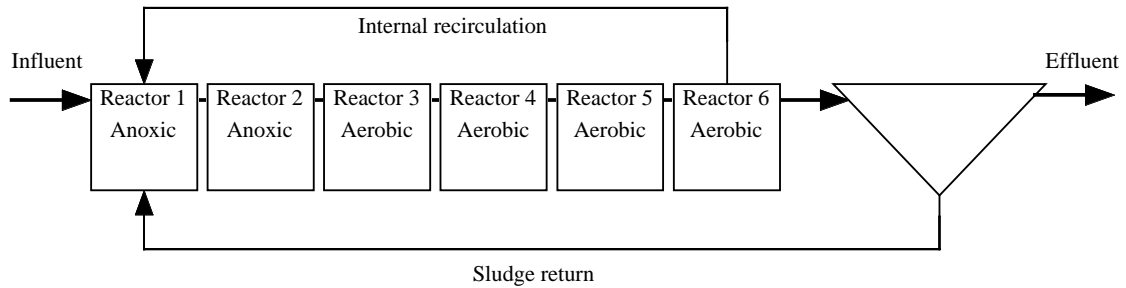


**Figure 7.5**   Principal layout of the simulated plant.

2. During dry-weather operation this implies 200-450% of the influent flow rate. The aeration in bioreactor 3, 4 and 5 is set to a constant value, causing the DO level to vary, due to load changes. The aeration in bioreactor 6 is controlled to a set point of 2.0 mg/l. The operational parameters are listed in Table 7.4.

|  | Operational parameter | Unit | Value |
|--|-----------------------|------|-------|
| Return sludge flow rate | $Q_r$ | % | 100 |
| $S_{NO}$ setpoint for internal recirculation | $S_{NO,ref}$ | mg N/l | 1.0 |
| Aeration reac. 3-5 | $K_L a$ | day$^{-1}$ | 240 |
| DO setpoint in reac.6 | $S_{O,ref}$ | mg -COD/l | 2.0 |

**Table 7.4**   Operational parameters of the simulated process.

# 7.2   General Operational Mode Monitoring

As discussed in Chapter 6, when monitoring a *general* operational mode, only the general operational conditions are considered without any specific subprocess or quality variable in mind. The aim is either to detect deviations from the normal mode (binary classification) or to classify the current mode into mode categories (multiple classification). Thus, all available measurements are normally used, as we are not focused on a specific deviation or disturbance. One can separate the disturbances into two subcategories:

- external disturbances;

- internal disturbances.

*External* disturbances are defined as those imposed upon the process from the outside and detectable when monitoring the influent characteristics. For instance, a change in the influent flow rate can be considered as an external disturbance. *Internal* disturbances are caused by changes within the process affecting the process behaviour. A pump failure is a typical internal disturbance. However, from a detection point of view, a disturbance imposed upon the process from the outside, may not be possible to detect directly. Instead, the disturbance may be detected as an effect on internal variables. An example of such an internal disturbance may be decreased nitrification, caused by non-measurable changes in the influent wastewater characteristics. The detection may be triggered by the decrease in oxygen demand.

## External process disturbances

Hydraulic disturbances are common at most wastewater treatment plants. In the influent data file developed by the COST group, there are three events associated with the influent flow rate. However, the appearance of the disturbances differ from each other. The first one imitates a sudden storm event after a long period of dry weather. This implies that there is a flush out of accumulated particulate matter in

the sewer system. The second event is also a storm event, but now the sewer is relatively empty of accumulated matter and, consequently, the influent characteristics differ from the first event. The third event is an extended period of rain, appearing after a longer period of dry weather. The following example shows how these disturbances appear using a PCA model for general operational mode monitoring.

A PCA model is built from a period of one week of dry weather (normal operation). The data used are the influent file and model outputs, all with noise added to mimic sensor noise and outliers as described in Equations 7.1 and 7.2. In the model building stage it is important to remove noise and outliers to get a representative model. This is done by an FMH filter applied iteratively until the noise and outliers were reduced to an acceptable level. In Table 7.5, the variables used to build the PCA model are listed. As is shown Table 7.6, the model

| Var no | Symbol | Variable |
|---|---|---|
| 1 | $S_{NH,in}$ | Influent ammonia conc. |
| 2 | $Q_{in}$ | Influent flow rate |
| 3 | TSS | Total suspended solids conc. (rector 4) |
| 4 | $S_{O,3}$ | Dissolved oxygen conc. (reactor 3) |
| 5 | $S_{O,4}$ | Dissolved oxygen conc. (reactor 4) |
| 6 | $S_{O,5}$ | Dissolved oxygen conc. (reactor 5) |
| 7 | $K_L a$ | Oxygen mass transfer coefficient (reactor 6) |

**Table 7.5**  Variables constituting the $X$-block in the PCA model.

is able to capture most of the variability of the $X$-block in two PCs. An investigation of the eigenvalues associated with the model shows that three components may be a reasonable number of PCs.

**Storm Events**

The measurement variables during the storm weeks are presented in Figure 7.6. The first storm is visible at around sample 850. The second storm can be seen at around sample 1100.

In Figure 7.7, the $SPE$ (top) and the filtered $SPE$ (bottom) measures are shown. The filtered $SPE$ is used to determine whether a deviation
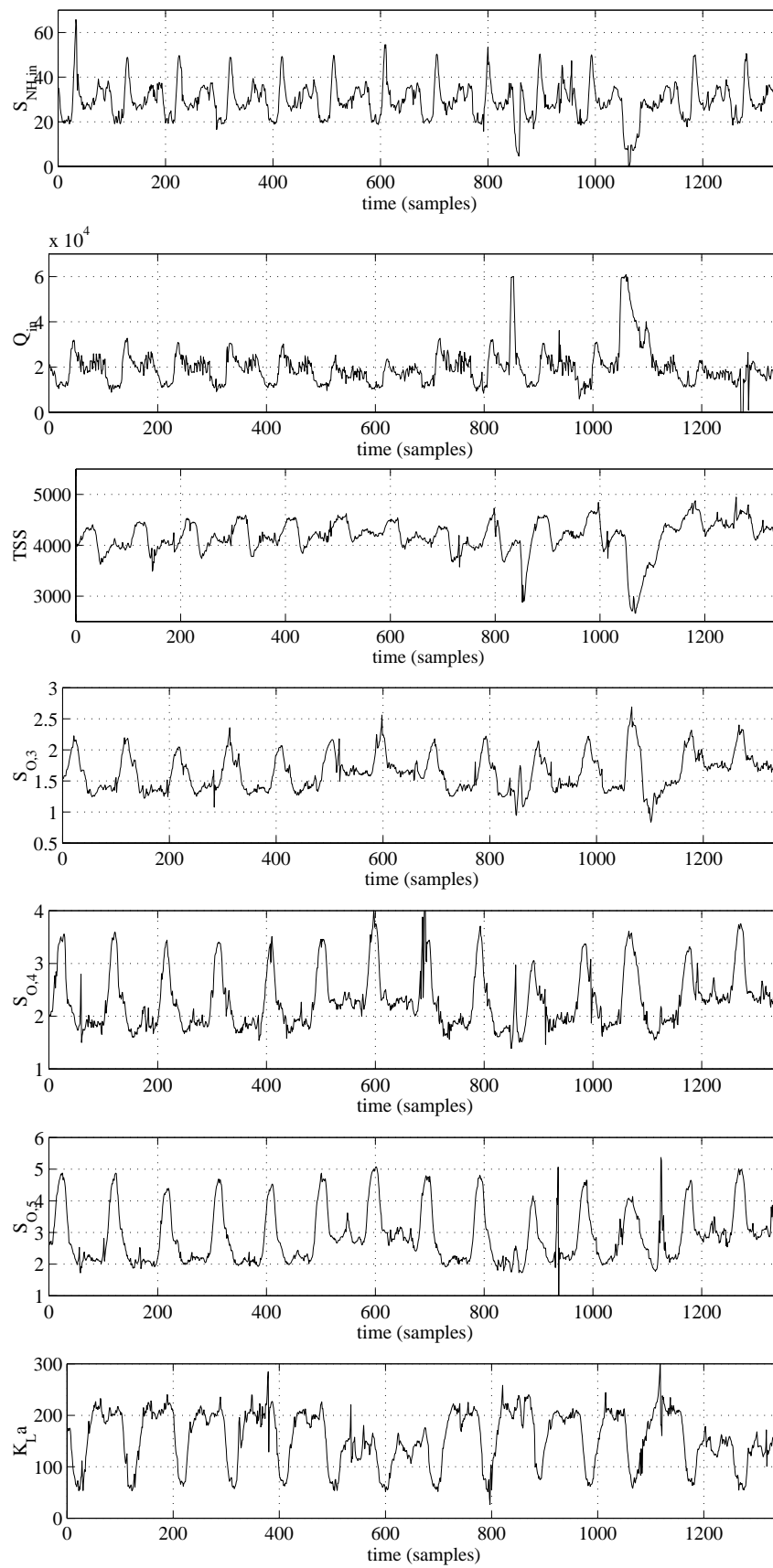
**Figure 7.6**  The monitored variables during the storm weeks.

| Principal component number | Eigenvalue of cov($\mathbf{X}$) | % Variance captured this PC | % Variance captured total |
|---|---|---|---|
| 1 | 5.27 | 75.30 | 75.30 |
| 2 | 1.09 | 15.52 | 90.81 |
| 3 | 0.40 | 5.69 | 96.50 |
| 4 | 0.14 | 1.95 | 98.45 |
| 5 | 0.06 | 0.88 | 99.33 |
| 6 | 0.04 | 0.56 | 99.89 |
| 7 | 0.01 | 0.11 | 100.00 |

**Table 7.6**  Variance captured by the PCA model.

in $SPE$ is caused by a single outlying value. Therefore, the $SPE$ is filtered by a causal 5-point median filter. This approximately corresponds to a detection rule requiring more than two consecutive samples to be above the limit. The limit is the 0.99 quantile of the training data $SPE$. This corresponds approximately to the 0.95 quantile of non-filtered training data. Since the model will be applied to non-filtered data it is reasonable to use a less stringent limit. It can be seen that besides a few exceeding samples during the first 800 samples, there is a significant deviation around sample 850. A second deviation is visible between samples 1050 to 1200.

The $T^2$ measure also displays significant deviations around samples 850 and 1050 (Figure 7.8). The same filtering as in the $SPE$ case has been used to produce the filtered $T^2$. The deviations in the $T^2$ measure are somewhat more significant than the deviations in the $SPE$ measure. The implication of this is that the deviations are especially large within the model, even though the deviations from the model plane are significant. A contribution plots is a fast way to investigate the event and to isolate the variables causing the deviation. Figure 7.9 displays the variables responsible for the deviation in the $SPE$ measure at samples 850 and 1052, respectively. The figure shows that during both events it is the variable 2 (influent flow rate) and variable 3 (TSS in reactor 4) that are primarily responsible for the deviations. If the signs of the elements constituting the loading matrix are investigated, it can be derived that there is an increase in the influent flow rate and a decrease in the TSS.
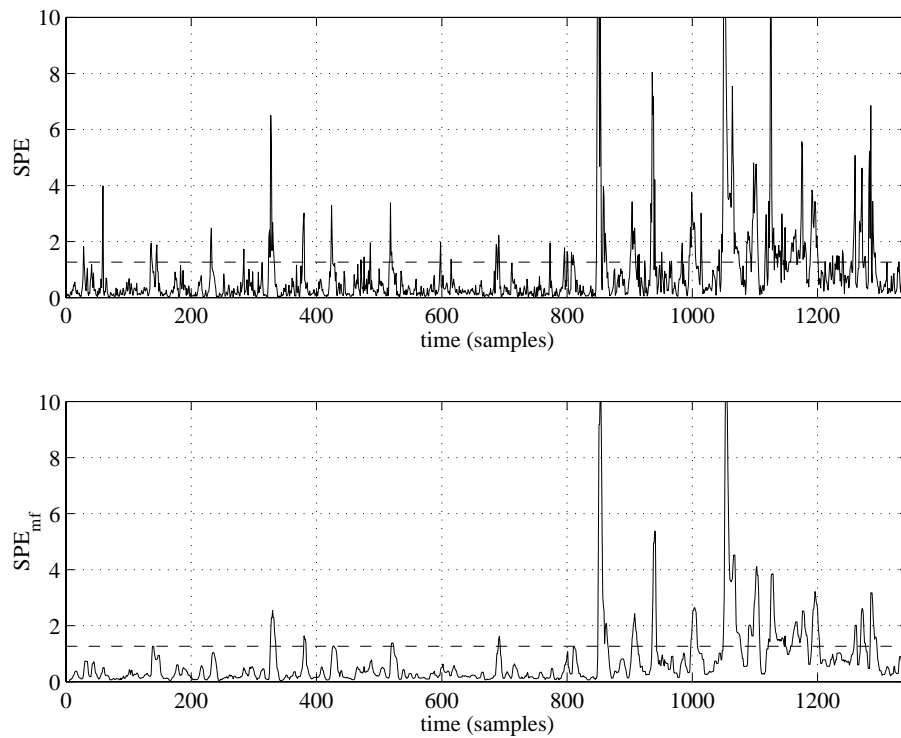
**Figure 7.7**  $SPE$ (top) and median filtered $SPE$ (bottom) during storm event. The dashed line corresponds to the 0.99 quantile of training data.
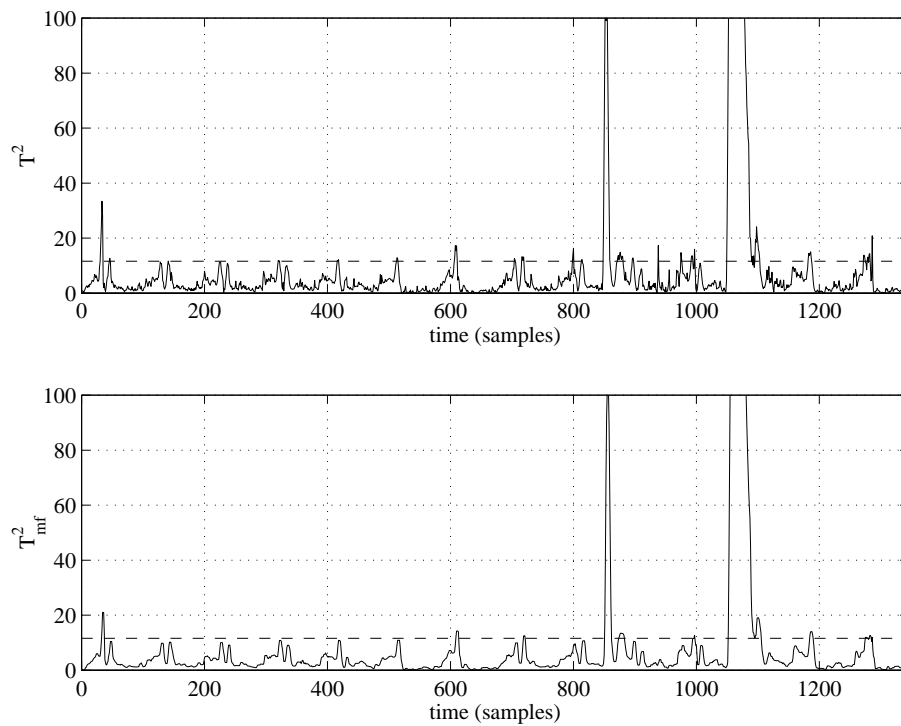


**Figure 7.8**  $T^2$ (top) and median filtered $T^2$ (bottom) during storm event. The dashed line corresponds to the 99% confidence level.
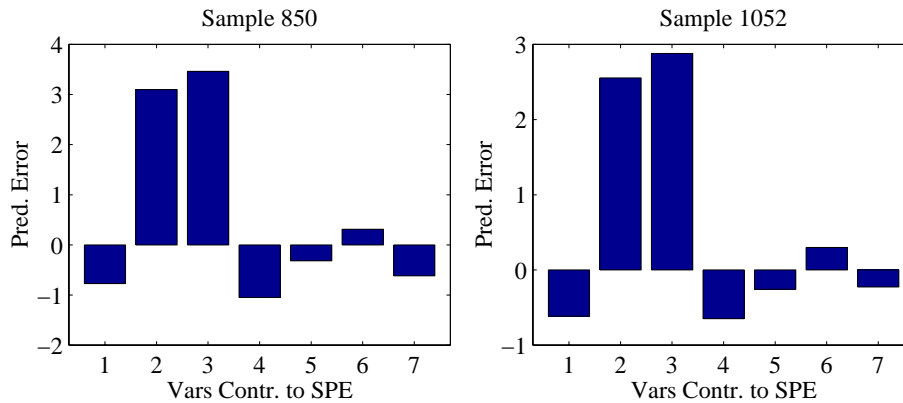
**Figure 7.9**   Variables contributing to the deviations in $SPE$ at sample 850 (left) and sample 1052 (right).

In order to determine variables which are contributing to the deviation in $T^2$, the most significant terms in Equation 6.36 must be found. Figure 7.10 shows that it is the third score vector that contributes the most to $T^2$ at samples 851 and 1052 (which in both cases represent the third consecutive sample above the significance limit for $T^2$, respectively). The second largest score contributing to $T^2$, is the score of PC no 2. In Figure 7.11, the variables contributing to the deviations in score vectors 2 and 3 are shown. The figure indicates that the largest contribution comes from variable 2 (influent flow rate), but it can also be seen that variable 1 (influent ammonia) has contributed significantly. An investigation of the loading matrix reveals that the influent flow rate is higher and that the influent ammonia concentration is lower than normal operating values.

The conclusion of the analysis of the contribution to the $SPE$ and $T^2$ measures during the storm events is that variables 2 and 3 (TSS) changes the mutual relations within the model and that especially variable 2 but also variables 1 and 3 are deviating from the normal daily pattern. Could this have detected seen by investigating the variables individually? The answer to that is yes, but it would not be that obvious how to rank the process influence of each variable and the task would involve monitoring of seven variables instead of two model residuals.

Another way of displaying the process mode is by score plots. Since Figure 7.11 indicates that all three score vectors play an important
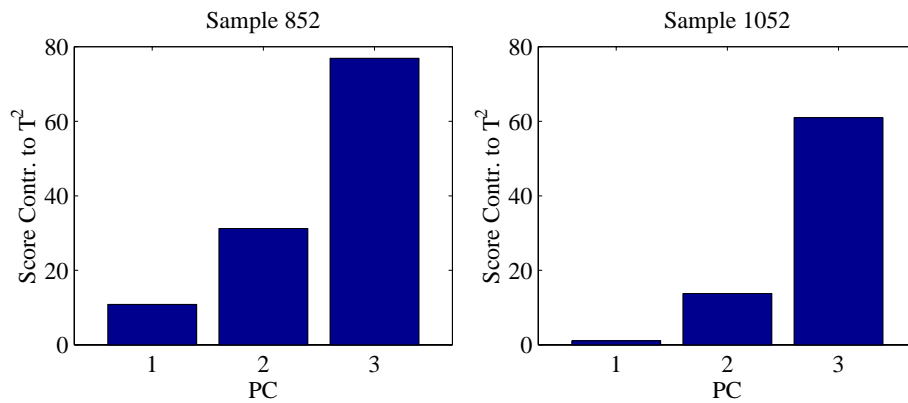
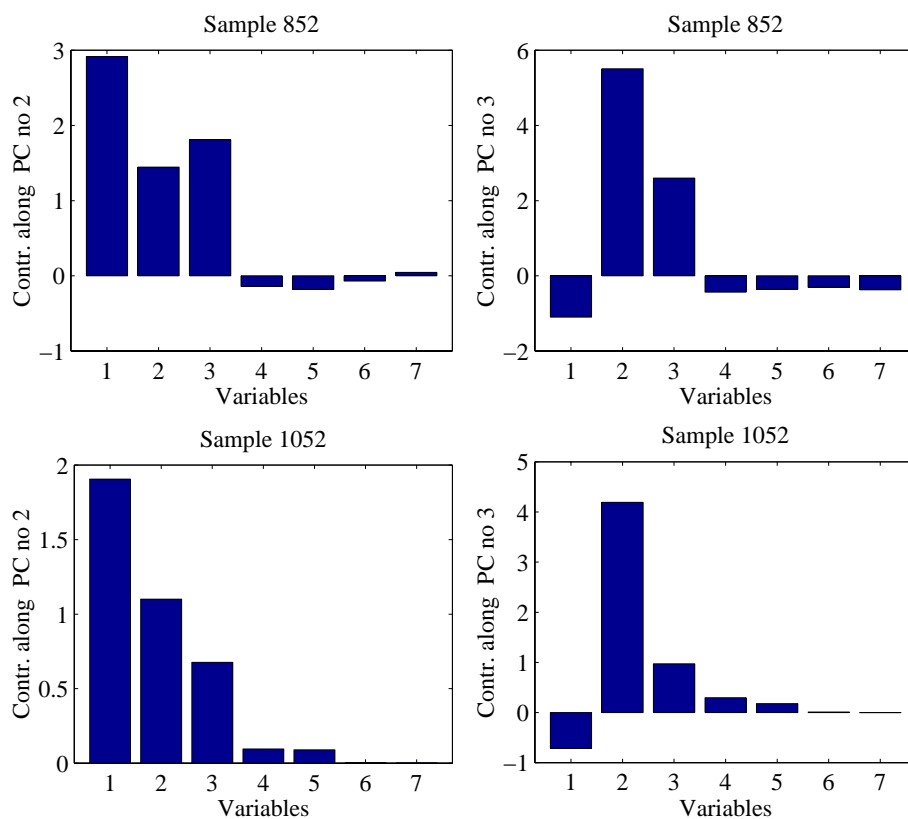**Figure 7.10**   Score vectors contributing to $T^2$ at sample 851.



**Figure 7.11**   Variables contributing to the deviations in $T^2$ along PC no 2 (top left) and 3 (top right) at sample 851 and along PC no 2 (bottom left) and 3 (bottom right) at sample 1052.

part for the deviations in $T^2$, every combination of the score vectors is plotted in Figure 7.12. During normal operation, there are still some points exceeding the 99% confidence limit of the scores, but the deviations are not significant. In the figure, a loop shaped pattern is visible, representing the changes over the 24 hours of the day. However, both the first ('*') and second ('+') storm event result in points located well outside the normal operating region.
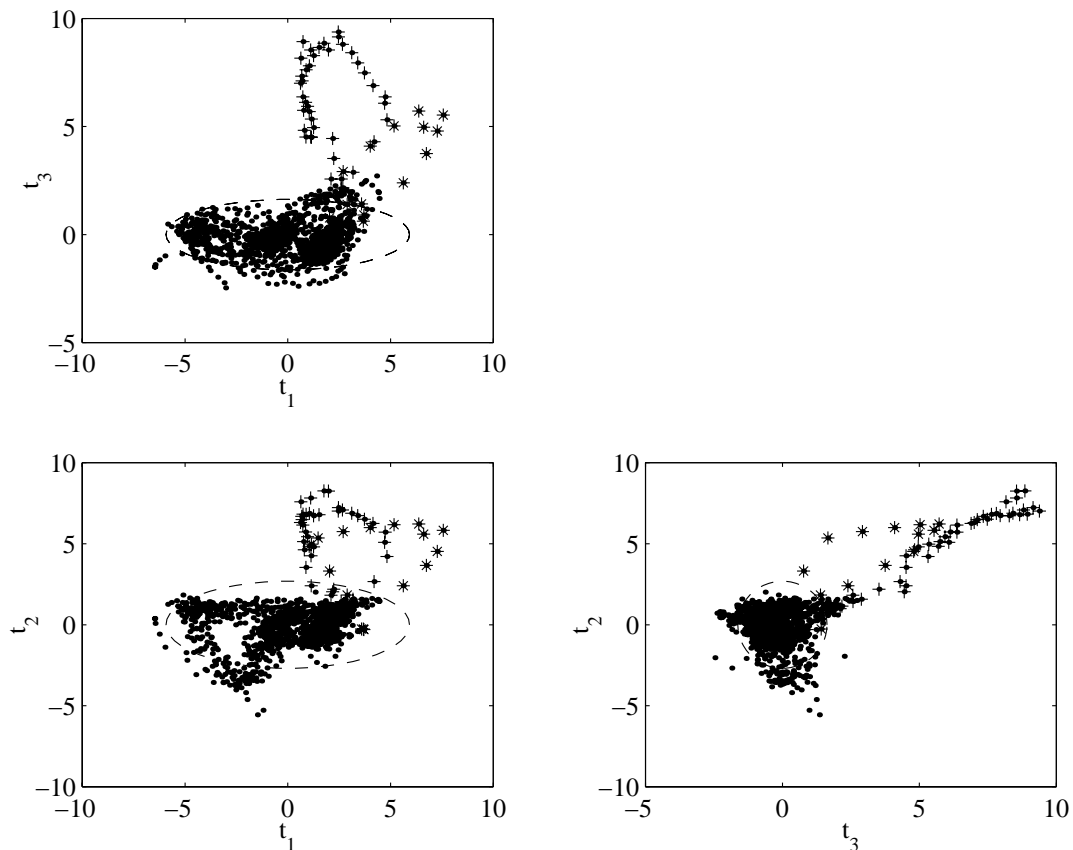


**Figure 7.12**   Score plots showing the process in the PC space. The '*' represents the first storm event and the '+' represents the second storm event.

An important observation is that after the second storm event the $T^2$ measure quickly resumes its normal operation value, while the $SPE$ measure does not (see Figures 7.7 and 7.8). This indicates that the external disturbance has distorted the internal relations between the variables and thus the process is still not in normal operational mode. The normal operational mode is not reached within the remaining time of the test period. This shows that monitoring the PC scores is not sufficient to determine the operational mode.

**Rain Event**

The measurement variables during the rain event are presented in Figure 7.13. The rain event is visible from samples 800 to 1000. The same PCA model as used for the storm events is used to monitor the rain event. Besides a continuously high level from samples 200 to 500, the $SPE$ does not display any significant deviation from normal operation (Figure 7.14). (The reason for the high level will be discussed later.) However, the $T^2$ measure (Figure 7.15) shows a significant deviation from samples 805 to 1000. The contribution from the scores to the deviation in $T^2$ shows that it is changes along the third PC that contribute the most to $T^2$ at sample 811 (Figure 7.16). The contributing variables to the change along PC nos 2 and 3 are shown in Figure 7.17. It is obvious that variable 2 (influent flow rate) is the main cause of the deviation. Variable 1 (influent ammonia concentration) is also a major contributor.

The implication of the $SPE$ and $T^2$ plots is that the disturbance is inside the model space, *i.e.* the deviations in the process are well described by the PCA model. The mutual relations between the variables are not distorted. This may be somewhat confusing, but when looking at how the rain data have been created, there is a simple explanation. The rain event data are constructed by simply adding a bias to the dry-weather data. This keeps the internal relation intact and, consequently, the model fit is still good. The rain data do not represent a totally realistic situation, but it is a good reminder of what the different measures express.

At first, the continuously high level of $SPE$ between samples 200 and 500, is confusing. A contribution plot would show that variables 2 (influent flow rate) and 3 (TSS concentration) are the main contributors to the prediction error. The low level of TSS is perhaps not surprising, since the data series is actually the continuation of the storm event data file, Thus, there is still a deviation from the second storm event. However, the high flow rate values are more intriguing. An investigation of the influent data reveals that flow rate is normal. However, one should not forget how the PCA model is constructed. The $SPE$ is a measure of the prediction error. A high level of TSS, which is highly (negatively) correlated to flow rate, will affect the prediction
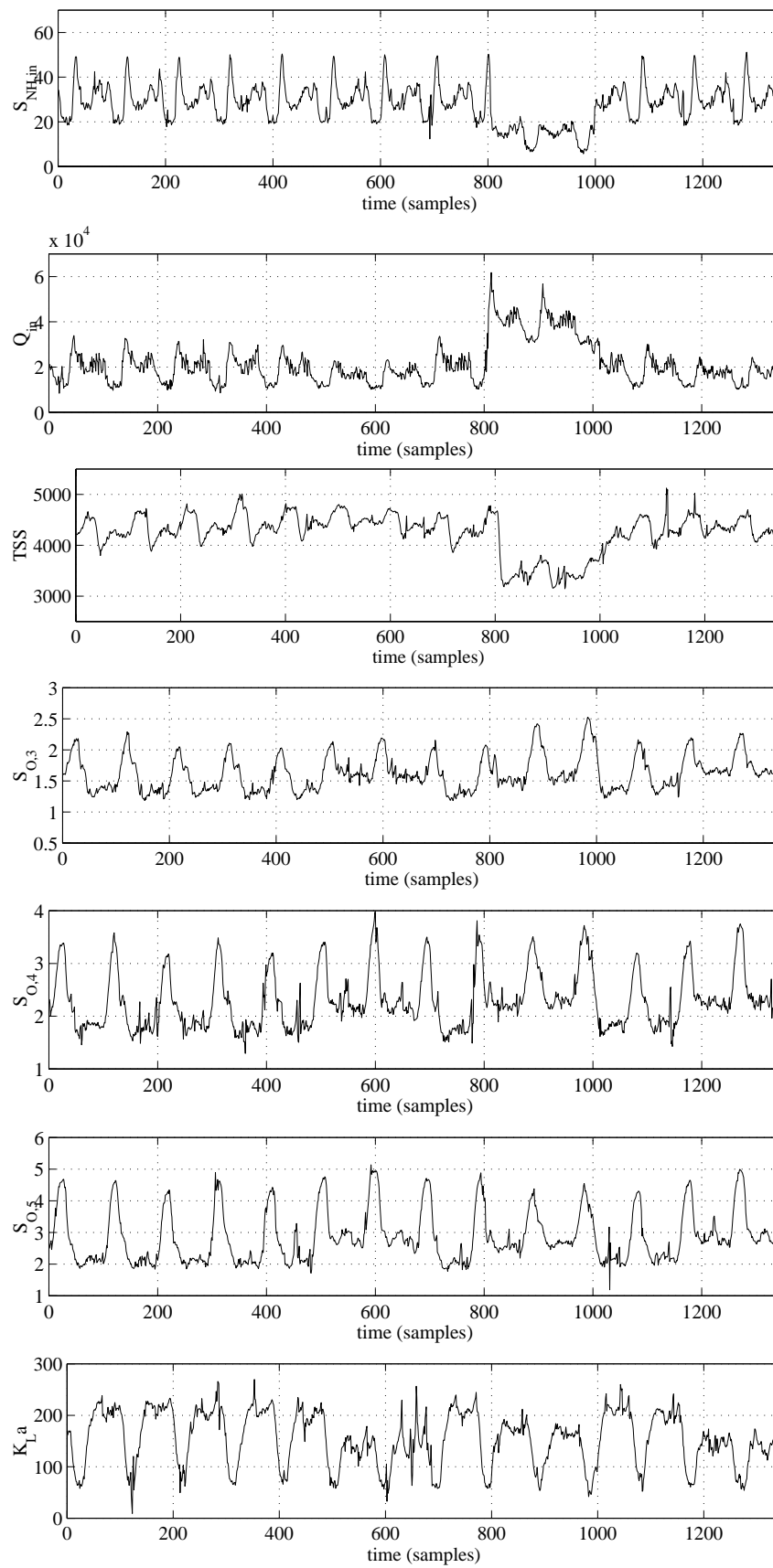
**Figure 7.13**  The monitored variables during the rain event.
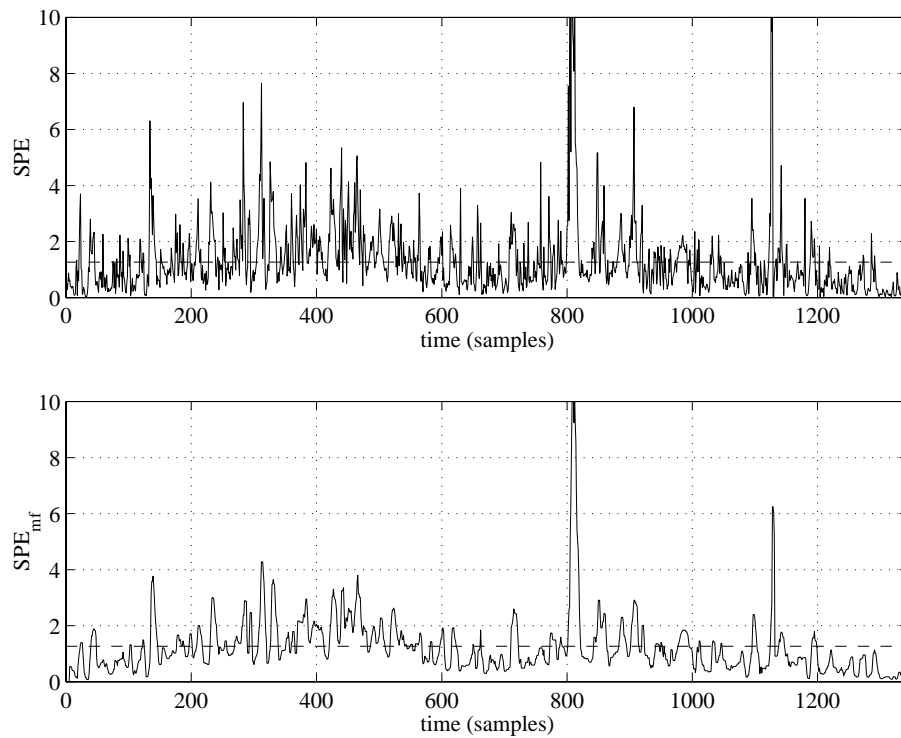
**Figure 7.14**   *SPE* (top) and median filtered *SPE* (bottom) during a rain
event.   The dashed line corresponds to the 0.99 quantile of
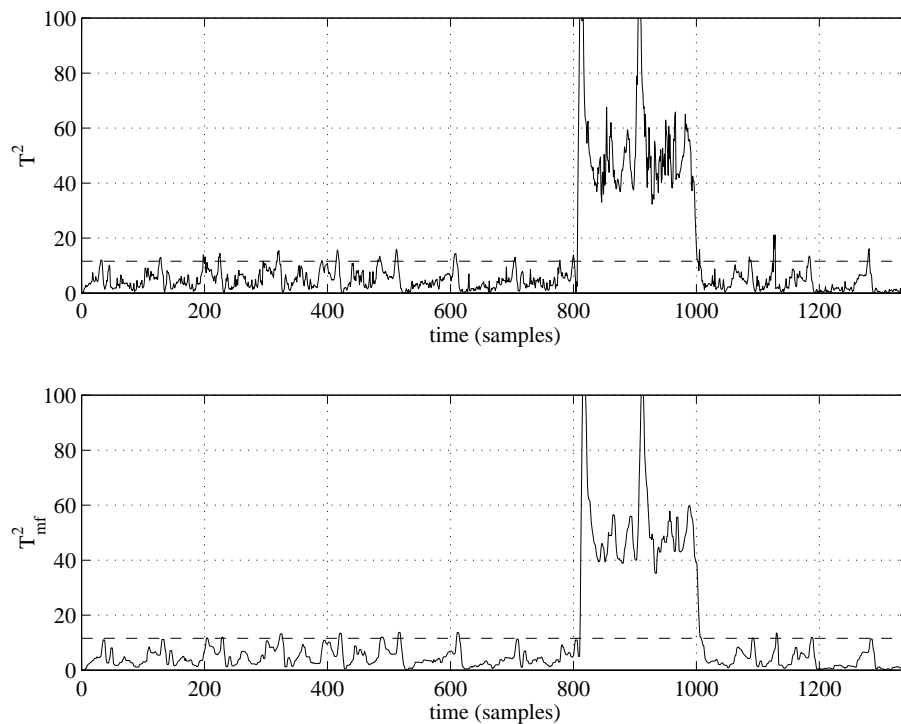training data.



**Figure 7.15**   $T^2$ (top) and median filtered $T^2$ (bottom) during a rain event.
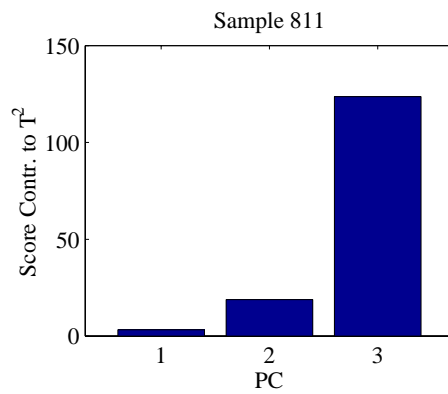The dashed line corresponds to the 99% confidence level.

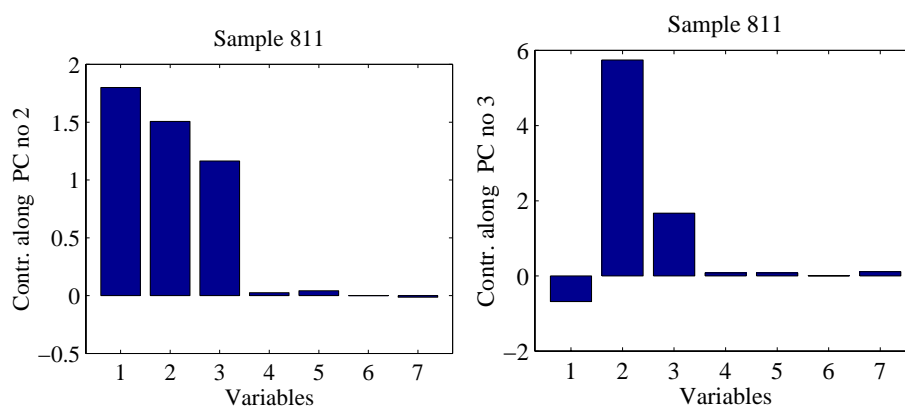**Figure 7.16**  Score vectors contributing to $T^2$ at sample 852.



**Figure 7.17**  Variables contributing to the deviations in $T^2$ along PC nos 2
(left) and 3 (right) at sample 811.

of the flow rate and, consequently, cause the prediction error to increase. This is an example of a disturbance or deviation difficult to detect by investigating a single variable, as the disturbance appears as a statistical misfit.

The storm and rain examples indicate the practicability of MVS for general operational mode monitoring. They also show that the $SPE$ and $T^2$ measures should be used complementarily for good monitoring results. This is further accentuated by the internal disturbance examples presented in the following in subsection.

## Internal Process Disturbances

Internal disturbances appear within the process or plant. Mechanical breakdowns and sensor failures or drift are typical internal disturbances. Other examples of internal disturbances are changes in reaction rates caused by external variations as discussed earlier.

A PCA model was built from a period of 14 days of dry-weather conditions. Noise was applied to the model output and influent data in the same way as discussed earlier. In the model building stage, it is important to remove noise and outliers to get a representative model. This was done by an FMH filter applied iteratively until the noise and outliers were reduced to acceptable levels. Five principal components were chosen and the captured variability is shown in Table 7.7.

| Principal component number | Eigenvalue of cov(X) | % Variance captured this PC | % Variance captured total |
|---|---|---|---|
| 1 | 5.00 | 71.56 | 71.56 |
| 2 | 1.09 | 15.60 | 87.16 |
| 3 | 0.47 | 6.71 | 93.88 |
| 4 | 0.22 | 3.09 | 96.97 |
| 5 | 0.09 | 1.32 | 98.29 |
| 6 | 0.07 | 1.07 | 99.36 |
| 7 | 0.05 | 0.64 | 100.00 |

**Table 7.7**  Variance captured by the PCA model.

## Deteriorating Nitrification

To simulate decreasing nitrification capability of the activated sludge, the specific growth rate for the autotrophs, $\mu_A$, is decreased. This is done as a step from $\mu_A$=0.5 to 0.4 day$^{-1}$ at day 2 (sample 192). The growth rate is then further decreased in a linear fashion. At day four the growth rate is 0.3 day$^{-1}$, and from that on it is constant according to Figure 7.18.
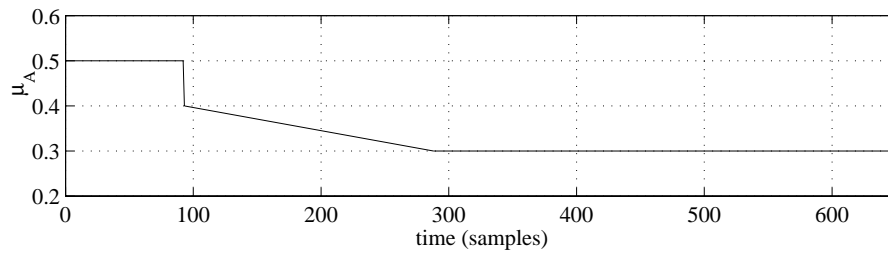


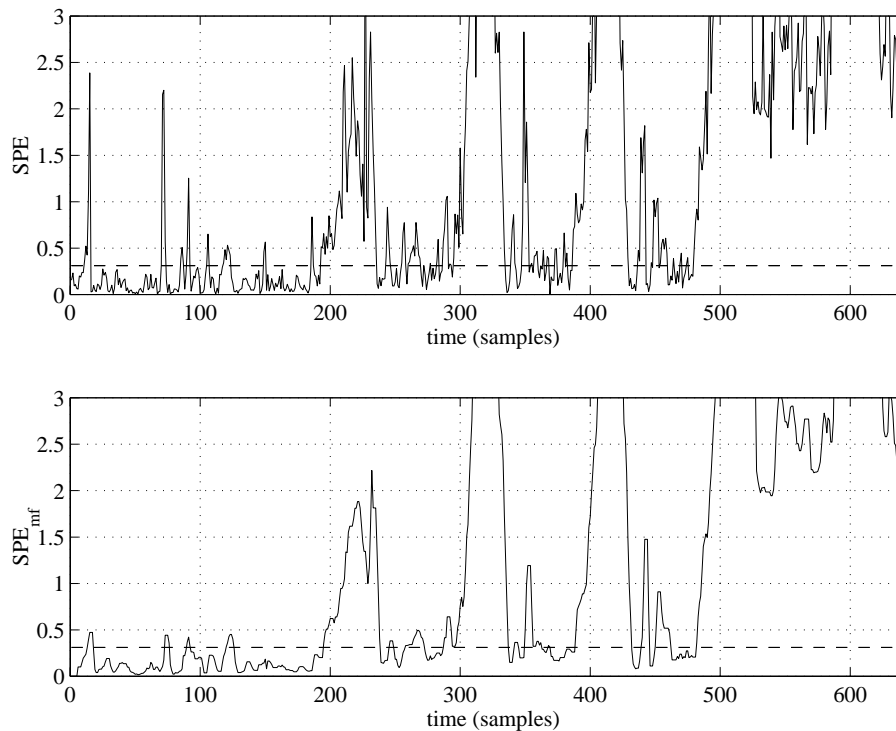**Figure 7.18**   The decrease of the specific growth rate $\mu_A$.



**Figure 7.19**   The *SPE* measure unfiltered (top) and filtered with a causal median filter of 5 points (bottom). Signs of a disturbance can be seen around sample 200. The decrease of autotrophic growth rate is imposed at sample 193.

In Figure 7.19 (top), the sum of the prediction error ($SPE$) is plotted. Apart from a few deviations before sample 200, the process can be regarded to be in normal operational mode. This is in accordance to the fact that the disturbance has not yet been introduced. However, at about sample 200, the $SPE$ increases and exceeds its limits significantly. Thus, the model does not cover the present variability of the process as well as before sample 200. We have a disturbance and this corresponds well to the decrease in the specific growth rate of autotrophs imposed at sample 192 (2 days). In Figure 7.19 (bottom), the median filtered $SPE$ is shown. The median filter introduces a delay of 2 samples, but the result is somewhat more robust. After sample 235, the $SPE$ measure is again located inside the normal region. Is the disturbance no longer present? The answer is that the disturbance is still present, but due to the variations in the process, the $SPE$ measure will differ during the hours of the day. This means that if the disturbance occurs when the $SPE$ measure is low, it will take longer time before the disturbance is detected. This points out the difficulties in detecting deviations in dynamic systems.

The $SPE$ measure reveals that the process has deviated from the normal operation mode in the sense that the fit of the model has decreased. In Figure 7.20 (top), the $T^2$ measure is plotted. The $T^2$ measure also reveals a deviation, but this seem to be a diurnal event occurring at this time every day. Looking at the whole week, there is a tendency towards higher peaks, but it is not obvious. This implies that the deviations within the model (that is the distances between each sample and the origin) are not significant. In Figure 7.20 (bottom), the median filtered $T^2$ measure is plotted. The $T^2$ together with the $SPE$ measure suggest that the disturbance has distorted the mutual relationships between the variables, but the mean values and extreme values are not significantly different from the normal operational mode. The reason for the deviation can be found by applying the methods discussed in Chapter 6. By examining at the variable contribution to the $SPE$ at, for instance, sample 220, the reason for the deviation can be found. The variable contribution is shown in Figure 7.21 (left). It is obvious that variable 4 (DO concentration in reactor 3) has contributed the most to the deviation in $SPE$. However, it may be wise to look at the mean contribution over a few samples to avoid the influence of single large variable values. The mean contribution
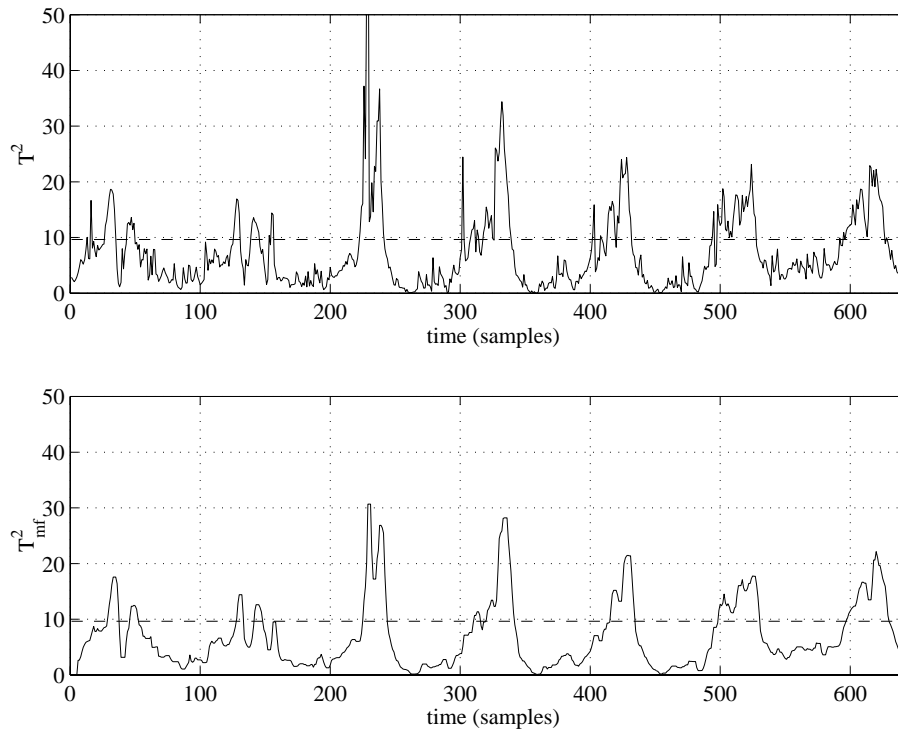
**Figure 7.20**  $T^2$ (top) and 5-point median filtered $T^2$ (bottom). No significant deviations visible - the $T^2$ does capture the disturbance. Consequently, the disturbance does not appear as deviating amplitudes or mean values of the scores.
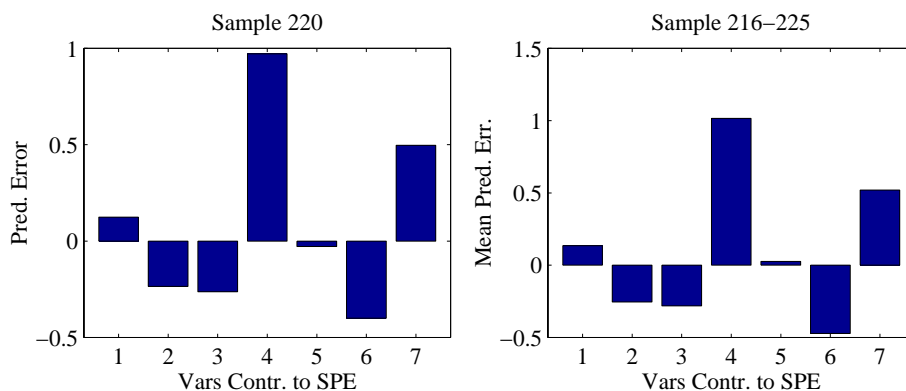


**Figure 7.21**  Variables contributing to $SPE$ at sample 220 (left) and variables contributing to the mean $SPE$ at sample 216 to 225 (right).

during samples 216 to 225 is shown in Figure 7.21 (right).

In this example, the detection and isolation of the disturbance do not tell us what has caused the disturbance. There are several possible causes for variable 4 to deviate but establishing these causes is the task of diagnosis and will not be discussed here.

## Mechanical Breakdown

A challenging problem is to detect changes or breakdowns of the mechanical equipment by monitoring the on-line measurements. For instance, a small decrease in the return sludge flow rate, due to poor pump performance, may not be detected by the pump alarm indicator. However, such an event will slowly change the behaviour of the process as, for example, the sludge content and, consequently, the sludge age is affected. In order to simulate a breakdown in the return sludge
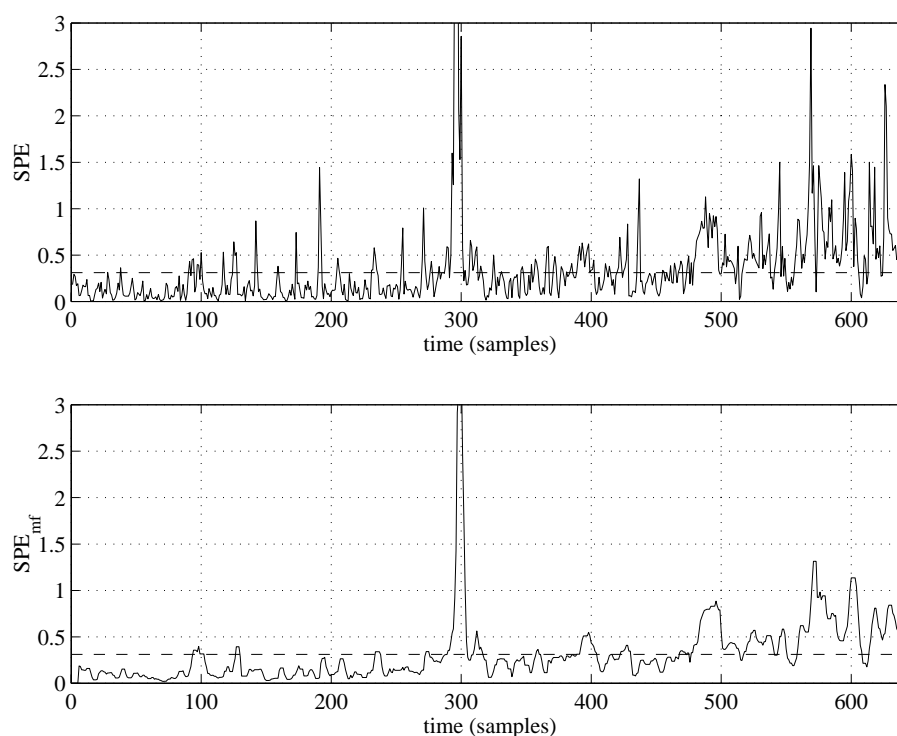


**Figure 7.22**  $SPE$ (top) and 5-points median filtered $SPE$ (bottom).

flow pumping, the flow rate is set to decrease in a linear fashion from its normal value at day 2 to 75% of it normal value 3 hours later. The same PCA model used in the previous example is applied. Is it then

possible to quickly detect the change in flow rate?
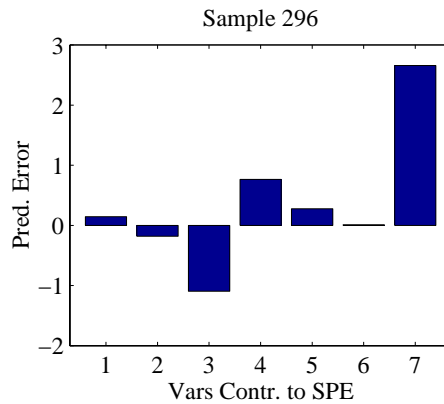


**Figure 7.23**   Variables contributing to the prediction error at sample 296.
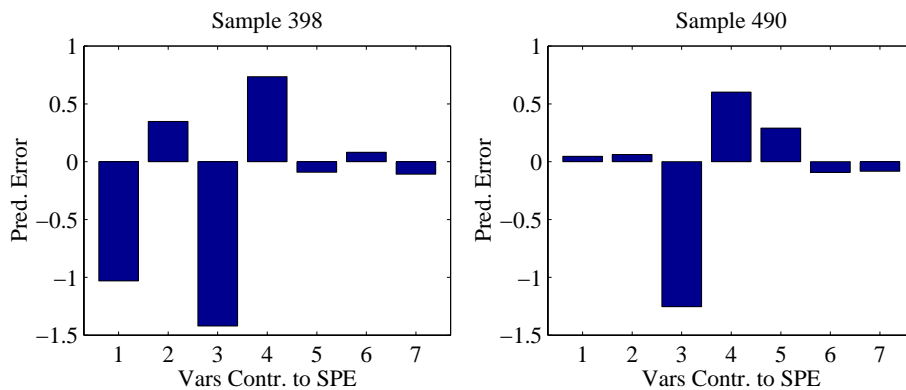


**Figure 7.24**   Variables contributing to the prediction error at sample 398 (left) and sample 490 (right).

When looking at the first 7 days, there is a slow trend in the $SPE$ measure (Figure 7.22 (top)). This trend becomes more visible when the $SPE$ is filtered, using a causal median filter of 5 points. There is a significant deviation around sample 295, but the impulse like shape indicates that it is a measurement disturbance. However, in Figure 7.23 the reason for the deviation at sample 296 is shown. The figure shows that it is mainly variable 7 ($K_L a$ in reactor 6) contributing to the deviation.

It is not until sample 480 that $SPE$ more consistently exceeds the limit. The variables contributing to this deviation at samples 398 and 490 is shown in Figure 7.24. In both figures it is variable no 3 (TSS)

that contributes the most. In Figure 7.25, the mean contribution over
a longer period is shown. This is done so that no momentary large
deviation will mislead us to draw a false conclusion. The contribution
from variable 3 is evident. The small contributions from variable 1 (in-
fluent ammonia) and 2 (flow rate) indicate that there are no trends in
the influent water characteristics, instead it is an internal disturbance.
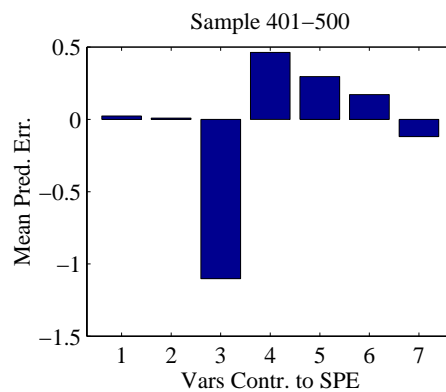


**Figure 7.25**    Variables contributing to the mean prediction error at sample
401 to 500.

The $T^2$ measure displays the same behaviour as in the previous ex-
ample. The disturbance is thus not clearly visible in the $T^2$ plot. The
disturbance consist of an internal distortion of the mutual relation-
ships of the variables.

## Cluster Classification

Different operational modes give rise to different patterns of the scores
in the score plots and clustering points represent similar conditions.
This can be used to empirically couple the score pattern to a certain
mode or a disturbance. An operator knows that if the points are
gathered in specific regions in the PC space, the process operates under
certain conditions. This can be used to classify several operational
modes with respect to the process location in the PC space, instead
of simply determining if the mode is normal or abnormal. Below two
simple examples are presented.

## General Classification of the Storm Event

In order to classify deviations some criteria are needed. The isolation of deviating variables during the storm events discussed on page 112 indicated that it was especially variables 2 (flow rate) and 3 (TSS), but also variable 1 (influent ammonia) that contributed to the disturbance (see Figure 7.10). In Figure 7.26, the first two loading vectors of the model used to monitor the storm event are plotted. As mentioned in Chapter 6, the load plot indicates how the variables influence the process representation in the PC plane. For instance, if $Q_{in}$ in Figure 7.26 increases (assuming that no other variables change), the points representing the process in a score plot will move diagonally towards the upper right corner. A decrease, on the other hand, will move the points in the opposite direction. Thus, it can be seen in the figure that in order to force the process towards the upper right corner of the score plot (Figure 7.12, lower left panel), variable 1 ($S_{NH,in}$) must be lower, variable 2 ($Q_{in}$) must be higher and variable 3 (TSS) must be lower than their normal mode values. The class (upper right corner of the score plot) are thus defined by:

- variable 1 , influent ammonia: low;

- variable 2, influent flow rate: high;

- variable 3, TSS in reactor 4: low.

Next time the process is located in the upper right corner of the PC space, the operators know that the variables 1, 2 and 3 are most likely deviating in the same manner. The classification gives a physical interpretation to the disturbance pattern seen in the score plot.

## Specific Classification of the Storm Event

The disturbance pattern can also be coupled to an effect of the disturbance. If, for instance, the effluent nitrate concentration ($S_{NO}$) is measured, a classification can be made with regard to the nitrogen removal performance.

The storm event data is used as training data for a simple specific classification. During the storm events, the effluent nitrate level is
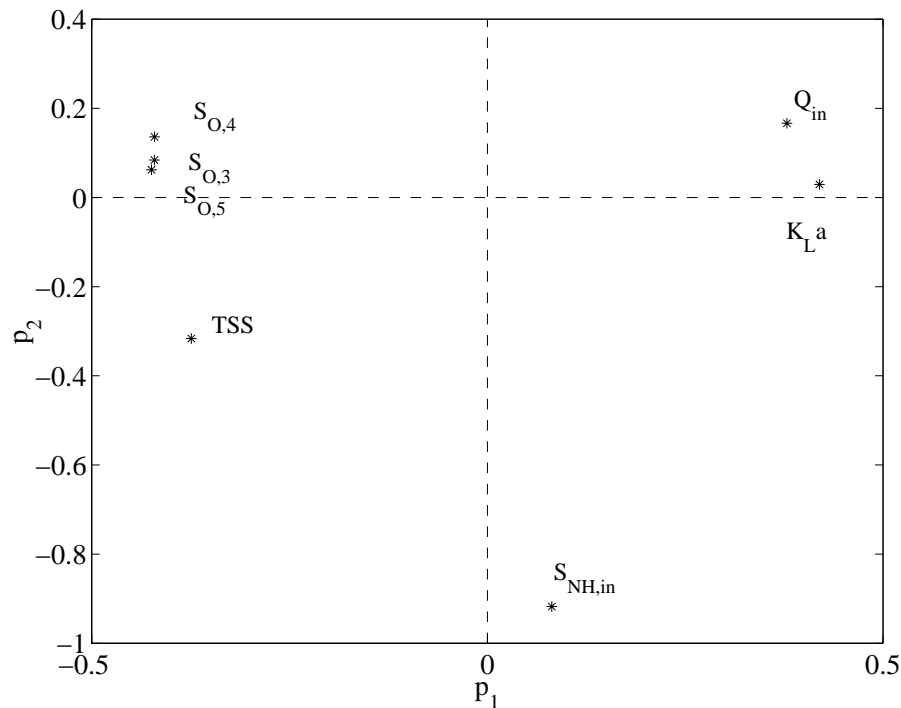
**Figure 7.26**  The first two loading vectors. The points indicate the influence
of a certain variable upon the process.

lower than normal. In order to create a simple criterion, the nitrogen
level is discretised into normal and low. Every value below the 0.10
quantile is labelled low, the rest is labelled normal. The aim is thus to
recognise a deviating score pattern when the nitrate level is low. The
rain data will serve as validation data of the classification.

As previously described in Chapter 6, the $k$-nearest clustering al-
gorithm is simple and easy to use. Training instances are the two
first score vectors and the discretised nitrate level is the class out-
come. Figure 7.27 (top), displays how the instances with an outcome
of low nitrate level cluster in the upper right corner ('+'= instances
with low nitrate level). 11-nearest, that is $k = 11$, classification is used
on the rain data and the outcome of is shown in Figure 7.27 (bottom).
The algorithm classifies most of the deviating scores as "low nitrate".
Consequently, the mechanism resulting in low nitrate during the storm
event, is also present during the rain event. The classification preci-
sion could probably be improved by filtering and introducing a time
delay. One way to monitor the reliability of the classification is to plot
the sum of the distances between a new instance and the $k$ nearest
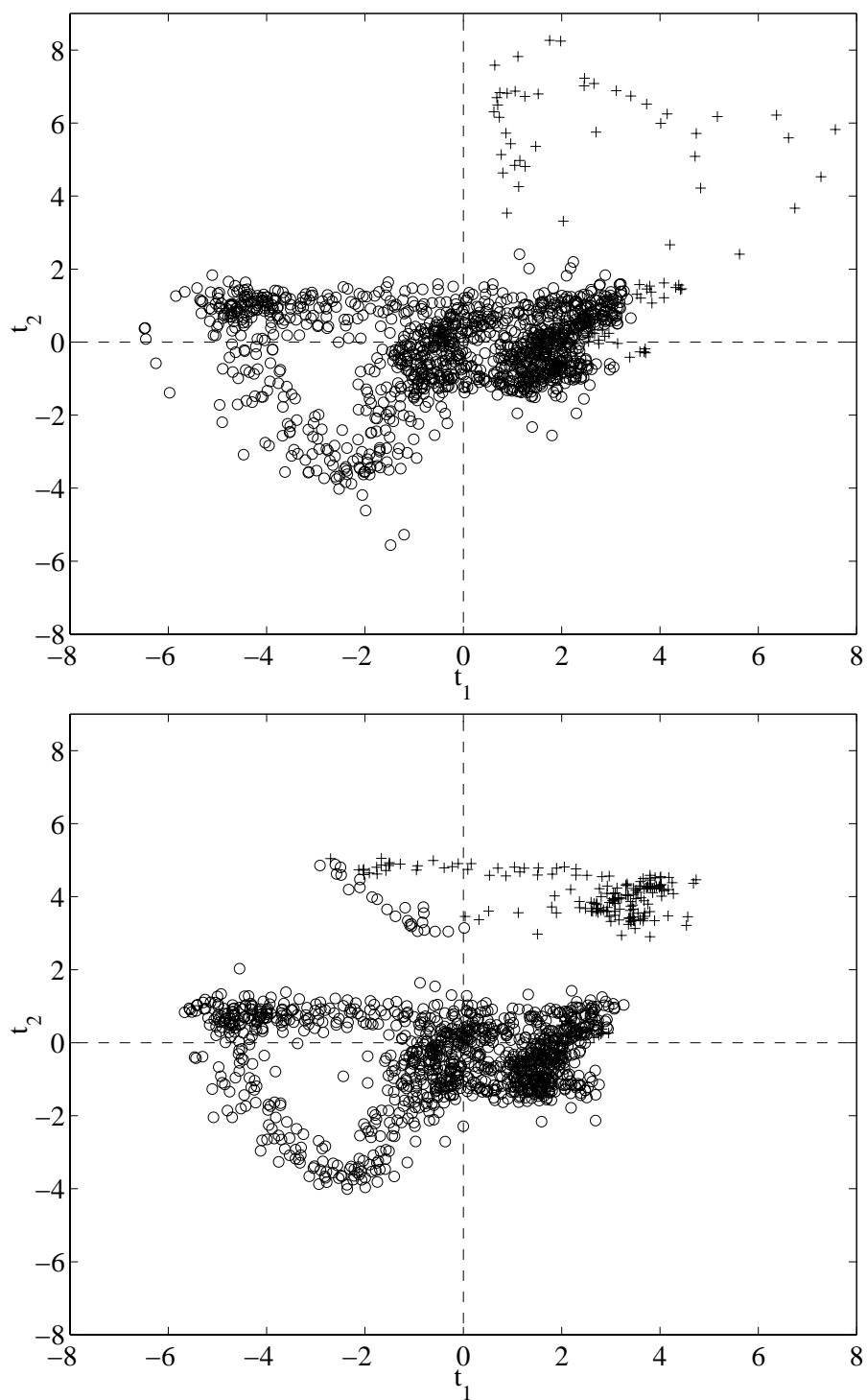
**Figure 7.27**    Training instances (top) and 11-nearest classified instances (bottom). '+'= low nitrate effluent level and 'o'= normal nitrate effluent level.

neighbours. High values of the sum indicate that the classification is somewhat uncertain and should be used with care. In Figure 7.28, the sum of distances is plotted for the rain data. It is clear that the classifications around samples 880 to 895 and 975 to 990 are not very reliable. As a matter of fact, these are actually the instances with an outcome of normal nitrate value in the upper cluster in shown Figure 7.27 (bottom).
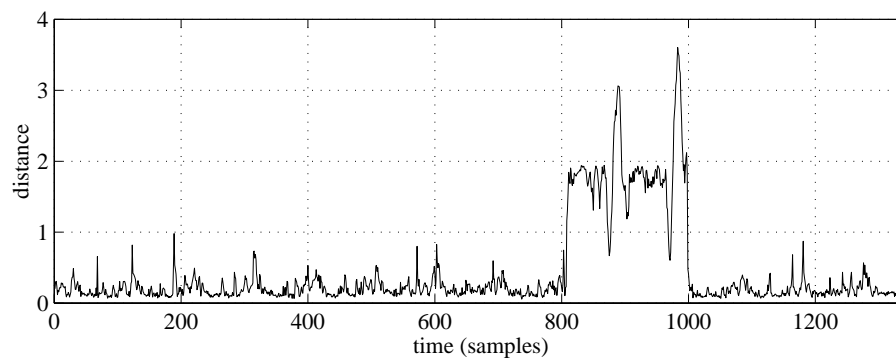


**Figure 7.28**   The sum of distances between a new instance and the 11-nearest neighbours.

When a new deviation occurs, the same procedure can be used to link this deviation to another important observation or key variable. Instances can also be added to already known classes in order to decrease the uncertainty, for example, since the rain event has the same effect on the effluent nitrate concentration as the storm events, the rain instances can be added to the training data for the low nitrate class. However, an increasing number of examples in the training data make the $k$-nearest algorithm slow, as every example must be checked in order to find the $k$ nearest neighbours.

# 7.3  Specific Operational Mode Monitoring

So far, the monitoring examples presented in this chapter have been focusing on the general operational mode. No consideration has been taken to the effluent or quality variables of the simulated plant. Consequently, the PCA models have been used as monitoring models. If the monitoring is to be emphasised upon a subprocess of the treatment process, the model must be able to take particular consideration to the variables influencing that subprocess. This can be achieved with PLS.

## Monitoring the Performance

Let us assume that the most critical requirements for the simulated wastewater treatment plant are on effluent nitrogen concentration. It would then be desirable to emphasise the monitoring task of variables influencing the effluent nitrogen. This can be achieved by PLS, where the input variables ($X$-block) are the same as in the PCA case listed in Table 7.5 and the output variables ($Y$-block) are the effluent nitrate and ammonia concentration. The monitoring model is then identified in such a way, that a maximum of the variance in both input and output variables is described. A static PLS model with time delays is identified from training data, which consist of 672 samples, *i.e.* one week's data. Time lags according to a crosscorrelation analysis between the input and output blocks are included in order to make the model more accurate. In this case, when the $Y$-block constitutes two output variables, the determination of the time lags becomes difficult. This is due to the fact that the time lags between the $X$-block and the separate variables in the $Y$-block differ. However, it turns out that the crosscorrelation is practically the same and, consequently, a compromise can be made. In Table 7.8 the explained variability of the $X$ and $Y$-block is listed, respectively. As shown in the table, the model is able to capture most of the variability of the $X$-block, which is desirable in a monitoring situation, and a large part of the variability of the $Y$-block. Best predictive ability is accomplished with six latent variables (LVs).

| LV | $X$-block total | $Y$-block total |
|----|----------|----------|
| 1 | 82.14 | 66.85 |
| 2 | 90.96 | 74.51 |
| 3 | 96.92 | 79.12 |
| 4 | 98.23 | 84.24 |
| 5 | 99.12 | 85.83 |
| 6 | 99.85 | 86.19 |

**Table 7.8**    Explained variability of the $X$ and $Y$-block, respectively.
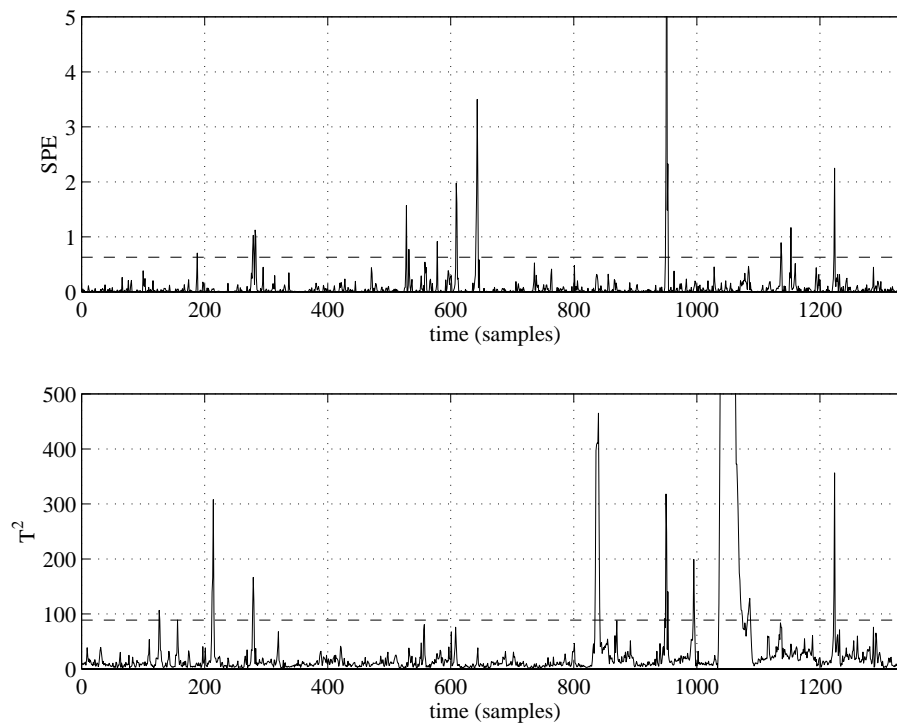


**Figure 7.29**    $SPE$ (top) and $T^2$ (bottom) measures during the storm events.

Figure 7.29 displays the behaviour of the model when the storm data are processed. The $SPE$ measure (top) is low, which is expected as six out of seven LVs are used. The $SPE$ does not increase during the storms and this is an indication that the internal relations are not altered according to the model. On the other hand, the $T^2$ measure displays significant deviations at both storm events (around samples 850 and 1100, respectively).
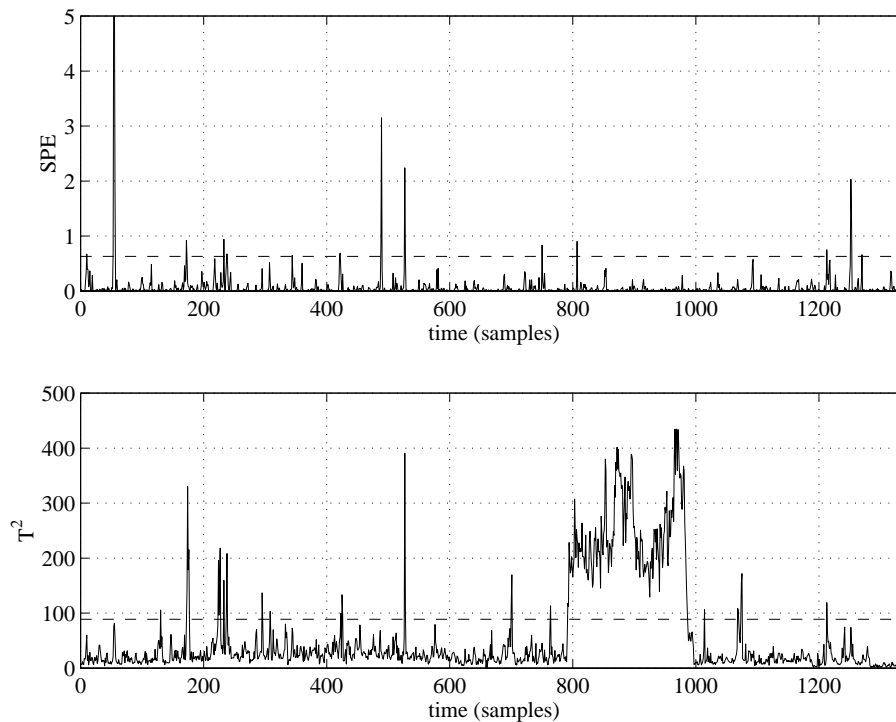


**Figure 7.30**   $SPE$ (top) and $T^2$ (bottom) measures during the rain events.

The rain event is monitored in Figure 7.30. Here, the $SPE$ is constantly low and the process is inside the model region. However, the $T^2$ measure deviates significantly during the rain event (samples 800 to 1000).

## Quality Variable Prediction

An appealing feature of the regression methods is the predictive capability. The predictive capability can be used directly to estimate variables not measured or measured only at sparse instances. Prediction can also be used for continuously validating the monitoring

| Model | No of LVs | $X$-block total | $Y$-block total |
|-------|-----------|-----------------|-----------------|
| 1     | 6         | 99.77           | 81.99           |
| 2     | 6         | 99.76           | 85.49           |
| 3     | 12        | 98.37           | 93.43           |

**Table 7.9**  Explained variability of the first (static, without time lags), second (static, with time lags) and third (FIR model) PLS model.

model. Here, examples of both fields of application are presented.

## Prediction of Effluent Nitrate

Measuring devices are expensive, both in terms of money and maintenance. Due to this, the number of measurements is often kept at a minimum. Therefore, it is important to be able to estimate variables not available from the measurement system. An example of this can be the effluent nitrate concentration. If a plant is built with parallel lines, a good model can reduce the need for nitrate sensors. Instead of installing one sensor in each line, only one can be installed and a model can be used to estimate the nitrate concentration in the other lines. The estimates will not be as good as a real sensor, but the results can be used to indicate disturbances, calling for deeper investigations.

The independent block consists of the variables listed in Table 7.5. The dependent block is the effluent nitrate $S_{NO}$, or more precisely the nitrate concentration in reactor 6. Three PLS models are built. The first is a static model, with no regard to time lags. The second model is a static model with time lags. The third model is a finite impulse response (FIR) PLS model. The time lags are determined with crosscorrelation analysis. The time lag demonstrating the best correlation is chosen as the time lag for the relation between the independent and dependent variable. The number of historic measurements included in the FIR model is also determined by crosscorrelation analysis. There are different numbers of historic measurements for each variable in the $X$-block and the numbers are chosen in such way that the time shift corresponding to the maximum crosscorrelation is included. In order to chose the appropriate number of components retained in each

model, crossvalidation is used.  In Table 7.9, the explained variability
of the three models is shown.
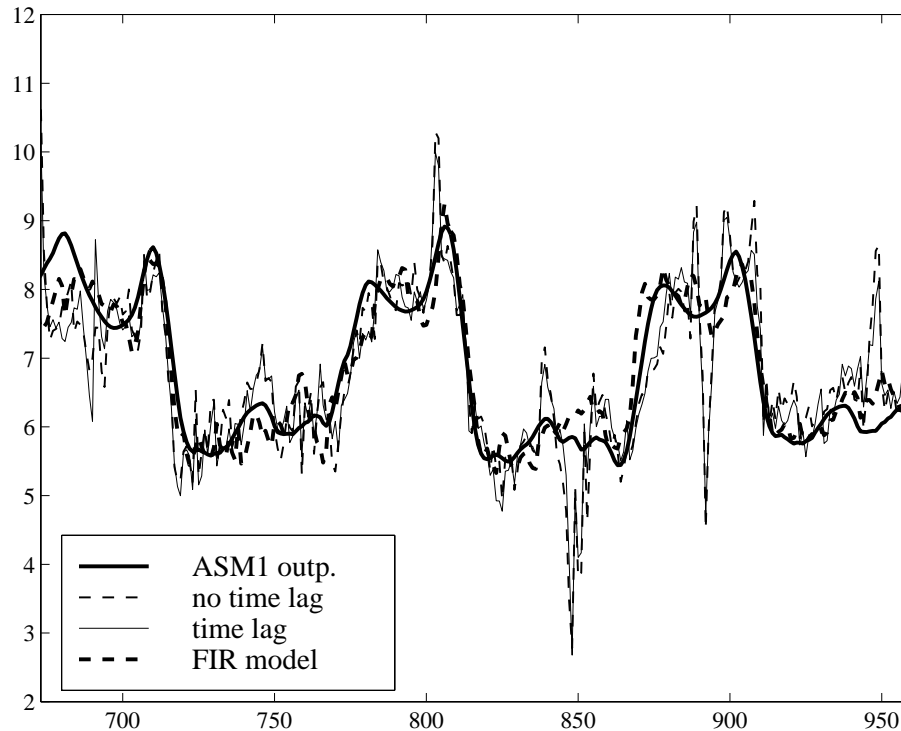


**Figure 7.31**   The performance of the three models during normal (training)
conditions.  The plot displays the results during three days,
of which the first is a Sunday (different operational conditions
during weekends).

In Figure 7.31, the ASM1 output value and the predictions from the
PLS models are shown.  Only the results during three days are plot-
ted to be able to discern the separate graphs.  The predictions are
good, no model results deviate significantly from the ASM1 output.
This is expected since the explained variability is high for all three
models.  However, more interesting is to investigate how the models
perform when a new situation, not encountered in the training data,
arises.  Figure 7.32 shows the prediction during the two storm events
(a total time period of six days).  It is obvious that the static model
with no time lags performs poorly when compared to the other two
models.  This is especially significant during the second rain event,
around samples 2300 to 2450.  Here, the first model predicts an in-
crease when the ASM1 output is actually decreasing.  The second
(static with time lags) and third (FIR model) perform well, and both
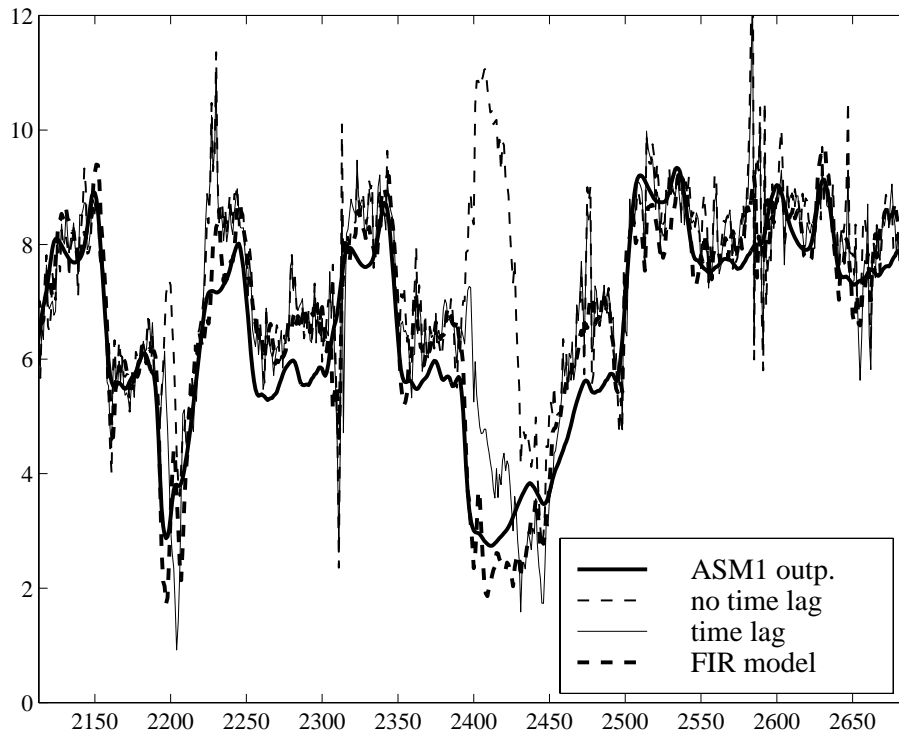
**Figure 7.32**   The performance of the three models during two storm events.

have captured the mechanisms that cause the nitrate concentration to decrease even though the FIR model is notably better. During the rain event the FIR model produces relatively good predictions. The static model with time delays also captures the main dynamics of the system. Which model produces the best prediction? One way to determine this is to examine the sum of squares of the prediction error (see Equation 6.26). The mean $SPE_Y$ of models 1, 2 and 3 is listed in Table 7.10.

The best predictive performance is achieved with the FIR model. This is not a surprising result as this model captures the most variability of the training data. The above is only an example of the performance of different models. In other situations, static models may perform better than FIR (or IIR) models. The situation and the aim of the model determine the best model structure.
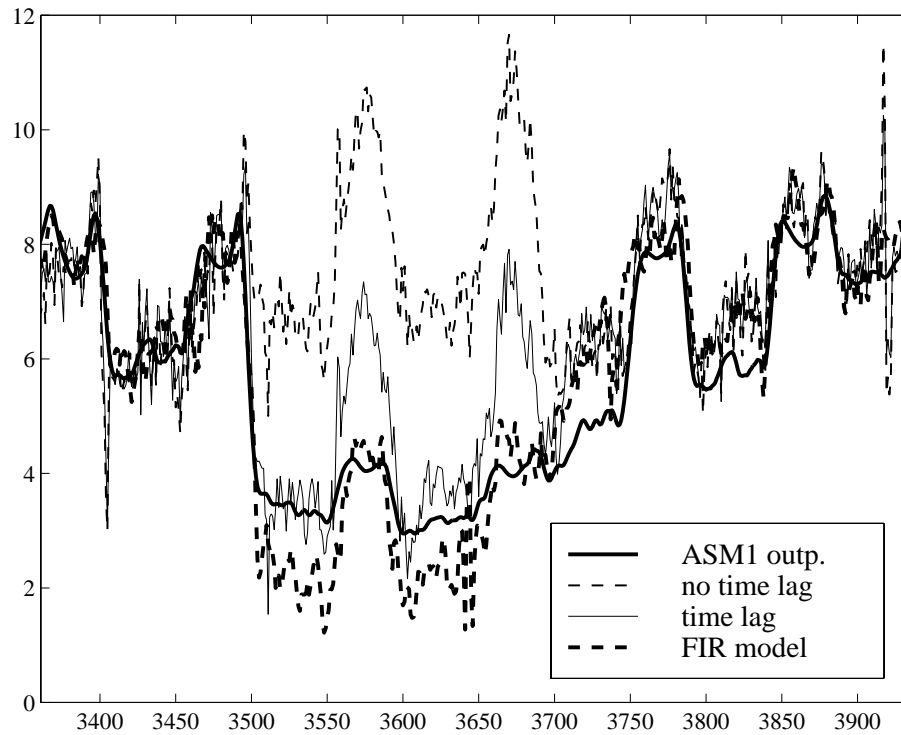
**Figure 7.33**   The performance of the three models during the rain event.

| Model type | mean $SPE_Y$ |
|---|---|
| Static without time lags | 2.10 |
| Static with time lags | 0.77 |
| FIR model | 0.59 |

**Table 7.10**   The mean $SPE_Y$ of the PLS models.

# Chapter 8

# MVS Applied to Real On-line Measurements

In this chapter a few detection examples are presented. They are chosen to be informative and representative for the operation of a treatment plant. The data that are used in this chapter, are real data from the Ronneby wastewater treatment plant in Sweden.

## 8.1   The Ronneby Treatment Plant

The Ronneby treatment plant was originally built in 1970 and is located on south-east coast of Sweden. The recipient, the Hanö bay, is considered to be an environmentally sensitive area, and the requirements on effluent quality have been increased over the years. This led to a major upgrade of the plant in the early nineties, aiming at nitrogen removal with a capacity for enhanced biological phosphorous removal. However, chemical post-precipitation is still used to remove phosphorous. The principal layout of the plant is shown in Figure 8.1. The Ronneby plant serves the city of Ronneby with a population of about 15.000. Some key dimensions of the plant are given in Table 8.1. The biological reactors at the Ronneby plant are divided into two parallel lines. This is done to ensure the capability to always keep one line intact in case of major disturbances, *e.g.* loss of nitrification. The intact line can then be used to recover the treatment capacity of the affected line. The Ronneby plant is operated at a specific DO setpoint concentration, using controllers to maintain the DO concentration. This is done successfully with rare deviations from the setpoint. The DO concentration is measured at two separate locations in each line. At the point of influent, flow rate, ammonia concentra-
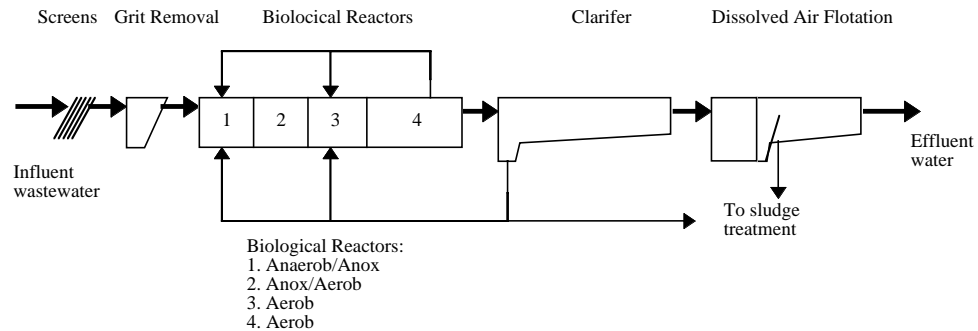
**Figure 8.1**   The principal layout of the Ronneby wastewater treatment plant.

| Design load | |
|---|---:|
| Average flow rate $(m^3/day)$ | 10.000 |
| BOD$_7$ $(kg/day)$ | 2.000 |
| Tot-N $(kg/day)$ | 400 |
| Tot-P $(kg/day)$ | 80 |

| Dimensions | |
|---|---:|
| Anaerobic* $(m^3)$ | 0 |
| Anoxic* $(m^3)$ | 3.000 |
| Aerobic $(m^3)$ | 3.200 |
| Clarifier $(m^2)$ | 2.010 |

| Effluent quality requirements | |
|---|---:|
| BOD$_7$ $(mg/l)$ | < 15 |
| Tot-N $(mg/l)$ | < 12 |
| Tot-P $(mg/l)$ | < 0.5 |

* The plant can be operated with either 3.000 $m^3$ anoxic volume or 2.000 $m^3$ anoxic volume and 1000 $m^3$ anaerobic volume.

**Table 8.1**   Some key dimensions and figures for the Ronneby plant.

tion, conductivity, pH and temperature are measured. Besides the DO concentration, sludge concentration and air valve position of the aeration systems are measured in. At the point of effluent from the biological reactors, ammonia and pH are measured, while phosphate, turbidity and pH are measured at the plant outlet. The measurement system collects data with a sampling interval of 5 minutes, *i.e.* 288 samples per day.

## 8.2  Monitoring General Operational Modes

As discussed in Chapter 6, a *general* operational mode describes the process mode without one or several target variables in mind. This makes PCA suitable for the task. A straightforward way of using PCA for classification of operational modes is to use the statistics described in Chapter 6. The PCA model is developed from data representing normal and/or desired operational behaviour of the process. Confidence limits of $SPE$ and $T^2$ are used to decide whether the process mode is normal or not. The mode definitions are thus restricted to normal and abnormal operation. As soon as the $SPE$ or $T^2$ measures exceed their limits, the process is said to be in an abnormal mode. This is of course based on the assumption that the measurements are correct. Consequently, we will have two cases of abnormal operation: truly abnormal mode and believed abnormal mode due to sensor failure. The PCA model will not distinguish between these cases. However, if there is a sensor failure, this is also important information. It is often easy to distinguish a sensor failure from a process failure, as the sensor failure will normally influence only one variable. Process failures on the other hand, can often be tracked in several variables. Also, sensor failures often appear more abruptly than process changes.

### Detection of a Sensor Failure

The general operational mode of the Ronneby wastewater treatment plant is monitored with PCA. The model is identified from data during

| Variable number | Measured entity |
|---|---|
| 1 | influent temperature |
| 2 | sludge concentration in line 1 |
| 3 | sludge concentration in line 2 |
| 4 | air valve position of blower 1 in line 1 |
| 5 | air valve position of blower 2 in line 1 |
| 6 | air valve position of blower 1 in line 2 |
| 7 | air valve position of blower 2 in line 2 |
| 8 | influent conductivity |
| 9 | influent ammonia |
| 10 | influent pH |
| 11 | influent flow rate |

**Table 8.2**   Variables used in the PCA model.

a period of 2500 samples, *i.e.* approximately 9 days, and the variables used are given in Table 8.2. During the period from which the training data are collected, the process demonstrates a normal and desired behaviour. Thus, the process mode described by the PCA model can be said to be a normal operational mode. In the PCA model, six principal components are retained, capturing approximately 90% of the variability of the original data matrix (Table 8.3). The $SPE$ and $T^2$ measures of the new data are shown in Figure 8.2 and it is obvious that everything appears relatively normal until sample 731. At this time, both $SPE$ and $T^2$ increase suddenly, and exceed the confidence limits by a wide margin. The mode can be classified as abnormal. The change is rapid, which suggests that the problem is not process related. Instead, the change may have been caused by a sensor failure. From Figure 8.3 it is concluded that the contribution to the deviation in $SPE$ at sample 731 is mainly caused by a change in variable 8, *i.e.* influent conductivity. There are also significant contributions from variables 1 and 2, influent temperature and sludge concentration, respectively. If the contribution to the changes along the PCs between sample 730, where the $SPE$ and $T^2$ measures are still small, and sample 731 is studied, the picture becomes clear (Figure 8.4). It is obvious that there is a change in variable 8 (influent conductivity) and that this has caused the $T^2$ measure to exceed its limits. It can be seen in Figure 8.2 that the residuals decrease at sample 1070 as suddenly as they increased at sample 731. This is caused by a corrective action

| Principal component number | Eigenvalue of cov(X) | % Variance captured this PC | % Variance captured total |
|---|---|---|---|
| 1 | 4.70e+00 | 42.74 | 42.74 |
| 2 | 1.89e+00 | 17.18 | 59.93 |
| 3 | 1.32e+00 | 11.97 | 71.89 |
| 4 | 9.26e-01 | 8.42 | 80.31 |
| 5 | 6.65e-01 | 6.05 | 86.36 |
| 6 | 4.28e-01 | 3.89 | 90.25 |
| 7 | 3.40e-01 | 3.09 | 93.34 |
| 8 | 3.00e-01 | 2.73 | 96.06 |
| 9 | 2.52e-01 | 2.29 | 98.35 |
| 10 | 1.23e-01 | 1.12 | 99.47 |
| 11 | 5.78e-02 | 0.53 | 100.00 |

**Table 8.3**   Percent variance captured by the PCA model.
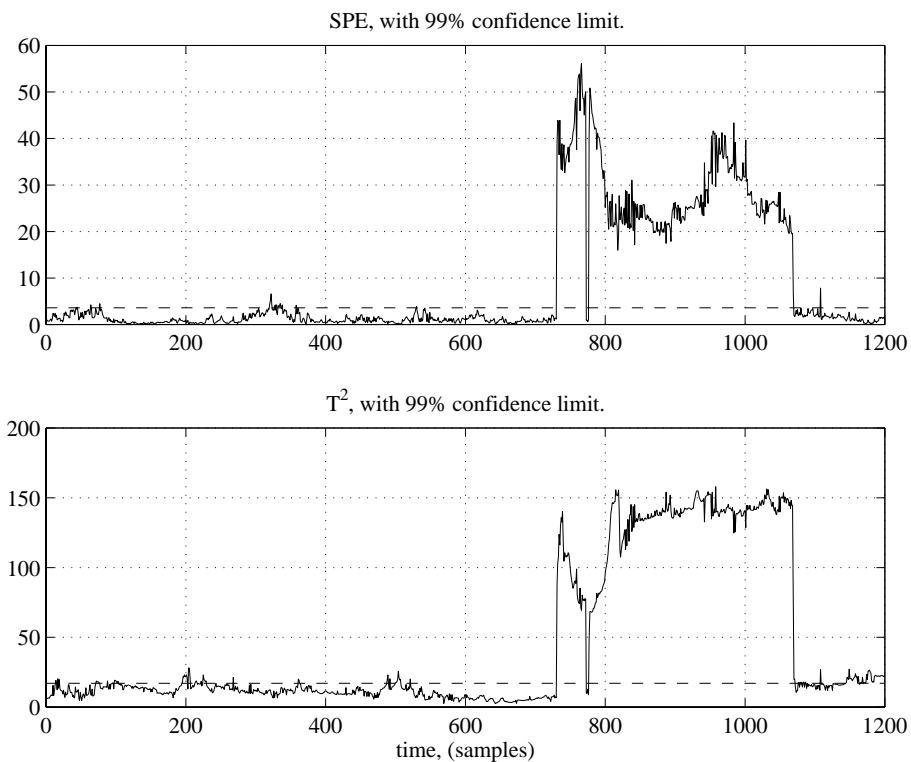


**Figure 8.2**   The $SPE$ and $T^2$ measures for new data.
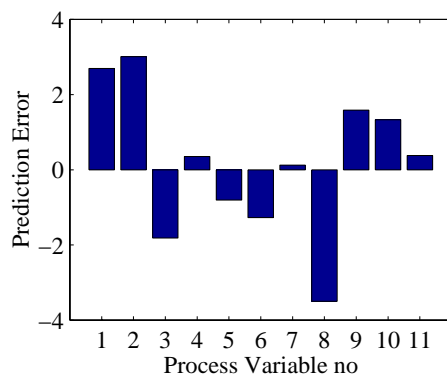
**Figure 8.3**   The contribution to the large $SPE$ in sample 731.
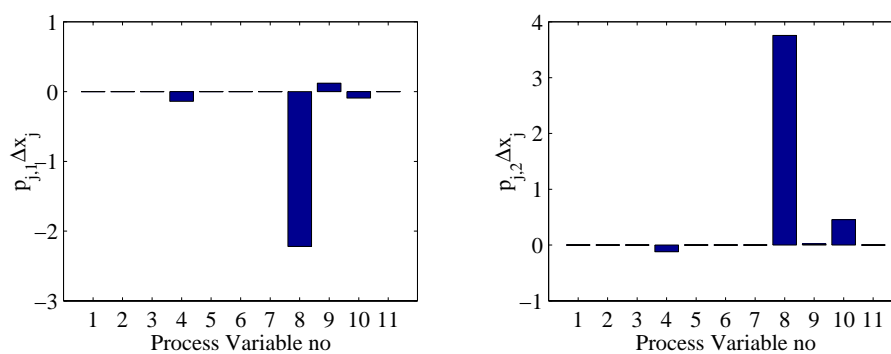


**Figure 8.4**   Variables contributing to change along PC no 1 (left) and PC
no 2 (right).

| Principal component number | Eigenvalue of cov(X) | % Variance captured this PC | % Variance captured total |
|:---:|:---:|:---:|:---:|
| 1 | 3.96e+00 | 33.03 | 33.03 |
| 2 | 2.43e+00 | 20.21 | 53.24 |
| 3 | 1.84e+00 | 15.37 | 68.61 |
| 4 | 1.31e+00 | 10.96 | 79.57 |
| 5 | 8.14e-01 | 6.79 | 86.36 |
| 6 | 6.89e-01 | 5.74 | 92.10 |
| 7 | 4.09e-01 | 3.41 | 95.50 |
| 8 | 2.31e-01 | 1.92 | 97.43 |
| 9 | 1.72e-01 | 1.43 | 98.86 |
| 10 | 7.61e-02 | 0.63 | 99.50 |
| 11 | 6.02e-02 | 0.50 | 100.00 |
| 12 | 1.14e-14 | 0.00 | 100.00 |

**Table 8.4**   Percent variance captured by the PCA model.

performed on the failing sensor. The significant increase in both $SPE$ and $T^2$ makes it difficult to draw any conclusions of how the process is operating during the sensor failure. A small but significant change of the process behaviour would "drown" in the residuals caused by the sensor failure. Thus, it is important that the misleading data from the erroneous sensor are replaced by data not distorting the monitoring.

## Detection of External Disturbance

In the previous example the cause of the change of operational mode was caused by a sensor failure. This should have been resolved during the screening stage of the data. A more interesting situation is if there are many concurrent variables driving the process in a certain direction. A PCA model is developed to monitor the process behaviour. In order to obtain a general model, more samples than in the previous example were included. The model is based on 6000 samples (approximately 21 days) collected during normal operational conditions. There are periods of rain and other minor disturbances, which make the model slightly more tolerant to such disturbances in the data. The data used for developing the model are the same as in the previous example, except that a variable describing the difference

between sludge concentration in line 1 and 2 is included as variable 12.
The captured variance is shown in Table 8.4. The number of retained
principal components are chosen to four. This implies that the model
is able to capture approximately 80% of the variance of the training
data.

In Figure 8.5, the $SPE$ (top) and $T^2$ (bottom) measures are plotted.
First we focus on the $SPE$ measure. The residual is increasing signifi-
cantly from sample 650 and forward. As mentioned before, the $SPE$
is the Euclidian distance between the sample and the model plane
(with four dimensions in this case). After sample 650 the process
leaves the model region and the distance to the model plane increases.
A residual contribution plot (Figure 8.6, top) reveals what has caused
the deviation. At sample 685 there is no single variable that can be
pointed out as the main cause. Variables 1 (influent temperature) and
9 (influent pH), together with variables 5 (air valve position) and 11
(influent flow rate) are slightly more dominant than the others. The
conclusion is that the process has left the model region and several
variables have contributed to this. In the residual contribution plot
at sample 852 (Figure 8.6, bottom), it is possible to distinguish a few
dominant variables contributing to the deviation. Variables 2 (sludge
concentration, line 1), 10 (influent pH) and 12 (difference in sludge
concentration between lines 1 and 2) appear to be the main contrib-
utors. The disturbance in sample 852 is thus not exactly the same as
in sample 685.

The $T^2$ measure also increases around sample 650. The residual
reaches a peak at sample 685, and the reason can be found in the
contribution plots. Figure 8.7 shows the variables contributing to the
change along the principal component between samples 640 and 685.
Here, variables 4, 5, 6, 7 (air valve positions) and 11 (influent flow
rate) are the most dominant variables. An increased influent flow rate
causing an increased demand of aeration seem to be the reason that
the $T^2$ measure exceeds its limits. The variables contributing to the
change along the PCs between samples 640 and 852 are shown in Fig-
ure 8.8. There are two dominant variables: 2 (sludge concentration
in line 1) and 12 (difference in sludge concentration). The conclusion
is that there is a change in the sludge concentration in line 1. Hence,
the disturbances at samples 685 and 852 are not the same.
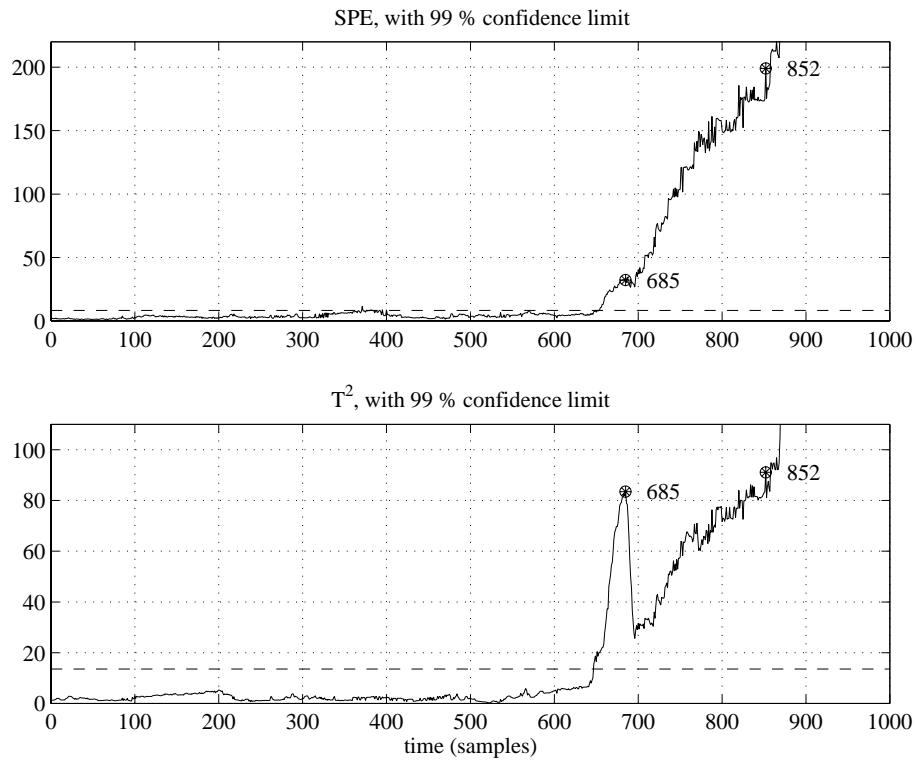
**Figure 8.5**   The $SPE$ and $T^2$ measures for the new data.
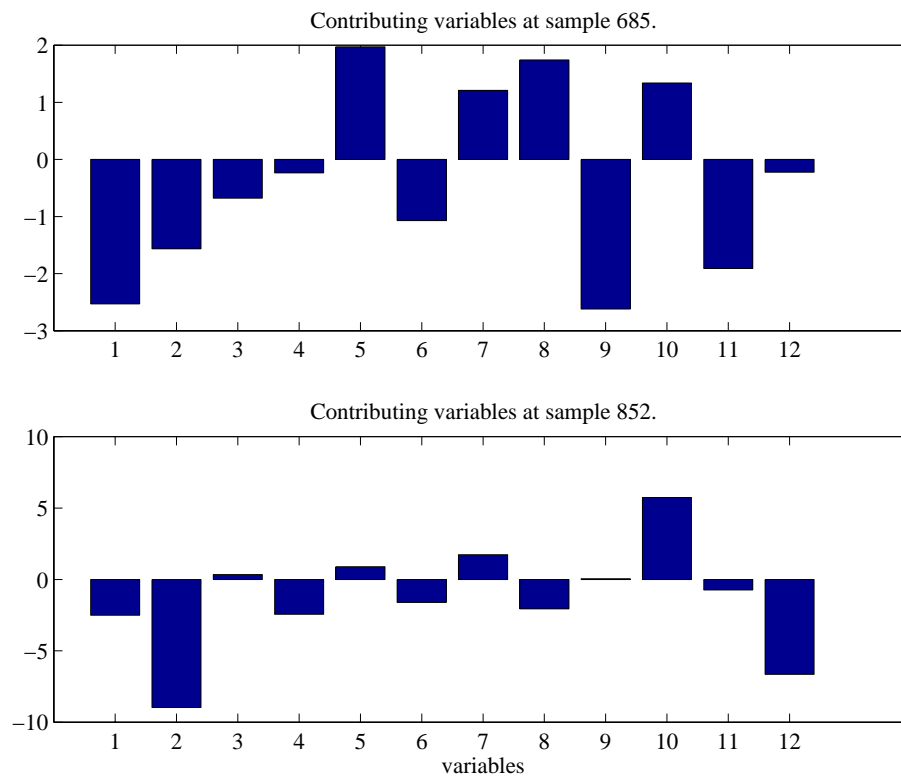


**Figure 8.6**   Variable contribution to $SPE$ at samples 685 (top) and 852 (bottom).
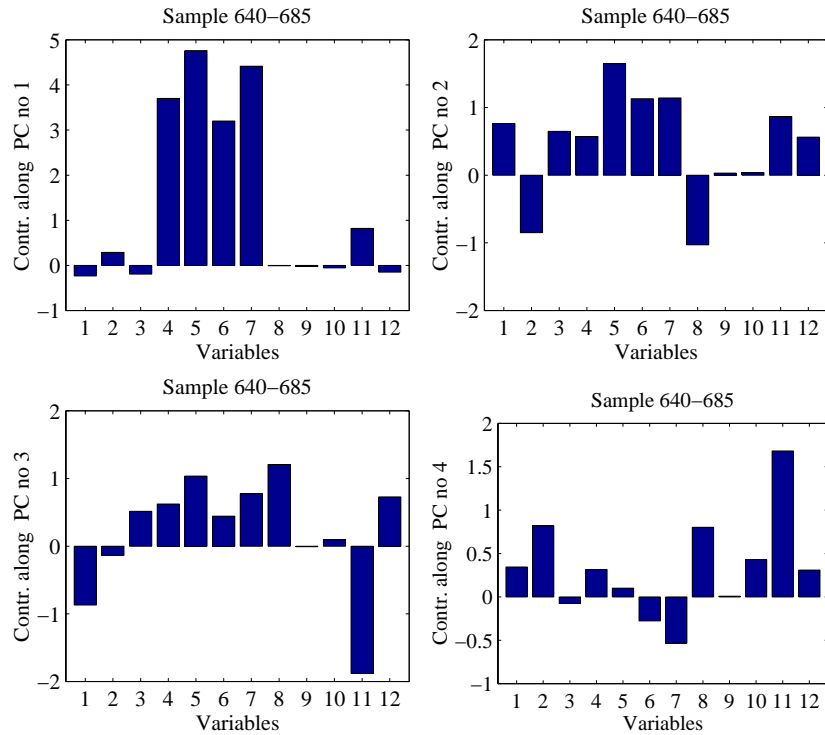
**Figure 8.7**    Variables contributing to the change along the PC nos 1, 2, 3 and 4 between samples 640 and 685.
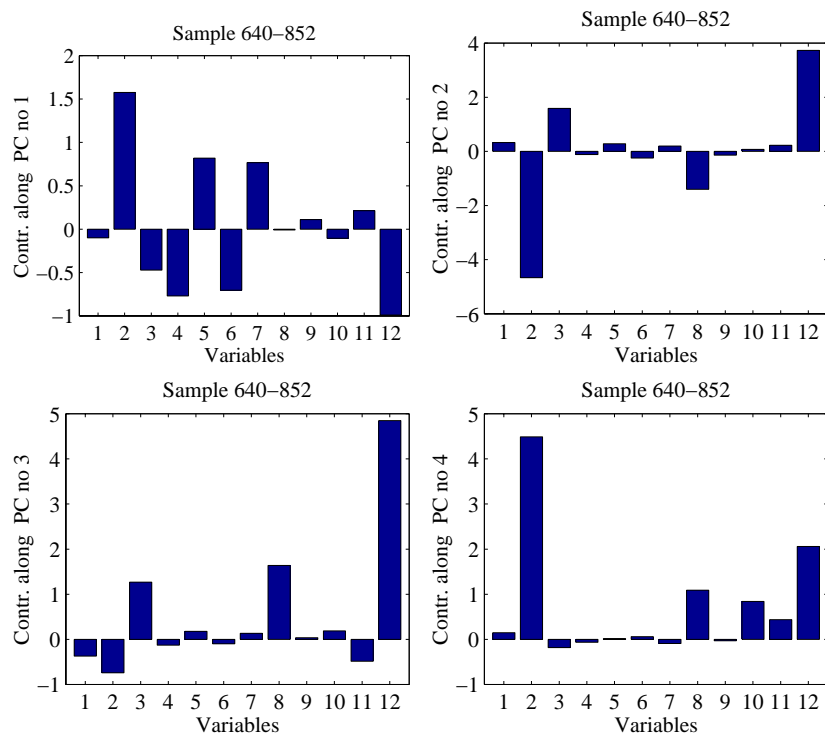


**Figure 8.8**    Variables contributing to the change along the PC nos 1, 2, 3 and 4 between samples 640 and 852.

The original variables are shown in Figures 8.9, 8.10 and 8.11. The limits are the approximate 95% confidence limits of the original training data. It is obvious that there are disturbances in most variables somewhere between samples 600 and 700, and it is difficult to determine which ones are responsible for the deviations in $SPE$ and $T^2$. The contribution plots make it easier to determine the most probable main contributors to the process deviation and, thus, to the change in mode from normal to abnormal operation.
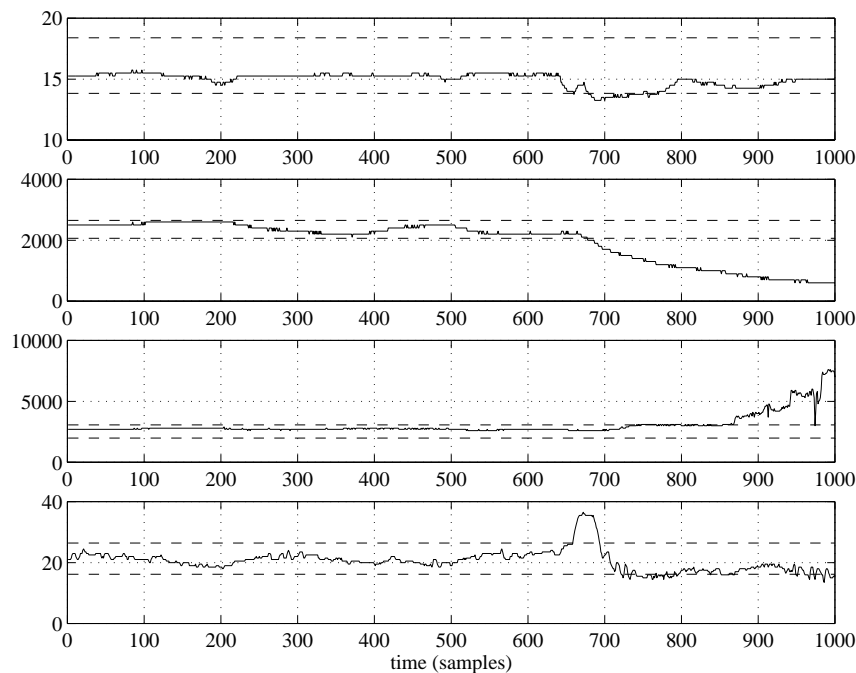


**Figure 8.9**   The original (measured) variables 1 to 4, plotted in order from top to bottom. The dashed lines correspond to the approximate 95% confidence limits of the training data.
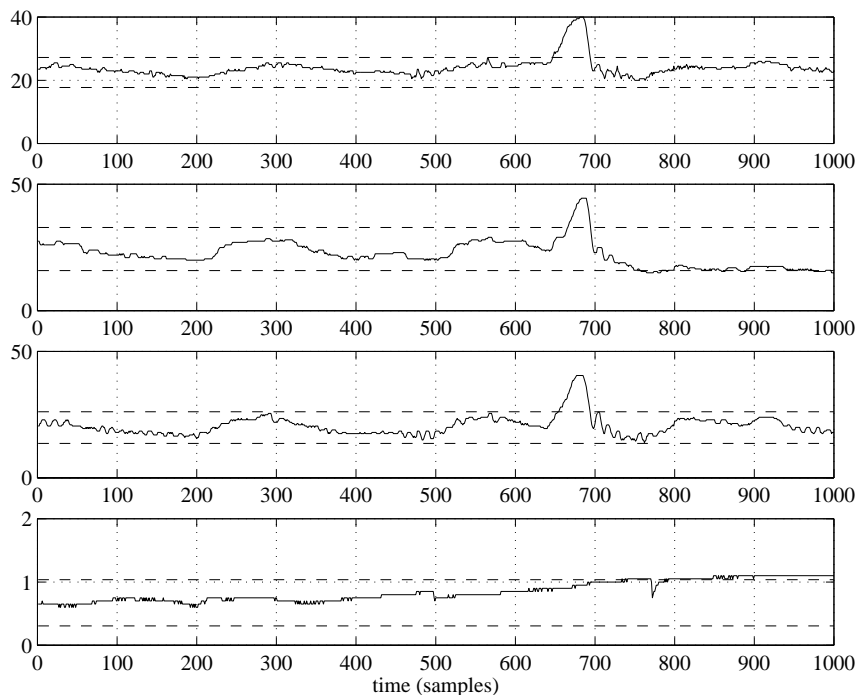
**Figure 8.10**    The original (measured) variables 5 to 8, plotted in order from top to bottom. The dashed lines correspond to the approximate 95% confidence limits of the training data.
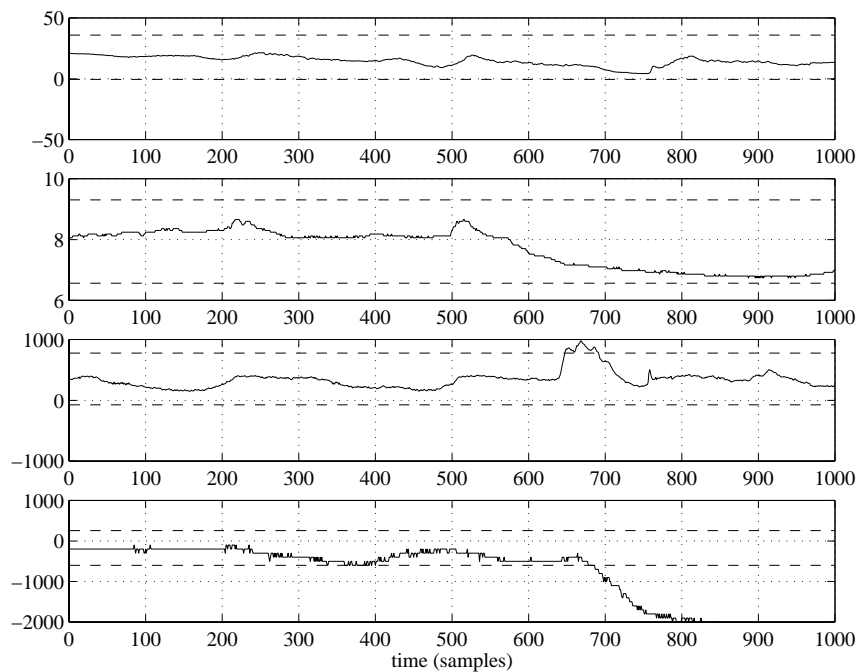


**Figure 8.11**    The original (measured) variables 9 to 12, plotted in order from top to bottom. The dashed lines correspond to the approximate 95% confidence limits of the training data.

| Principal component number | Eigenvalue of cov(X) | % Variance captured this PC | % Variance captured total |
|---|---|---|---|
| 1 | 3.56e+00 | 35.55 | 35.55 |
| 2 | 1.43e+00 | 14.30 | 49.86 |
| 3 | 1.34e+00 | 13.40 | 63.26 |
| 4 | 1.08e+00 | 10.77 | 74.02 |
| 5 | 8.27e-01 | 8.27 | 82.29 |
| 6 | 6.90e-01 | 6.90 | 89.19 |
| 7 | 5.02e-01 | 5.02 | 94.21 |
| 8 | 3.56e-01 | 3.56 | 97.77 |
| 9 | 1.69e-01 | 1.69 | 99.45 |
| 10 | 5.46e-02 | 0.55 | 100.00 |

**Table 8.5** Percent variance captured by the PCA model.

# Detection Using Multiple Operational Classes

Monitoring the $SPE$ and $T^2$ residuals is effective, but not especially transparent. As mentioned before, the nature of most industrial processes implies that only a few latent variables or principal components will cover most of the variability of the process space. By plotting, for instance, the first score vector against the second score vector the process changes can be viewed as a point moving around in the plane as new samples are added. Points that cluster represent similar process behaviour and, consequently, deviating points indicate process changes. This makes the score plot useful for classification purposes. A PCA model is identified from a set of data containing 10 000 samples (approximately 36 days) of process measurements. The variables included in the analysis is the same as the ones listed in Table 8.2. However, the temperature measurement is excluded for reasons discussed later. The model is able to capture 50% of the variability using two principal components (Table 8.5). In Figure 8.12, it is shown that the majority of the data is located in a cluster somewhat symmetrically located around the origin. There is one more cluster below the main cluster. The clusters are demarcated by class boundaries. These boundaries are determined empirically, by manually examining the plot. Four classes are defined from the numerical characteristics of the data. Is it possible to find a physical interpretation to the cluster appearances? Some of the variables of the data used to identify the
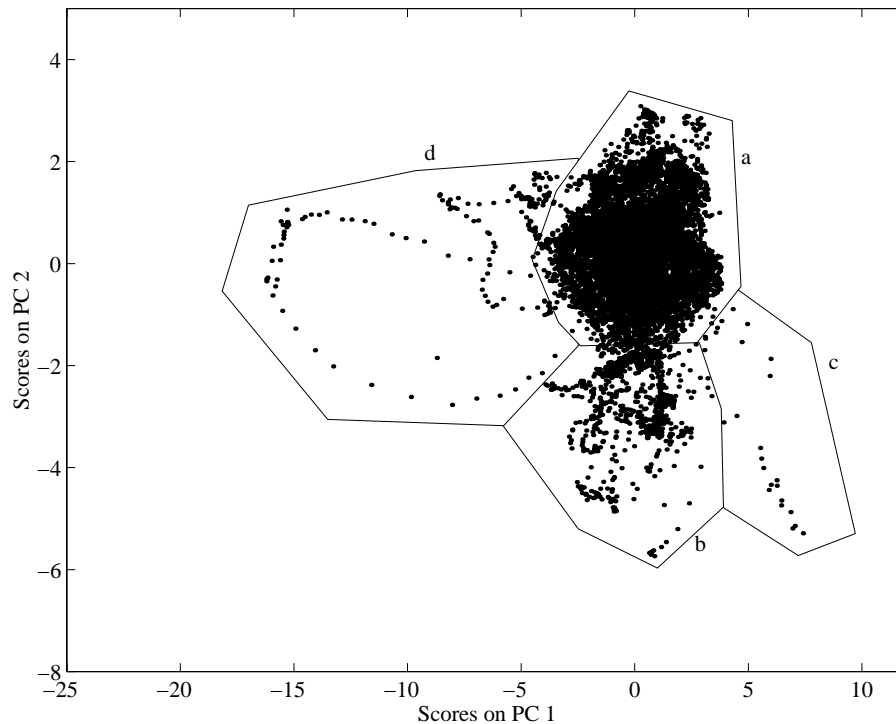
**Figure 8.12**   Score plot with classes manually defined from separate clusters
and patterns in the plane.

PCA model are shown in Figure 8.13. There are some events occur-
ring during the training period: immediately before sample 2000 there
are a few peaks in the influent flow rate (plot d) and in the air valve
position (plot c), around samples 4400, 5800 and 6900 there are peaks
in the suspended solids concentration (plots a and b) and from about
samples 7000 to 7500 there is a period of rain increasing the influent
flow significantly (plot d). All these events are represented by the
different class memberships in the score plot. Normal, dry-weather
conditions are covered by class a. The peaks in flow rate together
with the increased oxygen demand are represented by class d, longer
periods of high flow rate fall into class b and upsets in the suspended
solids concentrations belong to class c. As shown in Figure 8.12, differ-
ent operating conditions appear as clusters or deviations in the score
plot. Next step is to investigate how the PCA model performs when
it is applied to new (on-line) data. In Figure 8.14, the PCA model
and its classes, are used to classify new data (10000 samples). The
majority of the data falls into the normal class (a), but there are some
interesting deviations. Data are frequently classified as class b (high
flow rate) and some times as class d (high oxygen demand). There are

**Figure 8.13**  The original (measured) variables. Suspended solids concentration in line 1 (a) and in line 2 (b). Air valve position (c) and influent flow rate (d).

also samples falling outside all the defined classes, somewhere between and below classes b and d. In that case we have a situation not covered by the defined classes, and the set of classes may have to be updated for future use. The data falling outside the defined classes ranges from samples 1937 to 1972 in the first event (the loop below class d) and from samples 3090 to 3100 in the second event (the loop below class b). By examining Figure 8.15, both events can be traced to an increase in both oxygen demand (plot c) and influent flow rate (plot d). This is not surprising as the events occur in between and below classes b and d in Figure 8.14. The samples inside class c can be interpreted as an increase in the suspended solids concentration around samples 2150 and 3460. As a matter of fact, some samples fall outside the axis of the score plot and are not included for clarity reasons. An example of an event outside the score plot can be seen in Figure 8.15 around sample 500. It is obvious that something is wrong at this point in time.

In this example it is demonstrated that PCA can be used for classification of general operational modes, and that the number of classes

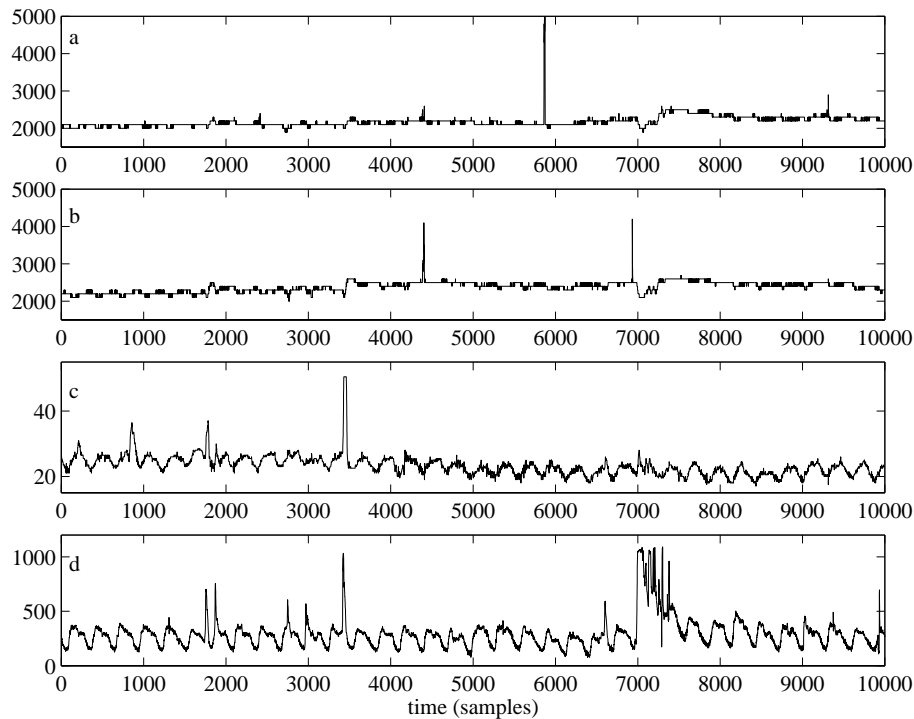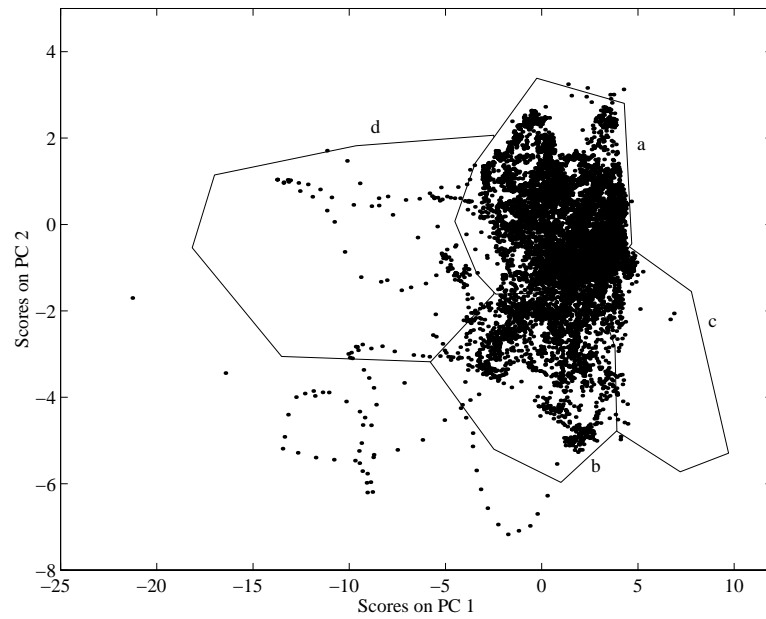**Figure 8.14**   Score plot with classes from Figure 8.14.
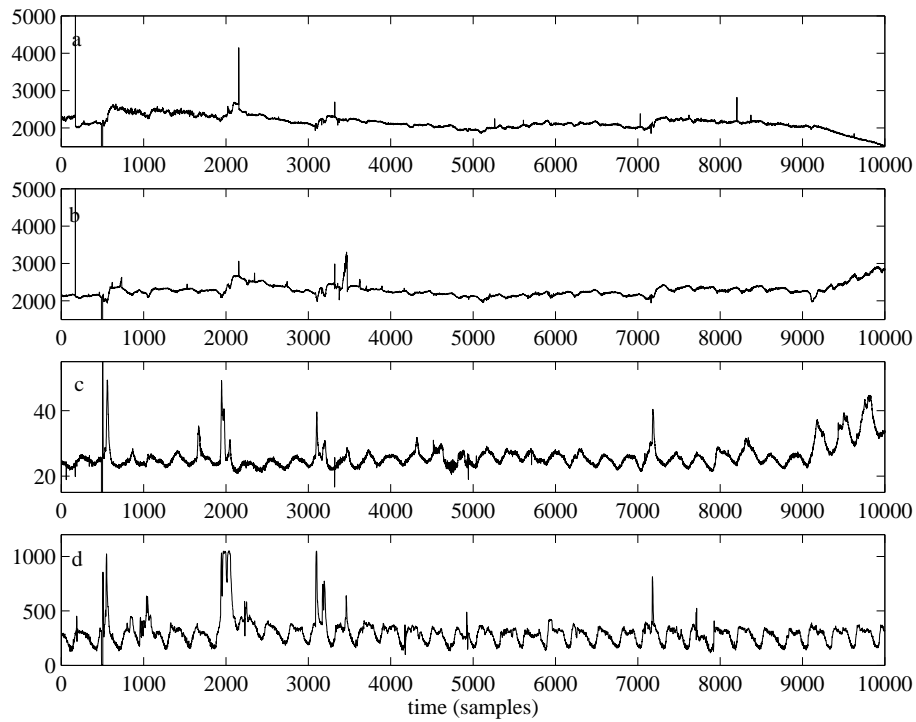


**Figure 8.15**   The original (measured) variables. Suspended solids concentration in line 1 (a) and in line 2 (b). Air valve position (c) and influent flow rate (d).

can be more than two, *i.e.* normal and abnormal operation. Here the classification was done manually, but there is no problem assigning a simple classification algorithm, such as *k-nearest neighbour*, to perform the task automatically (see Chapter 7).

# 8.3   Monitoring Specific Operational Modes

An advantage of PLS, in comparison with PCA, is the capability of linking a set of dependent variables to the independent variable block. This allows us to develop a model that focuses on the variability influencing the output variables of interest. Changes in independent variables influencing the dependent variables will have a larger impact on the monitoring model than variables not influencing the dependent block. Referring to what was discussed earlier about general and specific operational mode descriptions, PLS will serve as a tool for defining and classifying specific operational modes.

## Disturbances with Respect to Effluent Turbidity

The effluent turbidity is considered an important variable for monitoring the effluent water quality from the Ronneby plant. Thus, the effluent turbidity forms the $Y$-matrix (or a rather vector). The $X$-matrix consists of the variables listed in Table 8.6. The goal is to develop a model that will describe a normal operational mode including minor disturbances. Consequently, the period used for training contains mostly of dry-weather conditions, but with limited time periods of rain and storm events. The training period covers 10 000 samples, that is 35 days. Before the data are used, an exponential filter ($\alpha = 0.9$) is applied in order to remove outliers and suppress noise. The resulting model captures the variability of the $X$ and $Y$-blocks according to Table 8.7.

When the model has been identified, it is subjected to new data. The new period is immediately succeeding the training period which implies that the data should and the model result should agree well, at

| Variable number | Measured entity |
|---|---|
| 1 | sludge concentration in line 1 |
| 2 | sludge concentration in line 2 |
| 3 | air valve position, blower 1 in line 1 |
| 4 | air valve position, blower 2 in line 1 |
| 5 | air valve position, blower 1 in line 2 |
| 6 | air valve position, blower 2 in line 2 |
| 7 | influent flow rate |
| 8 | pH, bio reactors |

**Table 8.6**   Variables included in the PLS model.

| LV number | $X$-block this LV | total | $Y$-block this LV | total |
|---|---|---|---|---|
| 1 | 47.28 | 47.28 | 64.17 | 64.17 |
| 2 | 19.95 | 67.23 | 3.90 | 68.07 |
| 3 | 10.03 | 77.25 | 1.86 | 69.94 |
| 4 | 7.25 | 84.50 | 0.48 | 70.42 |
| 5 | 8.33 | 92.83 | 0.11 | 70.53 |
| 6 | 3.20 | 96.04 | 0.21 | 70.74 |
| 7 | 0.75 | 96.79 | 0.22 | 70.96 |
| 8 | 3.21 | 100.00 | 0.00 | 70.96 |

**Table 8.7**   Percent variance captured by the PLS model.
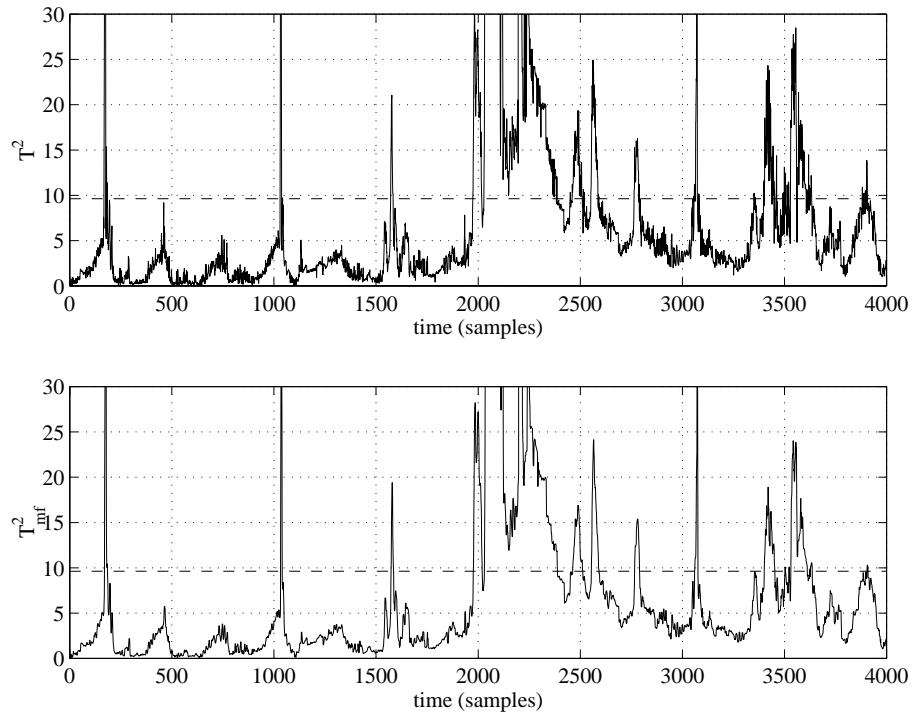
**Figure 8.16** The $T^2$ measure (top) and the five-points median filtered $T^2$ measure (bottom).
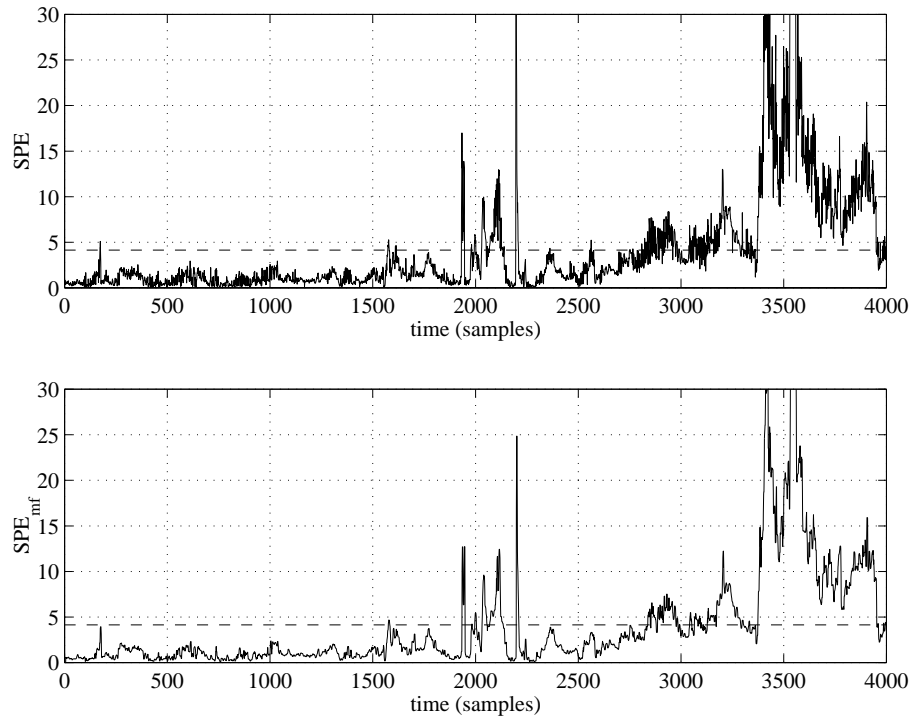


**Figure 8.17** The $SPE$ measure (top) and the five-points median filtered $SPE$ measure (bottom).
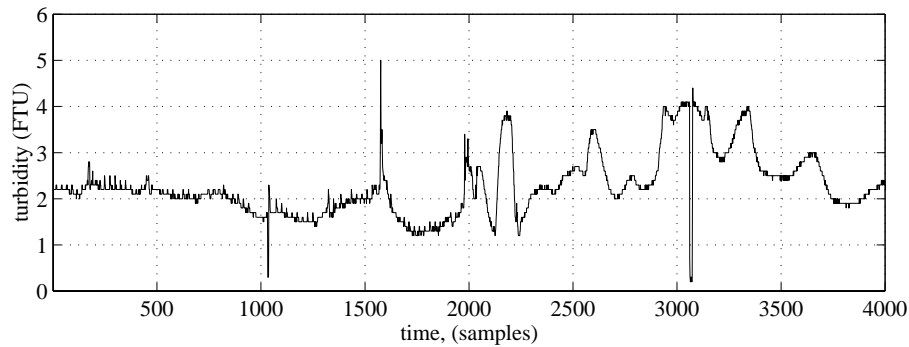
**Figure 8.18**   The effluent turbidity during the monitored period.
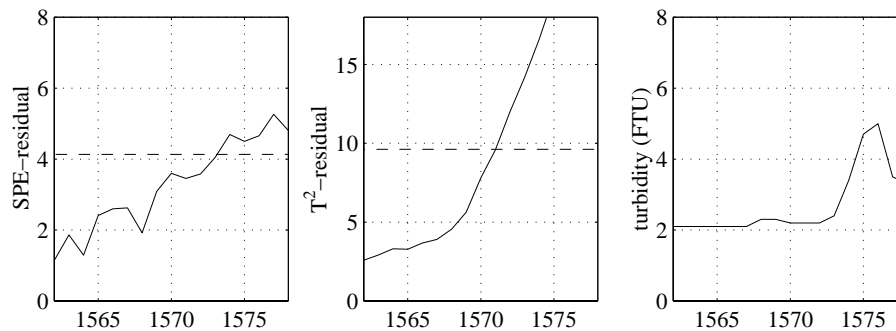


**Figure 8.19**   A closer look at the $SPE$, $T^2$ and effluent turbidity around sample 1570.

least in the beginning of the new period. In Figures 8.16 and 8.17, the $SPE$ and $T^2$ residuals are shown. Evidently, there are disturbances at several occasions during the period. The question is if they correspond to real disturbances. If so, the effect should be possible to observe in the effluent turbidity measurement. It is concluded from the figures that the disturbances in the beginning only affect the $T^2$ measure and, thus, they are inside the model region. However, at about sample 1900 and forward, the disturbances also affect the $SPE$ measure, which indicates that the process has drifted outside the model region (Figure 8.17). How does this difference in the disturbance appearance affect the effluent turbidity? In Figure 8.18, the effluent turbidity during the period is shown. During the first 2000 samples, the variations are short, almost impulse like. From sample 2000 and forward, the variations demonstrate a more continuous behaviour, with longer periods of high effluent turbidity. The difference in appearance coincides with the behaviour of the $SPE$ residual. When disturbances are more persistent, the $SPE$ residual increases.
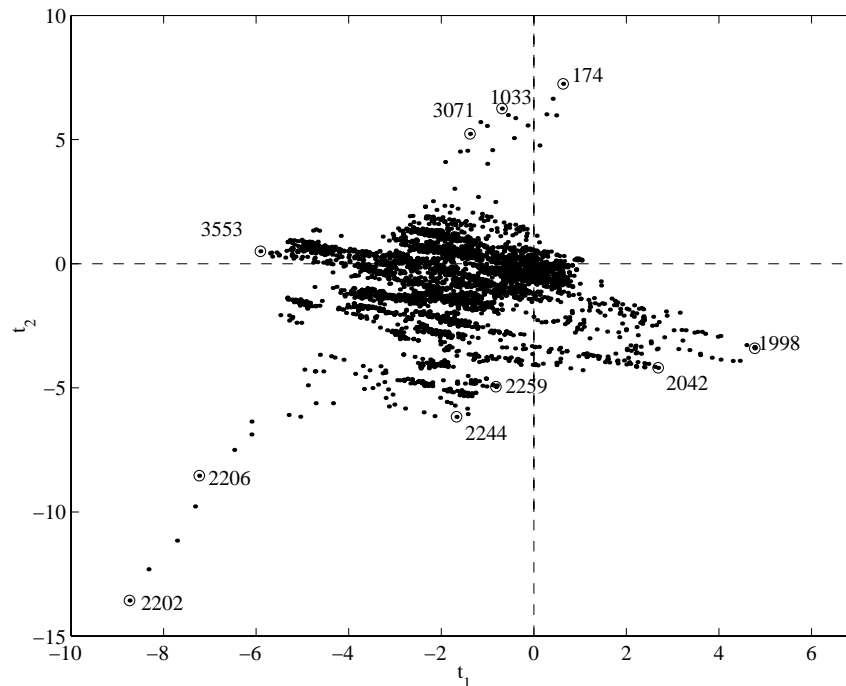
**Figure 8.20**  Score plot of the first two scores. A few specific deviating samples are indicated (compare with Figure 8.16).

Figures 8.16 and 8.17 span over a long period, approximately two weeks, and from the figure it is not possible to decide exactly when an indication of a disturbance occurs. A closer examination of the plots (Figure 8.19) shows that the indication (the residual breaking the confidence limit) not rarely occurs several samples before the increase in the effluent turbidity is visible. This is due to the time delay between, for instance, influent variables and the effluent variables. When independent variables influencing the dependent variable change, the residuals are affected before the dependent variable (if the dependent variable is affected at all).

In Figure 8.20, the first two scores are displayed. Some of the more deviating points are indicated by their sample number. At samples 174, 1033 and 3071 there are major deviations from the normal operational process region. One would expect that the variable or variables responsible for the deviations at these samples are the same ones. In Figure 8.21, the contributions to the deviation along the second PC at samples 174, 1033 and 3071 are shown. The figure clearly indicates variable 8 (pH in the biological reactor), as the main contributor for
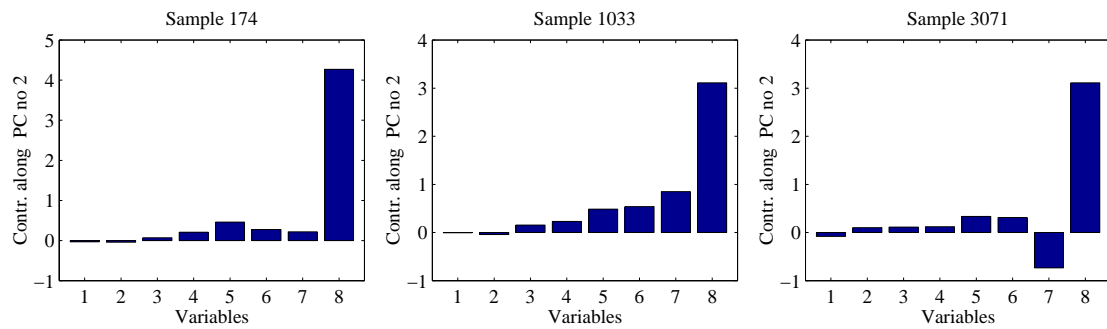
**Figure 8.21**  Variables contributing to the $T^2$ measure at specific samples.
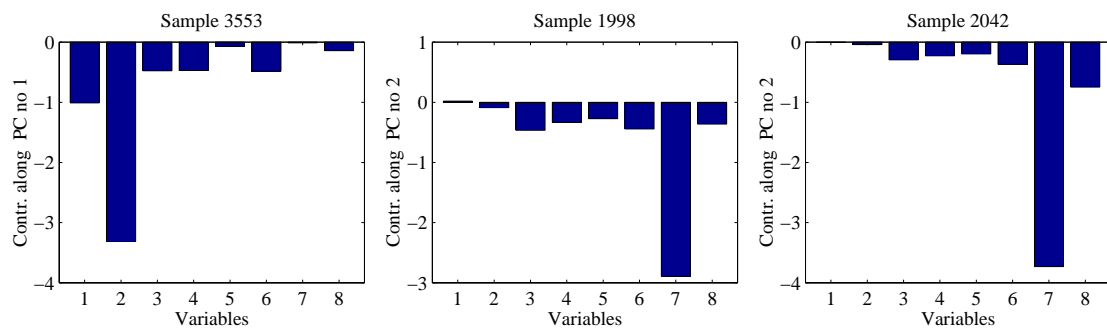


**Figure 8.22**  Variables contributing to the $T^2$ measure at specific samples.

all occasions. In the $T^2$ plot the events are seen as sudden peaks in the $T^2$ value (Figure 8.16). Sample 3553 is primarily deviating along the first PC axis. The reason for the deviation can be seen in Figure 8.22 (left). Variable 2 (sludge concentration in line 2) is the dominant contributor. In the same figure, the contributions to the high $T^2$ value at samples 1998 (middle) and 2042 (right) are shown. In both cases, variable 7 (influent flow rate) has moved the process in the PC space. In this way, all the deviating points can be investigated and the variables causing the deviations can be isolated. To be able to compare the PLS based monitoring with more conventional time series monitoring, the original variables are shown in Figure 8.23. The confidence limits are based on the approximate 95% confidence limits of the training data.
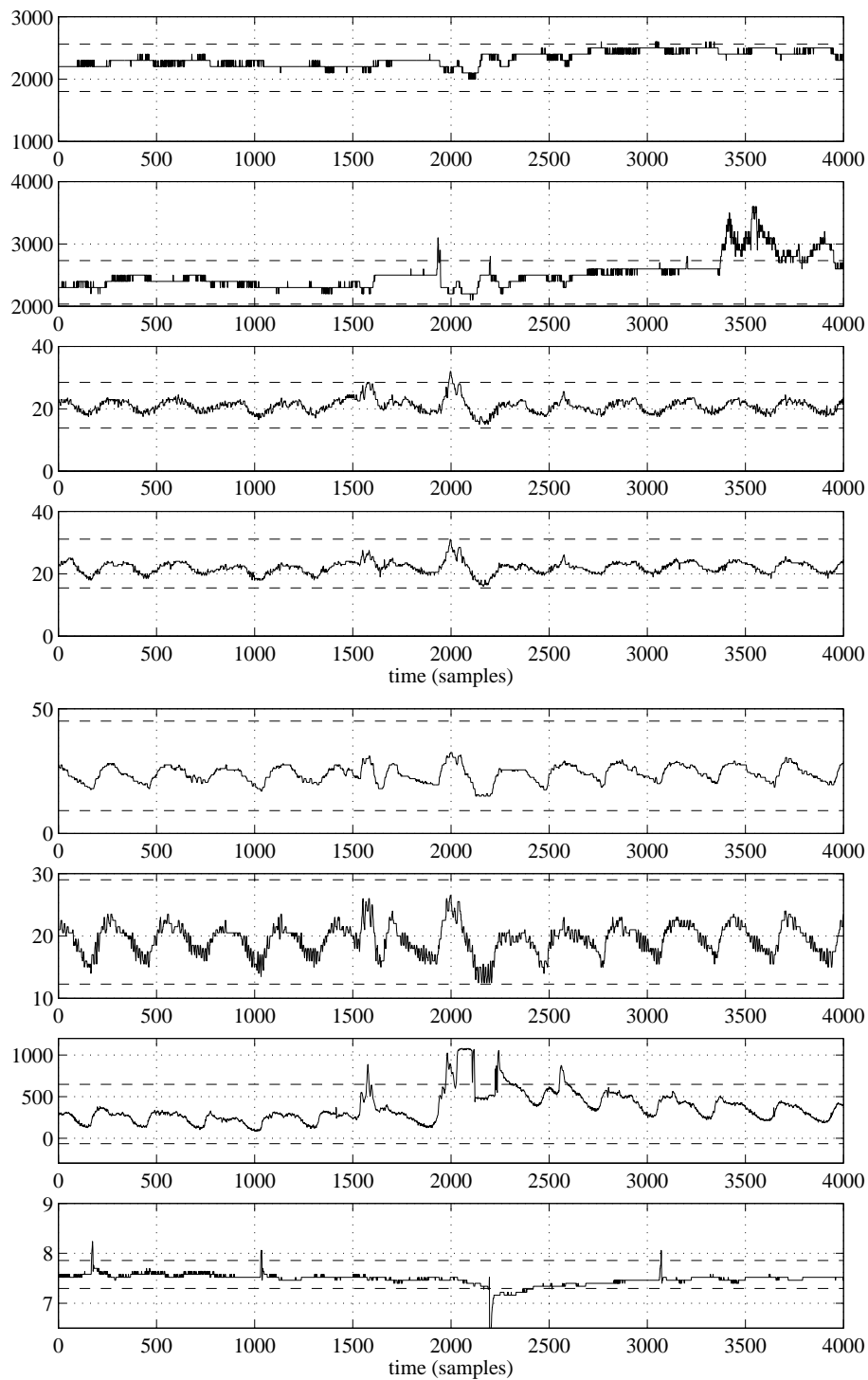
**Figure 8.23**  The original variables of the $X$-block. From the top: sludge concentration line 1, sludge concentration line, air valve position 1-line 1, air valve position 2-line 1, air valve position 1-line 2, air valve position 2-line 2, influent flow rate and pH in bioreactor.

# Chapter 9

# Conclusions

The development of measuring techniques for wastewater treatment purposes has put emphasis on the way the collected data are used. Methods for analysing large amounts of data are required in order to transform the data into information. Information extraction from on-line measurements will most likely become more and more important, partly, because the environmental requirements are becoming more stringent and, partly, because of the increased process complexity due to new and more efficient plant configurations.

## 9.1  Summary of Results

In this thesis, a number of different tools for monitoring on-line measurements are presented. Monitoring on-line measurements involves detection of deviating situations, such as faults, process disturbances and extraordinary events, not normally observed in the process. Monitoring also involves isolation of the deviating variables, so that the variables responsible for the deviating situation are located. Monitoring can be performed either on each variable individually, or simultaneously on many variables using multivariate monitoring techniques.

### Data Screening

Measurement data collected at real wastewater treatment plants are often distorted by noise, outliers, missing values and drifts. This calls for validation and reconstruction of data prior to any thorough analysis. Satisfactory noise reduction can be achieved by digital filters and especially by using non-linear filters. Median filters and *finite response*

*impulse median hybrid* (FMH) filters have proven to be effective, due to their capability to preserve discontinuities in measurement signals. Median filters with appropriate parameters can also be used for outlier removal. However, the median filter is coarse, and sometimes other detection techniques must be used. Multivariate statistics (MVS) has proven to be useful to detect deviating values in data.

## Single Variable Detection

In order to detect deviations in individual measurement signals the signal can be analysed in both the time and frequency domains. Detection in the time domain involves, for instance, analysis of amplitude, centre of location, spread and both short and long-term variability. Usable methods have been presented together with examples of their applicability. In the frequency domain, periodic behaviours can be detected both as long-term and short-term (noise) variations.

Individual investigation of each measurement signal results in a lot of information on the signal. However, the interpretation is sometimes difficult, since the information is not put into a context. Individual investigation of signals does not allow the consequence of any synergetic effects to be detected.

## Multivariate Detection

In order to detect synergetic effects, the measurements must be investigated simultaneously. Multivariate statistics (MVS) provides us with methods to accomplish this. MVS analysis makes it possible to determine the operational mode, that is the conditions under which the process is operated, and the information on the present operational mode is contextual. This makes the result easier to interpret and more suitable for operational decisions than information on individual measurements. In this thesis the concept of general and specific operational modes is introduced.

A *general operational mode* description aims at describing the operational mode without any consideration taken to one or several specific process output criteria. A method presented for general monitoring

is principal component analysis (PCA). Monitoring of the general operational mode, using PCA, is especially well suited for process mode monitoring, but can also be used for process output monitoring.

*Specific operational mode* descriptions aim at describing the process conditions that influence one or several process output criteria. Specific monitoring can be carried out using, for instance, projection to latent structures (PLS). Monitoring of the specific operational mode, using PLS, is suited for process output control, *i.e.* quality control of the product. PLS can also be used for estimation of process output variables.

Most of the information obtained by analysis of individual measurement signals can also be gained by using multivariate monitoring. However, the contextual information provided by multivariate monitoring, makes the multivariate monitoring advantageous in comparison with single variable monitoring. Thus, multivariate monitoring is well suited for wastewater treatment processes.

## 9.2 Implementation Aspects

Some aspects of implementation of the methods described in this thesis are appropriate to discuss. There are many factors to consider, and the best solution for disturbance detection and isolation may vary considerably from plant to plant. The comments in this section are the author's own opinions, which have evolved during the studies on which this thesis is based.

### Data Screening

The most important issue for collection of on-line measurements is the quality of the data. Low data quality limits the use considerably. Therefore, the measurement system, including sensors, devices and computers must be properly and continuously maintained and checked. However, measurement related disturbances will always occur, especially in an industrial environment. Digital filtering is a straightforward, and yet, flexible way to improve the data quality.

The median-based filters, used in this work, have proven to be effective. The frequently occurring step changes and discontinuities in data are preserved (which is not the case when using linear filters) while noise is reduced. The main drawback is the unavoidable time delay, which may cause problems in some applications where a fast response is important.

## Single Variable Detection

Analysis of a single measurement is done in order to extract information. The basic features, such as amplitude, mean and spread, can all be used for information extraction. However, the features must be put into context and presented in a comprehensible way. In time series plots, adaptive limits for detection are perhaps more suitable for the changing conditions common for wastewater treatment, whereas fixed limits are more appropriate when fixed requirements or goals are to be maintained.

## Multivariate Detection

The majority of the measurement features that are obtained by single variable analysis can also be obtained by multivariate analysis. This makes the multivariate approach more versatile, as the result of synergetic effects of several variables can be detected at the same time as basic single variable features are extracted. In this thesis, multivariate statistics (MVS) has been used for detection and isolation of disturbances in wastewater treatment processes. If the general mode of the process is to be monitored, a principal component analysis (PCA) is normally adequate. Since the present mode is inquired for, no time delays have to be considered and no historical measurements need to be incorporated. However, if predictive capability is desired, the monitoring method must take the output variables into consideration. With projection to latent structures (PLS) this is achievable. Since the analysis involves a coupling between input and output variables, time lags between the input and output block must be accounted for. Moreover, dynamics becomes important when the relations between the input and output blocks are to be described. Dynamics can be

incorporated in the analysis by identification of FIR or IIR models. Furthermore PLS, provide means to focus the detection on specific processes within the treatment process.

In order to detect process deviations, detection limits on the results of MVS can be used. Due to the fact that measurement series from wastewater treatment rarely display normal distribution, robust techniques, such as quantiles, are often more suitable for determining detection limits than methods based on, for instance, standard deviation. Moreover, the diurnal variations, common in wastewater treatment, lead to patterns in the process representation in a score plot. Ellipse-shaped boundaries often describe these patterns poorly. Therefore, empirically determined boundaries should be used to determine the normal operational mode.

## 9.3 Topics for Future Research

As the study presented in this thesis progressed, some interesting topics for further studies arose.

### Multivariate statistics (MVS)

In processes with many different separate subprocesses, the *multiblock analysis* approach may prove powerful. Multiblock analysis implies that the $X$-block is separated into several blocks, each one representing a subprocess. This makes the analysis more physically interpretable and the isolation task easier. If a wastewater treatment plant with separate processes is considered, this may significantly improve the isolation of a fault or disturbance.

Parallel MVS models can increase the applicability of monitoring. Instead of attempting to describe all operational modes with one model, several parallel models, each specialised for a certain operational mode, can be used. If an objective criterion of the performance of the model can be determined, this criterion can be used to weight the results of each model, giving high weights to well-performing models and low weights to poor performing models. In this way, the models will not

only produce accurate outputs, but the operational mode can be directly determined from the model currently used. A possible criterion for parallel models could be the $SPE$ residual, normalised by the standard deviation of the $SPE$ residual of the training period.

In order to take the dynamics with different time constants fully into consideration, decomposition of the signals into different time scales before analysis may be a successful approach. Tools for decomposition of signals may be based on *Fast Fourier Transformation* (FFT). In FFT a signal is decomposed into sinusoidal signals of different amplitudes and frequency. However, in wastewater treatment processes, this is not always suitable, as the signals cannot always be approximated by a sum of different sinusoidal signals. However, *wavelet theory* may then be an alternative. As opposed to a sinusoid, a wavelet is a wave form with limited duration and different amplitude, but with zero average. Therefore, wavelet transformations may be more suited to handle process signals with irregular features. The idea of using wavelet theory to decompose measurement signals into a few dominant time scales and then perform MVS analysis on the different time scales is appealing. Wavelets can also be used for noise reduction and detection of changes in signal characteristics (Misiti *et al.* 1996).

Identification of dynamic models using MVS has been discussed briefly in Chapter 6. However, there are many interesting aspects of the coupling between automatic control and chemometrics remaining to be investigated. Examples of this are presented Wise (1991) and Wise *et al.* (1990) where it is demonstrated how MVS can be used for monitoring and control of dynamic processes, or in Piovoso and Kosanovich (1994) where the possibility to use MVS for controller design is discussed.

## Qualitative Diagnosis

As mentioned in Chapter 3, the next logical step after detection and isolation is diagnosis of faults, disturbances and events. Graph-based methods for qualitative diagnosis, as discussed in Chapter 3, may be successful, but there are several interesting alternatives, such as various types of knowledge based or expert systems.

## Interpretation Tools

A significant amount of information can be gained by using different types of information extraction methods from on-line measurements and in this thesis a few methods have been presented. However, the interpretation part is not always straightforward, especially when experience and knowledge of the methods are limited. This calls for a good and easily interpretable man-machine interface, *i.e.* the system presenting of the information. This is a large topic, including research in, for instance, psychology and cognition. Much can be done to improve the comprehensibility of the information presented in order to make it easier for plant operators to quickly make correct decisions.

# Bibliography

Andrews, J.F., (ed.) (1992), *Dynamics and Control of the Activated Sludge, Water Quality Management Library—Volume 6*, Technomic Publishing Company, Inc., Lancaster, Pennsylvania, USA.

Åström, K.J., Wittenmark, B. (1997), *Computer Controlled Systems, Theory and design*, (3rd ed.), Prentice Hall, Inc., Englewood Cliffs, New Jersey, USA.

Barnett, V., Lewis, T. (1994), *Outliers in Statistical Data*, (3rd ed.), John Wiley & Sons Ltd, Chichester, UK.

Bergh, S.-G. (1996), *Diagnosis Problems in Wastewater Settling*, Licentiate's Thesis, Department of Industrial Electrical Engineering and Automation, Lund Institute of Technology, Sweden.

Bissel, D. (1994), *Statistical Methods for SPC and TQM*, Chapman and Hall, London, UK.

Box, G., Luceno, A. (1997), *Statistical Control by Monitoring and Feedback Adjustment*, John Wiley & Sons, Inc., New York, New York, USA.

Champely, S., Doledec, S. (1997), "How to Separate Long-Term Trends from Periodic Variation in Water Quality Monitoring", *Wat. Res.*, **31**(11), 2849-2857.

Chapman, D.T. (1992), "Statistics for Treatment Plant Operation", in Andrews, J.F. (ed.), *Dynamics and Control of the Activated Sludge, Water Quality Management Library—Volume 6*, Technomic Publishing Company, Inc., Lancaster, Pennsylvania, USA.

Davis, J.F., Bakshi, B.R., Kosanovich, K.A., Piovoso, M.J. (1996), "Process Monitoring, Data Analysis and Data Interpretation, *AIChE Symposium Series*, **92**, 1-11.

Dold, P.L., Marais, G.v.R. (1986), "Evaluation of the General Activated Sludge Model Proposed by the IAWPRC Task Group", *Wat. Sci. Tech.*, **18**(6), 63-89.

Dold, P.L., Wentzel, M.C., Billing, A.E., Ekama, G.A., Marais, G.v.R. (1991), *Activated Sludge System Simulation Programs*, Water Research Commission, Pretoria, RSA.

Geladi, P., Kowalski, B.R. (1986), "Partial Least-Squares Regression: A Tutorial", *Analytica Chemica Acta*, **185**, 1-17.

Hammer, M.J. (1986), *Water and Wastewater Technology*, (2nd ed.), Prentice Hall, Inc., Englewood Cliffs, New Jersey, USA.

Hellinga, C., Romein, B., Luyben, K.Ch.A.M., Heijnen, J.J. (1998), "Error Diagnosis and Data Reconciliation Using Linear Conservation Relations", in Van Impe, J.F.M, Vanrolleghem, P.A., Iserentant, D.M. (eds), *Advanced Instrumentation, Data Interpretation, and Control of Biotechnological Processes*, Kluwer Academic Publishers, Dordrecht, The Netherlands.

Henze, M., Grady Jr., C.P.L., Gujer, W., Marais, G.v.R., Matsuo, T. (1987), "Activated Sludge Model No.1", *IAWQ Scientific and Technical Report No.1*, IAWQ, London, UK.

Henze, M., Harremoes, P., Jansen, J. la C., Arvin, E. (1995a), *Wastewater treatment. Biological and Chemical Processes*, Springer Verlag, Berlin, Germany.

Henze, M., Gujer, W., Takahashi, M., Matsuo, T., Wentzel, M.C., Marais, G.v.R. (1995b), "Activated Sludge Model No.2", *IAWQ Scientific and Technical Report No.3*, IAWQ, London, UK.

Höskuldsson, A. (1988), "PLS Regression Methods", *Journal of Chemometrics*, **2**, 211-228.

Jeppsson, U. (1996), *Modelling Aspects of Wastewater Treatment Processes*, Ph.D. Dissertation, Department of Industrial Electrical Engineering and Automation, Lund Institute of Technology, Sweden.

Johansson, R. (1993), *System Modelling & Identification*, Prentice Hall, Inc., Englewood Cliffs, New Jersey, USA.

Kanaya T., Hirabayashi, I., Tsumura, K. (1996), "Detection of Unusual Data in Online Monitoring of Wastewater Processing", *Wat. Sci. Tech.*, **33**(1), 71-79.

Kramer, M.A., Mah, R.S.H. (1994), "Model-Based Monitoring", in Rippin, D., Hale, J., Davis, J. (eds), *Proc. Second Int. Conf. on Foundations of Computer Aided Process Operations*, 45-68.

Krauss, P.T., Shure, L., Little, J.N. (1994), *Signal Processing Toolbox User's Guide*, The MathWorks, Inc., Natick, Massachusetts, USA.

Kresta, J.V., MacGregor, J.F., Marlin, T.E. (1991), "Multivariate Statistical Monitoring of Process Operating Performance", *Can. J. Chem. Eng.*, **69**. 35-47.

Krofta, M., Herath, B., Burgess, D., Lampman, L. (1995), "An Attempt to Understand Dissolved Air Flotation Using Multivariate Analysis", *Wat. Sci. Tech.*, **31**(3-4), 191-201.

Kourti, T., MacGregor, J.F. (1994), "Multivariate SPC Methods for Monitoring and Diagnosing of Process Performance", *Proceedings of PSE '94*, 739-746.

Larsson, J.E. (1994), "Diagnosis Based on Explicit Mean-End Models", *Artificial Intelligence*, **80**, 29-93.

Lind, M. (1990), "Representing Goals and Functions of Complex Systems", Technical Report, Institute of Automatic Control Systems, Technical University of Denmark, Lyngby, Denmark.

MacGregor, J. F., Jaeckle, C., Kiparissides, C., Koutoudi, M. (1994), "Process Monitoring and Diagnosis by Multiblock PLS Methods", *AIChE Journal*, **40**(5), 826-838.

MathWorks (1996), *Using MATLAB - Version 5*, The MathWorks, Inc., Natick, Massachusetts, USA.

Miller, J.C., Miller, J.N. (1993), *Statistics for Analytical Chemistry*, (3rd ed.), Ellis Horwood Ltd, Chichester, UK.

Misiti, M., Misiti, Y., Oppenheim, G., Poggi, J.M. (1996), *Wavelet TOOLBOX, For Use with MATLAB*, The MathWorks, Inc., Natick, Massachusetts, USA.

Mossberg, M. (1995), *An Introduction to Biased Linear Regression*, Master Thesis, UPTEC 95120E, Department of Technology, Uppsala University, Sweden.

Olsson, G., Piani, G. (1992), *Computer Systems for Automation and Control*, Prentice Hall International (UK) Ltd, Hemel Hempstead, UK.

Olsson, G., Newell, R. (1998), *Control of Biological Wastewater Treatment Plants*, book manuscript, to be published in 1999.

Orhon, D., Artan, N. (1994), *Modelling of Activated Sludge Systems*, Technomic Publishing Company, Inc., Lancaster, Pennsylvania, USA.

Piovoso, M.J., Kosanovich, K.A. (1994), "Applications of Multivariate Statistical Methods to Process Monitoring and Controller Design", *Int. J. Control*, **59**(3), 743-756.

Piovoso, M.J., Kasanovich, K.A., Pearson, R.K. (1992), "Monitoring Process Performance in Real-Time", *Proc. Amer. Control Conf., 1992 Chicago*, 2359-2363.

Proakis, J.G., Manolakis, D.G. (1992), *Digital Signal Processing - Principles, Algorithms, and Applications*, (2nd ed.), Macmillan Publishing Company, New York, New York, USA.

Rosén, C., Olsson, G. (1997a), "From Data to Information - Analysis of Operational Data from Wastewater Treatment Plants" (in Swedish), *Proc. Ny teknik inom avloppsvattenrening 1997*, Lund, Sweden.

Rosén, C., Olsson, G. (1997b), *Analysis of On-line Measurements of Pt Loma Wastewater Treatment Plant, San Diego*, Report TEIE-7131, Department of Industrial Electrical Engineering and Automation, Lund Institute of Technology, Sweden.

Rosén, C., Olsson, G. (1998), "Disturbance Detection in Wastewater Treatment Systems", *Wat. Sci. Tech.*, **37**(12), 197-205.

Rosén, C. (1998), *Time Delays and Fault Propagation in Multilevel Flow Models*, Report TEIE-7132, Department of Industrial Electrical Engineering and Automation, Lund Institute of Technology, Sweden.

Söderström, T., Stoica, P., (1989), *System Identification*, Prentice-Hall, Inc., Englewood Cliffs, New Jersey, USA.

Sharaf, M.A., Illman, D.L., Kowalski, B.R. (1986), *Chemometrics*, John Wiley & Sons, Inc., New York, New York, USA.

Takács, I., Patry, G.G., Nolasco, D. (1991), "A Dynamic Model of the Clarification-Thickening Process", *Wat. Res.*, **25**(10), 1263-1271.

Thompson, J.R., Koronacki, J. (1993), *Statistical Process Control for Quality Improvement*, Chapman and Hall, New York, New York, USA.

Vanhooren, H., Nguyen, K. (1996), "Development of a Simulation Protocol for Evaluation of Respirometry-Based Control Strategies", *Technical Report*, BIOMATH department, University of Gent, Belgium.

Van Impe, J.F.M, Vanrolleghem, P.A., Iserentant, D.M., (eds) (1998), *Advanced Instrumentation, Data Interpretation and Control of Biotechnological Processes*, Kluwer Academic Publishers, Dordrecht, The Netherlands.

Wise, B. M., Ricker, N.L., Veltkamp, D.F., Kowalski, B.R. (1990), "A Theoretical Basis for the Use of Principal Component Models for Monitoring Multivariate Processes", *Process Control and Quality*, **1**, 41-51.

Wise, B. M. (1991), *Adapting Multivariate Analysis for Monitoring and Modeling of Dynamic Systems*, Ph.D. Dissertation, Department of Chemical Engineering, University of Washington, Seattle, Washington, USA.

Wise, B. M., Gallagher, N. B. (1996), *PLS_Toolbox for Use with MAT-LAB*, Eigenvector Research, Inc., Manson, Washington, USA.

Wold, S. (1978), "Cross-Validatory Estimation of the Numbers of Components in Factor and Principal Component Models", *Technometrics*, **20**(4), 397-405

Wold, S., Esbensen, K., Geladi, P. (1987), "Principal Component Analysis", *Chemometrics and Intelligent Laboratory Systems*, **2**(4), 37-52

Qin, S.J., McAvoy, T.J. (1991), "Nonlinear PLS Modelling Using Neural Networks", *Computers & Chemical Engineering*, **16**, 379-392.

# Appendix A

# Notation and Abbreviations

## A.1 Notation

| | |
|---|---|
| $A$ | Area of settler |
| $a$ | Number of dimensions retained in the MVS model |
| $\alpha$ | Forgetting factor |
| $\mathbf{B}$ | Regression matrix |
| $\mathbf{B}_{FIR}$ | Regression matrix of a FIR model |
| $\mathbf{B}_{IIR}$ | Regression matrix of an IIR model |
| $\mathbf{b}$ | Regression vector |
| $b$ | Regression scalar |
| $d$ | Euclidian distance or delay |
| $\mathbf{E}$ | General matrix of errors |
| $E_f$ | Detection measure based on a periodogram |
| $\mathbf{e}$ | General vector of errors |
| $\mathbf{F}$ | Matrix of errors of independent block in PLS |
| $f_p$ | General function describing a process |
| $G$ | Goal in a success-tree model |
| $h$ | Sampling time |
| $J_{dn}$ | Flux associated with downward bulk movement |

$J_s$                           Flux associated with gravity settling

$J_{up}$                        Flux associated with upward bulk movement

$K_L a$                         Oxygen transfer rate coefficient

$k$                             Point in time

$l$                             Number of historic values in a model

$\Lambda$                       Diagonal matrix of eigenvalues

$\lambda$                       Eigenvalue

$\mathbf{M}$                    General matrix

$m$                             Number of samples in a data series

$n$                             Number of variables in a data matrix

$\mathbf{P}$                    Loading matrix

$\mathbf{p}$                    Loading vector

$\mathbf{Q}$                    Loading matrix of the dependent block in PLS

$Q_e$                           Effluent flow rate

$Q_f$                           Feed layer flow rate

$Q_u$                           Underflow rate

$Q_r$                           Return sludge flow rate

$\mathbf{q}$                    Loading vector of the dependent block in PLS

$R_{per}^*$                     Periodogram

$r$                             Rank

$r_h$                           Settling characteristic parameter of the hindered settling zone

$r_p$                           Settling characteristic parameter at low solids concentrations

$\sigma$                        Standard deviation

$\sigma^2$                      Variance

| | |
|---|---|
| $S_{ALK}$ | Alkalinity |
| $S_I$ | Inert organic matter concentration |
| $S_{ND}$ | Biodegradable organic nitrogen concentration |
| $S_{NH}$ | Ammonia nitrogen concentration |
| $S_{NO}$ | Nitrate and nitrite nitrogen concentration |
| $S_O$ | Dissolved oxygen concentration |
| $S_S$ | Readily biodegradable substrate concentration |
| $\tau$ | Time shift |
| $\mathbf{T}$ | Score matrix |
| $\hat{\mathbf{T}}$ | Estimated score matrix |
| $T^2$ | Hotelling's $T^2$ statistics |
| $\mathbf{t}$ | Score vector |
| $t_{i,\alpha}$ | Confidence limit for the $i$th score |
| $\mathbf{U}$ | General data matrix of controlled variables or score matrix of the dependent block in PLS |
| $\mathbf{u}$ | Score vector of the dependent block in PLS |
| $v_s$ | Settling velocity |
| $v_0$ | Maximum practical settling velocity |
| $v_0'$ | Maximum theoretical settling velocity |
| $\mathbf{W}$ | General matrix of weights |
| $\mathbf{w}$ | General vector of weights |
| $\mathbf{X}$ | General data matrix of independent variables |
| $\mathbf{x}$ | General data vector of independent variables |
| $\hat{x}$ | Estimated value of an independent variable |
| $X_{B,A}$ | Active autotrophic biomass concentration |

$X_{B,H}$          Active heterotrophic biomass concentration

$X(f)$          Fourier transform of $x(k)$, $x(k-1)$, ... , $x(k-m)$

$X_f$          Particulate concentration in feed layer

$X_I$          Particulate inert organic matter concentration

$X_n$          Particulate concentration in layer $n$

$X_{ND}$          Particulate biodegradable organic nitrogen concentration

$X_P$          Particulate product concentration from biomass decay

$x_q$          New instance in $k$-nearest neighbour

$X_S$          Slowly biodegradable substrate concentration

$\mathbf{Y}$          General data matrix of dependent variables

$Y(f)$          Fourier transform of $y(k)$, $y(k-1)$, ... , $y(k-m)$

$\mathbf{y}$          General vector of measurements or model outputs

$\hat{\mathbf{y}}$          General vector of filter outputs

$\hat{\mathbf{y}}_{FMH}$          FMH-filter outputs

## A.2    Abbreviations

**AR**          Autoregressive filter or process

**ARMA**          Autoregressive moving average filter or process

**AS**          Activated sludge

**ASM1**          Activated Sludge Model No.1

**CCF**          Crosscorrelation function

**COD**          Chemical oxygen demand

*cov*          Covariance

| | |
|---|---|
| **CUSUM** | Cumulative sum |
| **DAF** | Dissolved air flotation |
| **DFT** | Discrete Fourier transform |
| **D²C** | Detection, diagnosis and consequence analysis |
| **DO** | Dissolved oxygen |
| **EWMA** | Exponentially weighted moving average |
| **FIR** | Finite impulse response |
| **FMH** | FIR median hybrid |
| **IAWQ** | International Association on Water Quality |
| **IIR** | Infinite impulse response |
| **IQR** | Interquartile range |
| **LV** | Latent vector |
| **MA** | Moving average filter or process |
| **MAX** | Moving average adaptive exponential filter |
| **MIMO** | Multiple input, multiple output |
| **MISO** | Multiple input, single output |
| **MLR** | Multiple linear regression |
| **MVS** | Multivariate statistics |
| **NIPALS** | Nonlinear partial least squares |
| **PC** | Principal component |
| **PCA** | Principal component analysis |
| **PCR** | Principal component regression |
| **PLC** | Programmable logic controller |
| **PLS** | Projection to latent structures or partial least squares |
| **R** | Range |

**SISO**             Single input, single output

**SPC**              Statistic process control

**SPE**              Squared prediction error

**SS**               Suspended solids

**TSS**              Total suspended solids

# Appendix B

# The NIPALS Algorithm for PLS

In this appendix the basic algorithm for projection to latent structures (PLS) is presented. The algorithm can be found in Geladi and Kowalski (1986) or in Sharaf $et\ al.$ (1986).

It is assumed that $\mathbf{X}$ and $\mathbf{Y}$ are mean-centred and scaled to unit variance.

For each component:

$$\mathbf{u}_{start} = some\ \mathbf{y}_i \tag{B.1}$$

In the $X$-block:

$$\mathbf{w}^T = \frac{\mathbf{u}^T\mathbf{X}}{\mathbf{u}^T\mathbf{u}} \tag{B.2}$$

Normalisation:

$$\mathbf{w}_{new}^T = \frac{\mathbf{w}_{old}^T}{\|\mathbf{w}_{old}^T\|} \tag{B.3}$$

$$\mathbf{t} = \frac{\mathbf{X}\mathbf{w}}{\mathbf{w}^T\mathbf{w}} \tag{B.4}$$

In the $Y$-block:

$$\mathbf{q}^T = \frac{\mathbf{t}^TY}{\mathbf{t}^T\mathbf{t}} \tag{B.5}$$

Normalisation:

$$\mathbf{q}_{new}^T = \frac{\mathbf{q}_{old}^T}{\|\mathbf{q}_{old}^T\|} \tag{B.6}$$

$$\mathbf{u} = \frac{\mathbf{Y}\mathbf{q}}{\mathbf{q}^T\mathbf{q}} \tag{B.7}$$

The weights $\mathbf{w}^T$ replace the $\mathbf{p}^T$ in order to get orthogonal $\mathbf{t}$ values.

Check convergence: compare the $\mathbf{t}$ with the preceding $\mathbf{t}$:

$$error = t - t_{preceding} \tag{B.8}$$

If *error* is below a certain threshold, then go to Equation B.9, otherwise return to Equation B.2 until convergence is obtained. (If the $Y$-block has only one variable, Equations B.5-B.8 can be omitted by putting $q = 1$, and no further iteration is necessary.)

Calculate the $\mathbf{X}$ loadings and rescale the scores and weights accordingly:

$$\mathbf{p}^T = \frac{\mathbf{t}^T \mathbf{X}}{\mathbf{t}^T \mathbf{t}} \tag{B.9}$$

Normalisation:

$$\mathbf{p}^T_{new} = \frac{\mathbf{p}^T_{old}}{\|\mathbf{p}^T_{old}\|} \tag{B.10}$$

$$\mathbf{t}_{new} = \mathbf{t}_{old} \|\mathbf{p}^T_{old}\| \tag{B.11}$$

$$\mathbf{w}^T_{new} = \mathbf{w}^T_{old} \|\mathbf{p}^T_{old}\| \tag{B.12}$$

($\mathbf{p}^T$,$\mathbf{q}^T$ and $\mathbf{w}^T$ should be stored for prediction; $\mathbf{t}$ and $\mathbf{u}$ can be stored for isolation and classification purposes).

Find the regression coefficient $b$ for the inner relation:

$$b = \frac{\mathbf{u}^T \mathbf{t}}{\mathbf{t}^T \mathbf{t}} \tag{B.13}$$

Calculation of the residuals. The general outer relation for the $X$-block (for component $i$) is:

$$\mathbf{E}_i = \mathbf{E}_{i-1} - \mathbf{t}_i \mathbf{p}^T_i \; ; \; \mathbf{X} = \mathbf{E}_0 \tag{B.14}$$

$$\mathbf{F}_i = \mathbf{F}_{i-1} - b_i \mathbf{t}_i \mathbf{q}^T_i \; ; \; \mathbf{Y} = \mathbf{F}_0 \tag{B.15}$$

From here, one goes to Equation B.1 to implement the procedure for the next component. (Note: after the first component, $\mathbf{X}$ in Equations B.2, B.5 and B.9 and $\mathbf{Y}$ in Equation B.7 are replaced by their corresponding residual matrices $\mathbf{E}_i$ and $\mathbf{F}_i$, respectively).

# Appendix C

# The IAWQ Activated Sludge Model no.1

This appendix contains the complete IAWQ Activated Sludge Model no.1 (ASM1), developed by Henze *et al.* (1987). It is a result of the work carried out by *Task Group on Mathematical Modelling for Design and Operation of Biological Wastewater Treatment Systems*, formed by *International Association on Water Quality* (IAWQ). On the next three pages, Tables C.1 and C.2 list the processes and reactions of the model and the default values of the parameters for 10 and 20° C

**Table C.1**    (Next two pages) The ASM1 model in matrix format (Jeppsson 1996).

**Table C.2**    (Page 190) The default set of parameter values for the ASM1 model (Jeppsson 1996).

| | Component → i | 1 | 2 | 3 | 4 | 5 | 6 | 7 | 8 | 9 |
|---|---|---|---|---|---|---|---|---|---|---|
| $j$ | Process ↓ | $S_I$ | $S_S$ | $X_I$ | $X_S$ | $X_{B,H}$ | $X_{B,A}$ | $X_P$ | $S_O$ | $S_{NO}$ |
| 1 | Aerobic growth of heterotrophs | | $-\dfrac{1}{Y_H}$ | | | $1$ | | | $-\dfrac{1-Y_H}{Y_H}$ | |
| 2 | Anoxic growth of heterotrophs | | $-\dfrac{1}{Y_H}$ | | | $1$ | | | | $-\dfrac{1-Y_H}{2.86\,Y_H}$ |
| 3 | Aerobic growth of autotrophs | | | | | | $1$ | | $-\dfrac{4.57}{Y_A}+1$ | $\dfrac{1}{Y_A}$ |
| 4 | 'Decay' of heterotrophs | | | | $1-f_P$ | $-1$ | | $f_P$ | | |
| 5 | 'Decay' of autotrophs | | | | $1-f_P$ | | $-1$ | $f_P$ | | |
| 6 | Ammonification of soluble organic nitrogen | | | | | | | | | |
| 7 | 'Hydrolysis' of entrapped organics | | $1$ | | $-1$ | | | | | |
| 8 | 'Hydrolysis' of entrapped organic nitrogen | | | | | | | | | |
| | Observed Conversion Rates [ML⁻³T⁻¹] | $r_i = \sum\limits_j \nu_{ij}\rho_j$ | | | | | | | | |
| | Stoichiometric Parameters: Heterotrophic yield: $Y_H$ Autotrophic yield: $Y_A$ Fraction of biomass yielding particulate products: $f_P$ Mass N/Mass COD in biomass: $i_{XB}$ Mass N/Mass COD in products from biomass: $i_{XP}$ | Soluble inert organic matter [M(COD)L⁻³] | Readily biodegradable substrate [M(COD)L⁻³] | Particulate inert organic matter [M(COD)L⁻³] | Slowly biodegradable substrate [M(COD)L⁻³] | Active heterotrophic biomass [M(COD)L⁻³] | Active autotrophic biomass [M(COD)L⁻³] | Particulate products arising from biomass decay [M(COD)L⁻³] | Oxygen (negative COD) [M(−COD)L⁻³] | Nitrate and nitrite nitrogen [M(N)L⁻³] |

| 10 $S_{NH}$ | 11 $S_{ND}$ | 12 $X_{ND}$ | 13 $S_{ALK}$ | Process Rate, $\rho_j$ [ML$^{-3}$T$^{-1}$] |
|---|---|---|---|---|
| $-i_{XB}$ | | | $-\dfrac{i_{XB}}{14}$ | $\hat{\mu}_H\left(\dfrac{S_S}{K_S+S_S}\right)\left(\dfrac{S_O}{K_{O,H}+S_O}\right)X_{B,H}$ |
| $-i_{XB}$ | | | $\dfrac{1-Y_H}{14\cdot 2.86Y_H}$ $-\dfrac{i_{XB}}{14}$ | $\hat{\mu}_H\left(\dfrac{S_S}{K_S+S_S}\right)\left(\dfrac{K_{O,H}}{K_{O,H}+S_O}\right)$ $\cdot\left(\dfrac{S_{NO}}{K_{NO}+S_{NO}}\right)\eta_g X_{B,H}$ |
| $-i_{XB}-\dfrac{1}{Y_A}$ | | | $-\dfrac{i_{XB}}{14}-\dfrac{1}{7Y_A}$ | $\hat{\mu}_A\left(\dfrac{S_{NH}}{K_{NH}+S_{NH}}\right)\left(\dfrac{S_O}{K_{O,A}+S_O}\right)X_{B,A}$ |
| | | $i_{XB}-f_Pi_{XP}$ | | $b_H X_{B,H}$ |
| | | $i_{XB}-f_Pi_{XP}$ | | $b_A X_{B,A}$ |
| 1 | $-1$ | | $\dfrac{1}{14}$ | $k_a S_{ND} X_{B,H}$ |
| | | | | $k_h\dfrac{X_S/X_{B,H}}{K_X+\left(X_S/X_{B,H}\right)}\left[\left(\dfrac{S_O}{K_{O,H}+S_O}\right)\right.$ $\left.+\eta_h\left(\dfrac{K_{O,H}}{K_{O,H}+S_O}\right)\left(\dfrac{S_{NO}}{K_{NO}+S_{NO}}\right)\right]X_{B,H}$ |
| | 1 | $-1$ | | $\rho_7(X_{ND}/X_S)$ |
| | $r_i=\sum\limits_{j} v_{ij}\rho_j$ | | | |
| NH$_4$+NH$_3$ nitrogen [M(N)L$^{-3}$] | Soluble biodegradable organic nitrogen [M(N)L$^{-3}$] | Particulate biodegradable organic nitrogen [M(N)L$^{-3}$] | Alkalinity – Molar units | Kinetic Parameters:<br>Heterotrophic growth and decay: $\hat{\mu}_H$, $K_S$, $K_{O,H}$, $K_{NO}$, $b_H$<br>Autotrophic growth and decay: $\hat{\mu}_A$, $K_{NH}$, $K_{O,A}$, $b_A$<br>Correction factor for anoxic growth of heterotrophs: $\eta_g$<br>Ammonification: $k_a$<br>Hydrolysis: $k_h$, $K_X$<br>Correction factor for anoxic hydrolysis: $\eta_h$ |

| IAWQ model parameters | symbol | unit | 20 °C | 10 °C | literature |
|---|---|---|---|---|---|
| *Stoichiometric parameters* | | | | | |
| Heterotrophic yield | $Y_H$ | g cell COD formed (g COD oxidized)⁻¹ | 0.67 | 0.67 | 0.38-0.75 |
| Autotrophic yield | $Y_A$ | g cell COD formed (g N oxidized)⁻¹ | 0.24 | 0.24 | 0.07-0.28 |
| Fraction of biomass yielding particulate products | $f_P$ | dimensionless | 0.08 | 0.08 | – |
| Mass N/mass COD in biomass | $i_{XB}$ | g N (g COD)⁻¹ in biomass | 0.086 | 0.086 | – |
| Mass N/mass COD in products from biomass | $i_{XP}$ | g N (gCOD)⁻¹ in endogenous mass | 0.06 | 0.06 | – |
| *Kinetic parameters* | | | | | |
| Heterotrophic max. specific growth rate | $\hat{\mu}_H$ | day⁻¹ | 6.0 | 3.0 | 0.6-13.2 |
| Heterotrophic decay rate | $b_H$ | day⁻¹ | 0.62 | 0.20 | 0.05-1.6 |
| Half-saturation coefficient (hsc) for heterotrophs | $K_S$ | g COD m⁻³ | 20 | 20 | 5-225 |
| Oxygen hsc for heterotrophs | $K_{O,H}$ | g O₂ m⁻³ | 0.20 | 0.20 | 0.01-0.20 |
| Nitrate hsc for denitrifying heterotrophs | $K_{NO}$ | g NO₃-N m⁻³ | 0.50 | 0.50 | 0.1-0.5 |
| Autotrophic max. specific growth rate | $\hat{\mu}_A$ | day⁻¹ | 0.80 | 0.30 | 0.2-1.0 |
| Autotrophic decay rate | $b_A$ | day⁻¹ | 0.20 | 0.10 | 0.05-0.2 |
| Oxygen hsc for autotrophs | $K_{O,A}$ | g O₂ m⁻³ | 0.4 | 0.4 | 0.4-2.0 |
| Ammonia hsc for autotrophs | $K_{NH}$ | g NH₃-N m⁻³ | 1.0 | 1.0 | – |
| Correction factor for anoxic growth of heterotrophs | $\eta_g$ | dimensionless | 0.8 | 0.8 | 0.6-1.0 |
| Ammonification rate | $k_a$ | m³ (g COD day)⁻¹ | 0.08 | 0.04 | – |
| Max. specific hydrolysis rate | $k_h$ | g slowly biodeg. COD (g cell COD day)⁻¹ | 3.0 | 1.0 | – |
| Hsc for hydrolysis of slowly biodeg. substrate | $K_X$ | g slowly biodeg. COD (g cell COD)⁻¹ | 0.03 | 0.01 | – |
| Correction factor for anoxic hydrolysis | $\eta_h$ | dimensionless | 0.4 | 0.4 | – |